ERDA/JPL-1012-77/2
Distribution Category UC-63

# LSSA
## LOW-COST SILICON SOLAR ARRAY PROJECT

# Project QUARTERLY REPORT -3

**FOR THE PERIOD OCTOBER 1976 - DECEMBER 1976**

**5101-24**

## DISCLAIMER

ENERGY RESEARCH AND DEVELOPMENT ADMINISTRATION

# LSSA
## LOW-COST SILICON SOLAR ARRAY PROJECT



# Project QUARTERLY REPORT-3

## FOR THE PERIOD OCTOBER 1976 - DECEMBER 1976

**5101-24**

NATIONAL AERONAUTICS AND SPACE ADMINISTRATION
JET PROPULSION LABORATORY
CALIFORNIA INSTITUTE OF TECHNOLOGY
PASADENA, CALIFORNIA

THIS PAGE

WAS INTENTIONALLY

LEFT BLANK

CONTENTS

Figures

Tables

DISTRIBUTION

Adolph Meller Co.
Attn: R. R. Monchamp
Providence RI

AeroChem Research Labs.
Attn: Dr. H. F. Calcote
Princeton NJ

Aerospace Corp.
Attn: Larry Gibson
Los Angeles CA

Aerospace Corp.
Attn: H. J. Killian
Los Angeles CA

Aerospace Corp.
Attn: Dr. S. L. Leonard
Los Angeles CA

Alcoa
Attn: Gregory Barthold
Washington DC

Amp, Inc.
Attn: E. J. Whiteman
Harrisburg PA

Arizona State Univ.
Attn: Dr. C. E. Backus
Tempe AZ

ARK
Attn: Eugene Findl
Farmingdale NY

Battelle Memorial Inst.
Attn: J. Blocher
Columbus OH

Battelle Memorial Inst.
Attn: Dr. M. F. Browning
Columbus OH

Battelle Memorial Inst.
Attn: Dr. D. C. Carmichael
Columbus OH

Battelle Memorial Inst.
Attn: G. Derringer
Columbus OH

Battelle Memorial Inst.
Attn: G. Gaines
Columbus OH

Battelle Memorial Inst.
Attn: F. Sliemers
Columbus OH

Battelle Memorial Inst.
Attn: R. Thomas
Columbus OH

Bendix Corp.
Attn: L. M. Farrell
Teterboro NJ

The Boeing Company
Attn: Dr. C. J. Bishop
Seattle WA

The Boeing Company
Attn: J. Lowe
Seattle WA

Boston College
Attn: Dr. P. H. Fang
Chestnut Hill MA

Brown Univ.
Attn: Prof. J. J. Loferski
Providence RI

California Polytechnic
State Univ.
Attn: Univ. Library
San Luis Obispo CA

Calspan Corp.
Attn: Dr. C. W. Sauer
Buffalo NY

Carnegie-Mellon Univ.
Attn: Dr. Art Milnes
Pittsburgh PA

Case Western Reserve Univ.
Attn: A. B. Kuper
Cleveland OH

Case Western Reserve Univ.
Attn: C. E. Rogers
Cleveland OH

Christian Science Monitor
Attn: D. F. Salisbury
Boston MA

Clarkson College of Tech.
Attn: W. R. Wilcox
Potsdam NY

Columbia Univ.
Attn: C. E. Meyer
New York NY

Comsat Corp.
Attn: L. C. Meyer
Washington DC

Comsat Labs.
Attn: D. J. Curtin
Clarksburg MD

Comuntzis, M.
Pasadena CA

Cornell Univ.
College of Engr.
Attn: D. G. Ast
Ithaca NY

Crystal Systems, Inc.
Attn: B. Reynolds
Salem MA

Crystal Systems, Inc.
Attn: Frederick Schmid
Salem MA

Delson Corp.
Attn: Marketing Mgr.
Glendale CA

Dow Corning Corp.
Attn: C. G. Currin
Hemlock MI

Dow Corning Corp.
Attn: Vishu Dosaj
Hemlock MI

Dow Corning Corp.
Attn: L. P. Hunt
Hemlock MI

Dow Corning Corp.
Attn: J. McCormick
Hemlock MI

Electric Power Res. Inst.
Attn: E. A. De Meo
Palo Alto CA

Electro Sol Labs.
Attn: Dr. H. R. Dessau
Winter Park FL

ERDA
Attn: T. B. Abernathy
Oak Ridge TN

ERDA
Sandia Labs.
Attn: R. Berg
Albuquerque NM

ERDA
Div. Solar Energy
Attn: Dr. H. R. Blieden
Washington DC

ERDA
Div. Solar Energy
Attn: Dr. D. L. Feucht
Washington DC

ERDA
Argonne National Lab.
Attn: P. R. Fields
Argonne IL

ERDA
Div. Solar Energy
Attn: Dr. L. O. Herwig
Washington DC

ERDA
Div. Solar Energy
Attn: Dr. L. M. Magid
Washington DC

ERDA
Sandia Labs.
Attn: B. Marshall
Albuquerque NM

ERDA
Div. Solar Energy
Attn: Dr. Henry Marvin
Washington DC

ERDA
Div. Solar Energy
Attn: Dr. Paul Maycock
Washington DC

ERDA
Oakland Ops. Office
Attn: D. Neely
Oakland CA

ERDA
Div. Solar Energy
Attn: Dr. Morton Prince
Washington DC

ERDA
Div. Solar Energy
Attn: Dr. H. L. Macomber
Washington DC

ERDA
Argonne National Lab.
Attn: A. Rabl
Argonne IL

ERDA
Sandia Lab.
Attn: R. P. Stromberg
Albuquerque NM

ERDA
San Francisco Ops. Office
Attn: Suite 2560
San Francisco CA

ERDA
Div. Solar Energy
Attn: Dr. Douglas Warschauer
Washington DC

ERDA
Argonne National Lab.
Attn: S. Zwerdling
Argonne IL

ESB Technology Center
Attn: Librarian
Yardley PA

Exotic Materials, Inc.
Attn: W. L. Loucks
Costa Mesa CA

Federal Energy Adm.
Attn: Solar Energy Div.
Washington DC

Federal Power Commission
Attn: Library
Washington DC

Four Corners Envir. Res. Inst.
Attn: Dr. Roy Cruz
Project Manager
Durango CO

General Electric Co.
Attn: R. N. Hall
Schenectady NY

General Electric Co.
Attn: M. Garfinkel
Schenectady NY

General Electric Co.
Valley Forge Space Center
Attn: G. J. Rayl
Philadelphia PA

General Electric Co.
Valley Forge Space Center
Attn: Dr. T. Riethof
Philadelphia PA

General Electric Co.
Valley Forge Space Center
Attn: W. Terrill
Philadelphia PA

Georgia Inst. of Tech.
Attn: R. Larson
Consultant
Atlanta GA

Georgia Inst. of Tech.
Attn: D. Williams
Atlanta GA

Goodyear Aerospace Corp.
Attn: D. E. Zesinger
Litchfield Park AZ

Gulf & Westinger
Attn: R. G. Brownstein
Swarthmore PA

Rodney Hippenhammer
Pasadena CA

Honeywell, Inc.
Attn: J. D. Heaps
Bloomington MN

Honeywell, Inc.
Attn: R. Maciolek
Bloomington MN

Honeywell, Inc.
Attn: O. Tufte
Bloomington MN

Honeywell, Inc.
Attn: D. Zook
Bloomington MN

Hughes Aircraft Co.
Attn: C. W. Jackson
Fullerton CA

IBM Corp.
Attn: T. Ciszek
Hopewell Junction NY

IBM Corp.
Attn: Dr. A. Kran
Hopewell Junction NY

IBM Corp.
Attn: Dr. G. H. Schwuttke
Hopewell Junction NY

ICT, Inc.
Attn: L. P. Kelley
Shelby MI

Info. Inc.
Attn: D. N. Jewett
Ayer MA

International Rectifier
Attn: M. F. Gift
El Segundo CA

IRT
Attn: R. Mertz
San Diego CA

IRT Corp.
Attn: J. A. Naber
San Diego CA

Kayex Corp.
Attn: R. L. Lane
Rochester NY

Lamar Univ.
Attn: K. Hansen
Beaumont TX

Lamar Univ.
Attn: Dr. C. L. Yaws
Beaumont TX

Arthur D. Little, Inc.
Attn: Dr. D. W. Almgren
Cambridge MA

Lockheed Missles & Space Co.
Attn: Paul Dillard
Sunnyvale CA

M7 International, Inc.
Attn: R. Ignatius
Arlington Heights IL

M7 International, Inc.
Attn: E. Gabrenya
Arlington Heights IL

MIT
Attn: J. Fan
Lexington MA

MIT
Attn: P. Jarvinen
Lexington MA

MIT
Lincoln Lab.
Attn: E. B. Murphy
Lexington MA

MIT
Lincoln Lab.
Attn: Mr. Marvin Pope
Lexington MA

Matare, Dr. H. F.
Los Angeles CA

Mc Donnell Douglas
Attn: L. G. Harmon
St. Louis MO

Mc Graw-Edison Co.
Attn: D. P. Spittlehouse
Bristol CT

Metallurgie Hoboken-Overpelt
Attn: I. H. Guislain
Belgium

Mettallurgie Hoboken-Overpelt
Attn: L. Van Hecke
Belgium

Mitre Corp.
Attn: A. Cherdak
Mc Lean VA

Mitre Corp.
Attn: Dr. Gregory Haas
Mc Lean VA

Mobile-Tyco Solar Energy Corp.
Attn: D. N. Jewett
Waltham MA

Mobile-Tyco Solar Energy Corp.
Attn: A. I. Mlavsky
Waltham MA

Mobil-Tyco Solar Energy Corp.
Attn: H. Rao
Waltham MA

Mobil-Tyco Solar Energy Corp.
Attn: K. V. Ravi
Waltham MA

Mobil-Tyco Solar Energy Corp.
Attn: T. Surek
Waltham MA

Modern Optics Corp.
Attn: I. C. Neufeld
El Monte CA

Monsanto Research Corp.
Attn: D. Hill
St. Peters MO

Monsanto Research Corp.
Attn: H. Gutsche
St. Peters MO

Monsanto Research Corp.
Attn: F. J. Winslow
St. Peters MO

Motorola, Inc.
Attn: A. Baghdadi
Phoenix AZ

Motorola, Inc.
New Venture Lab.
Attn: M. Coleman
Phoenix AZ

Motorola, Inc.
Attn: R. Chaney
Phoenix AZ

Motorola, Inc.
Attn: R. Gurtler
Phoenix AZ

Motorola, Inc.
Attn: M. Ingle
Phoenix AZ

Motorola, Inc.
Attn: Dr. I. A. Lesk
Phoenix AZ

Motorola, Inc.
Attn: B. McGinnis
Phoenix AZ

Motorola, Inc.
Attn: E. Philofsky
Phoenix AZ

Motorola, Inc.
Attn: R. Pryor
Phoenix AZ

Motorola, Inc.
Attn: C. Varker
Phoenix AZ

Multi-Systems Associates
Attn: P. J. Shlichta
San Diego CA

NASA Headquarters
Attn: R. D. Ginter
Washington DC

NASA Headquarters
Attn: L. Holcomb
Washington DC

NASA Headquarters
Attn: J. C. Loria
Washington DC

NASA Johnson Space Center
Attn: Harold Benson
Houston TX

NASA Lewis Research Center
Attn: R. Easter
Cleveland OH

NASA Lewis Research Center
Attn: R. S. Palmer
Cleveland OH

National Bureau of Standards
Attn: S. R. Coriell
Washington DC

National Science Foundation
Attn: Dr. Tapan Mukherjee
Washington DC

North Americal Philips Corp.
Attn: J. Kostelec
Briarcliff Manor NY

Northeastern Univ.
Attn: W. B. Nowak
Boston MA

Northrop Res. & Tech. Ctr.
Attn: S. Othmer
Hawthorne CA

Northrop Res. & Tech. Ctr.
Attn: J. Srour
Hawthorne CA

Oak Ridge National Lab.
Attn: Dr. W. J. Lackey
Oak Ridge TN

Opto Technology, Inc.
Attn: W. E. Hegberg
Wheeling IL

Optical Coating Lab., Inc.
Attn: T. Chao
City of Industry CA

Optical Coating Lab., Inc.
Attn: D. Sharman
City of Industry CA

Owens Illinois, Inc.
Attn: G. L. Glen
Toledo OH

Pennwalt Corp.
Attn: Piero Nannelli
King of Prussia PA

The Perkin-Elmer Corp.
Attn: Dr. B. E. Nelson
Norwalk CT

Purdue Univ.
Attn: R. W. Vest
West Lafayette IN

RCA Labs.
Attn: A. Bell
Princeton NJ

RCA Labs.
Attn: S. Berkman
Princeton NJ

RCA Labs.
Attn: G. W. Cullen
Princeton NJ

RCA Labs.
Attn: Paul Rappaport
Princeton NJ

RCA Labs.
Attn: D. Richman
Princeton NJ

RCA Labs.
Attn: B. Shelpuk
Princeton NJ

RCA Labs.
Attn: J. Toner
Princeton NJ

RCA Labs.
Attn: B. F. Williams
Princeton NJ

Res. & Dev. System Sics.
Attn: Wayne Maynard
Washington DC

Rockville Refining Co.
Attn: Bernard Free
Gaithersburg MD

Rockwell International
Attn: J. Farrar
Anaheim CA

Rockwell International
Attn: J. M. Kolyer
Anaheim CA

Rockwell International
Attn: Dr. H. M. Manasevit
Anaheim CA

Rockwell International
Attn: N. Mann
Thousand Oaks CA

Rockwell International
Attn: J. Page
Anaheim CA

Rockwell International
Attn: Dr. R. P. Ruth
Anaheim CA

Rockwell International
Attn: J. Yang
Anaheim CA

Ross, Dr. Bernd
San Diego CA

C. T. Sah Associates
Attn: Dr. C. T. Sah
Urbana IL

Sandia Labs.
Attn: J. Banas
Albuquerque NM

Sandia Labs.
Attn: Dr. D. G. Schueler
Albuquerque NM

Santa Barbara Res. Ctr.
Attn: D. D. La Porte
Goleta CA

J. C. Schumacher Co.
Attn: J. C. Schumacher
Oceanside CA

Science Magazine
Attn: Arthur Robinson
Washington DC

Sensor Technology, Inc.
Attn: P. Dennis
Chatsworth CA

Siltec Corporation
Attn: R. E. Lorenzini
Menlo Park CA

Simulation Physics, Inc.
Attn: A. R. Kirpatrick
Burlington MA

Simulation Physics, Inc.
Attn: R. Little
Burlington MA

Simulation Physics, Inc.
Attn: R. Minnucci
Burlington MA

Sensor Technology, Inc.
Attn: I. Rubin
Chatsworth CA

Sensor Technology, Inc.
Attn: K. Van Der Pool
Chatsworth CA

Sensor Technology, Inc.
Attn: I. Wu
Chatsworth CA

SERI
State of New Mexico
Attn: K. M. Fox
Albuquerque NM

Solar Energy Systems, Inc.
Attn: Robert Johnson
Newark DE

Solar Power Corp.
Attn: R. Addiss
North Billerica MA

Solar Power Corp.
Attn: P. Caruso
North Billerica MA

Solar Power Corp.
Attn: W. T. Kurth
North Billerica MA

Solar Tech. International
Attn: J. W. Yerkes
Chatsworth CA

Solarex Corp.
Attn: A. E. Clifford
Rockville MD

Solarex
Attn: Joseph Lindmayer
Rockville MD

Solec International, Inc.
Attn: Ishaq Shahryar
Los Angeles CA

Southern Methodist Univ.
Attn: T. L. Chu
Dallas TX

Spectrolab, Inc.
Attn: J. Albeck
Sylmar CA

Spectrolab, Inc.
Attn: E. L. Ralph
Sylmar CA

Spectrolab, Inc.
Attn: W. Taylor
Sylmar CA

Spectrolab, Inc.
Attn: G. Wrench
Sylmar CA

Springborn Labs. Inc.
Attn: Dr. Bernard Baum
Enfield CT

Springborn Labs. Inc.
Attn: R. White
Enfield CT

Springborn Labs. Inc.
Attn: P. Willis
Enfield CT

Stanford Research Inst.
Attn: Dr. Vijay Kapur
Menlo Park CA

Stanford Research Inst.
Attn: Dr. Leonard Nanis
Menlo Park CA

Stanford Univ.
Attn: J. F. Gibbons
Stanford CA

Stanford Univ.
Attn: Prof. G. Pearson
Stanford CA

State Univ. of New York
Attn: F. F. Y. Wang
Stony Brook NY

Stone & Webster Engr. Corp.
Attn: Reiner Kuhr
Boston MA

Synthatron Corp.
Attn: C. C. Herrman
Edgewater NJ

Technion, Inc.
Attn: G. L. Cann
Irvine CA

Texas Instruments, Inc.
Attn: B. Carbajal
Dallas TX

Texas Instruments, Inc.
Attn: T. Hasty
Dallas TX

Texas Instruments, Inc.
Attn: S. N. Rea
Dallas TX

Texas Instruments, Inc.
Attn: R. Roques
Dallas TX

Texas Instruments, Inc.
Attn: Dr. Gene Wakefield
Dallas TX

TRW Systems Group
Attn: Paul Goldsmith
Redondo Beach CA

TRW Systems Group
Attn: R. Yasui
Redondo Beach CA

US Army
Mobility Equipment
Res. & Dev. Command
Attn: Mr. D. D Faehn
Fort Belvoir VA

U. S. Congress
Off. of Tech. Assessment
Attn: John Furber
Washington DC

U. S. Senate
Attn: Senator Mike Gravel
Washington DC

Union Carbide Corp.
Attn: D. Bailey
Sistersville WV

Union Carbide Corp.
Attn: W. Breneman
Sistersville WV

Union Carbide Corp.
Attn: R. Elbert
Sistersville WV

Union Carbide Corp.
Attn: J. Y. Mui
Sistersville WV

Union Carbide Corp.
Attn: J. Rexor
Sistersville WV

United Detector Tech., Inc.
Attn: P. Wendland
Santa Monica CA

Universal Plastic Mold Co.
Attn: Ronald L. Cruci
Irwindale CA

Univ. of Delaware
Attn: Prof. K. W. Boer
Newark DE

Univ. of Delaware
Attn: J. D. Meakin
Newark DE

Univ. of Michigan
Attn: Raoul Kopelman
Ann Arbor MI

Univ. of New Mexico
Attn: W. W. Grannemann
Albuquerque NM

Univ. of New Mexico
Attn: M. W. Wildin
Albuquerque NM

Univ. of Pennsylvania
Attn: Dr. D. P. Pope
Philadelphia PA

Univ. of Pennsylvania
Attn: Prof. Martin Wolf
Philadelphia PA

Univ. of South Carolina
Attn: J. W. Faust Jr.
Columbia SC

Univ of South Carolina
Attn: R. B. Hilborn, Jr.
Columbia SC

Univ. of South Carolina
Attn: C. Rhodes
Columbia SC

Univ. of Utah
Attn: A. Sosin
Salt Lake City UT

Varian Associates
Attn: M. Hablanian
Lexington MA

Varian Associates
Attn: S. Holden
Lexington MA

Varian Associates
Attn: R. Wolfson
Lexington MA

Welch, Dr. Bruce L.
Woodbridge CT

Westech Systems, Inc.
Attn: G. L. Gill, Jr.
Phoenix AZ

Westinghouse Electric Corp.
Attn: F. G. Arcella
Pittsburgh PA

Westinghouse Electric Corp.
Attn: P. Blaise
Pittsburgh PA

Westinghouse Electric Corp.
Attn: C. Duncan
Pittsburgh PA

Westinghouse Electric Corp.
Attn: Dr. M. Fey
Trafford PA

Westinghouse Electric Corp.
Attn: F. J. Harvey
Pittsburgh PA

Westinghouse Electric Corp.
Attn: R. H. Hopkins
Pittsburgh PA

Westinghouse Electric Corp.
Attn: J. R. Davis
Pittsburgh PA

Westinghouse Electric Corp.
Attn: Dr. R. Mazelsky
Pittsburgh PA

Westinghouse Electric Corp.
Attn: R. Riel
Pittsburgh PA

Westinghouse Electric Corp.
Attn: Dr. R. G. Seidensticker
Pittsburgh PA

The Whittaker Corp.
Attn: Dr. Sol Aisenberg
Waltham MA

Worcester Polytechnic Inst.
Attn: Dr. E. N. Clarke
Worcester MA

Zaromb Research Corp.
Attn: Dr. Solomon Zaromb
Newark NJ

JPL ADDRESSEES

Abrahamson, R. C.
Alper, Dr. M. E.
Anhalt, K. J.
Anspaugh, Dr. B. E.
Arnett, J. C.
Bank, H.
Barlow, R. A.
Baugh, E. R.
Beale, R. J.
Bickler, D. B.
Bishop, W. E.
Briglio, Jr., A.
Cantu, A. H.
Carroll, W. F.
Chamberlain, R. G.
Christensen, E. M.
Cleland, E. L.
Costogue, E. N.
Coulbert, C. D.
Cuddihy, E. F.
Cumming, Dr. G. D.
Davis, C.
Dawson, K. M.
Digges, Jr., T. G.
Divita, E. L.
Doane, J. W.
Downing, R. G.
Dumas, L. N.
Forburger, D. C.
Forney, R. G.
Gallagher, B. D.
Gant, D. T.
Gardner, K. L.
Gates, Dr. C. R.
Goldsmith, J. V.
Gonzalez, C. C.
Greenwood, R. F.
Griffith, J. S.
Grippi, Jr., R. A.
Hagan, M. A.
Harkey, R. L.
Hasbach, W. A.
Headrick, E. L.
Heftman, K.
Henry, Dr. P. K.
Herrera, J. G.
Hogle, R. A.
Holtze, R. F.
Hsu, Dr. G. C.
Jaffe, P.
Josephs, R. H.
Knauss, W. G.
Kocsis, R. W.
Koliwad, Dr. K. M.
Larson, M. N.
Lawson, A. C.
Leipold, Dr. M. H.
LSSA Data Center
Lutwack, Dr. R.
Mallock, I. A.
Maxwell, H. G.
McDonald, R. R.
Mitchell, G. A.
Moacanin, Dr. J.
Moore, D. M.
Patterson, H. E.
Radics, C.
Rose, A.
Ross, Jr., Dr. R. G.
Rowe, W. M.
Salama, A. M.
Salama, Dr. M. A.
Schneider, E. B.
Schurmeier, H. M.
Sears, C. B.
Sequeira, E. A.
Sheldon, E. L.
Simoneau, F. R.
Smokler, M. I.
Sollock, S. G.
Speck, L. P.
Stephenson, Dr. R. R.
Stirn, Dr. R. J.
Stultz, J. W.
Surber, F. T.
Technology Utilization
Tomlin, C. S.
Tseng, Wen
Tsou, Dr. Peter
Turner, Dr. G. B.
Von Roos, Oldwig
Weiner, Howard
Wheelock, H. J.
Wilbur, P. R.
Wilson, J. H.
Wolf, F. N.
Yamakawa, K. A.
Zoutendyk, J. A.

# SECTION I

# INTRODUCTION AND PROJECT OVERVIEW

## A. INTRODUCTION

The potential for future widespread use of photovoltaic systems for the generation of electric power was the motivation for the establishment, in January 1975, of the Photovoltaic Conversion Program by ERDA's Division of Solar Energy. The Program's activities are planned to develop and to promote the use of photovoltaic systems to such an extent that the private sector will produce and utilize cost-competitive photovoltaic systems. As part of the ERDA Program, the Low-Cost Silicon Solar Array Project (LSSA) was established in January 1975.

This report describes the activities and progress of the LSSA Project during the months of October, November, and December 1976.

The Project objective is to develop the national capability to produce low-cost, long-life photovoltaic arrays at a rate greater than 500 megawatts per year and a price of less than $500* per kilowatt peak by 1986. The array performance goals include an efficiency greater than 10% and an operating lifetime in excess of 20 years.

The approach is to reduce the cost of solar cell arrays by improving solar array manufacturing technology and by increasing solar array production capacity and quantity. Forty-seven contracts have been awarded to date, to industrial firms and university and independent laboratories for experimental work, process development and analysis, technology assessment, and the production of solar-array modules. Approximately 58 kW of state-of-the-art modules have been delivered; design development is under way for a second block of moderately advanced modules, and planning for subsequent module procurements has begun.

Efforts of the LSSA Project are organized into an Analysis and Integration Task, four Technology Development Tasks - covering the areas of Silicon Material, Large Area Silicon Sheet, Encapsulation, and Automated Array Assembly - and a Large Scale Procurement Task, an Engineering Task, and an Operations Task.

## B. PROJECT OVERVIEW

With the period of October, November, and December 1976 the LSSA Project completed the second calendar year since its inception. The first year had been occupied principally with planning and the solicitation, negotiation, and execution (extending into CY 76) of contract efforts for technology development and module production by industry.

---

*In 1975 dollars.

The second year, ending with the quarter reported here, saw the major part of performance under these contracts and the corresponding planned in-house work through the first phase of activity.

During this quarter, the focus of Project activity emerged in the area of economic analysis. The Fourth Project Integration Meeting, held in October, applied this perspective to the fabrication and assembly processes in discussions based on work-in-process presentations by the three technology-assessment contractors of the Array Assembly Task. Another session of the meeting discussed economic analyses of various crystal growth and ingot/slicing approaches. With these and related assessments as points of departure, the various Technology Development Task teams iterated their views and conclusions through the quarter, and further discussions were held at the next Integration Meeting in January. Interaction between these analytical efforts on the one hand, and the module-production elements of the Project (notably Large-Scale Production contractors) on the other, was vigorous and helped to move these discussions forward.

At the same time, the Analysis and Integration team carried forward their work in developing a costing methodology, the industry simulation, the revised allocation of cost goals, and economic models of the industry. This task also performed various planning tasks in support of the Program Office, and strengthened its support of the Program Planning Group, an ad hoc body formed to develop a national PV program plan.

Deliveries for the initial block procurement of solar-array modules (nominal total 46 kW) were completed in October, and a required extension to this block had been initiated; deliveries on this extension proceeded through the quarter, to be completed in January. Contracts for the second block procurement (nominally 130 kW) had previously been executed, and prototype work and design reviews were carried out during this quarter, with production scheduled to start early in 1977.

# SECTION II

# SUMMARY

## A. PROJECT ANALYSIS AND INTEGRATION

During this quarter, the Planning and Integration Subtask continued to write a National Photovoltaic Energy Conversion Plan for ERDA Headquarters, and continued its effort to improve internal Project communications. The Array Technology Cost Analysis Subtask made progress in uniform costing methodology (SAMICS), industry simulation (SAMIS), and price goal allocations. The Economics and Industrialization Subtask continued its involvement in life-cycle cost of energy systems and industry modeling and program planning, and issued a report of its analysis of capital requirements implied by Program quantity goals.

## B. SILICON MATERIAL TASK

Installation of Union Carbide's miniplant was completed at the end of the quarter, with operation to begin after safety approval. The Battelle contract was extended, and will produce designs for a $ZnCl_2$ condensation system and for a 25-metric-ton fluidized bed reactor. The Westinghouse contract to study the effects of impurities was being negotiated for an 18-month extension. The Texas Instruments contract was limited to a study of the reduction of $SiO_2$ by C, while the Dow Corning effort on the purification of Si by vacuum evaporation was deleted. Results from Lamar University concerning vapor pressure data for $SiH_4$ as a function of temperature will be used in analyzing Union Carbide's process; formulations of a process flow diagram and material balance for the process also began during the quarter.

## C. LARGE AREA SILICON SHEET TASK

Routine growth of EFG ribbons 50 mm wide at 50 mm/min was achieved during the quarter, and other processes were able to routinely grow somewhat smaller ribbons. Great difficulty has been experienced using the inverted Stepanov process, and alternative inverted Stepanov techniques are being considered. The use of an aluminum pedestal and improved heat shielding has yielded greater control of the dendritic web process. A final forming limit diagram plotted for the hot rolling process showed that deformation of silicon is quite possible. Data on dip-coated cells indicated a corrected conversion efficiency of about 6%. A fused silica coating was developed that prevented cracking of the quartz crucible for a 1-1/2 inch diameter ingot. JPL completed the economic modeling of Czochralski growth. Studies on ingot growth during this quarter showed that it has excellent potential for providing low-cost silicon of acceptable quality.

## D. ENCAPSULATION TASK

A literature search completed this quarter shows that worldwide experience with accelerated/abbreviated lifetime test methods yields little useful understanding. Data are now being correlated and interpreted from studies of accelerated/abbreviated test methods, performed by a contractor using recently-developed universal test specimens. Progress this quarter on electrostatically bonded integral glass covers shows them to be quite promising. Work continues to develop a better understanding of polymeric properties and aging. Development of an in-house JPL test module, and failure analysis of modules from Blocks 1 and 2 were temporarily suspended due to a manpower shortage.

## E. AUTOMATED ARRAY ASSEMBLY TASK

Contractors presented a number of different manufacturing sequences during this quarter. Evaluation has led to recommendations for modification or more detailed development. A process cost analysis chart was prepared by task personnel from contractor data. Three contracts were recommended for extension so that process tolerances vs. cost ratios can be established. Detailed process technique studies continued. Contractors submitted three different encapsulation designs.

## F. ENGINEERING TASK

During this quarter, work by the Engineering Task was focused on the development of requirements for future large-scale procurements. The most important accomplishment in this regard was the development of a nominal terrestrial environment and a nominal cell operating temperature. These will allow uniform measurements of module performance characteristics in test situations that will accurately reflect the performance of those modules under field conditions. An improved definition of module power output was also created. The procedure developed from this, involving average power output at reference voltage, was found to be accurate to better than 1%. Work was begun in several other areas that will underly future designing and requirements.

## G. OPERATIONS TASK

Qualification testing of late-production Block 1 modules was completed this quarter. Modules from a manufacturer not previously involved with the Project were also tested. Environmental testing of the Block 1 "add-on" modules was begun. Humidity/freezing tests were completed for all but one type of Block 1 module. A wind load simulation apparatus was fabricated. Field installation of 30 more modules at Goldstone and Table Mountain was accomplished. Of 26 problem/failure reports generated, 25 were analyzed during the quarter. The JPL failure laboratory developed a nondestructive method for testing for module open circuits. Interlab (JPL/LeRC) measurement comparisons were performed with large- and small-area pulsed solar simulators; agreement was typically within 1%.

## H. LARGE SCALE PRODUCTION TASK

The Block 1 procurement, including the 15 kW "add-on", was completed during this quarter. Conclusions from experiences in this procurement include: (1) silicone pottant is very expensive and difficult in encapsulation; and (2) manufacturers say fabrication labor costs may be reduced through design of larger modules. Preliminary design reviews for the Block 2 buy were completed. Modules began arriving at JPL in December. Block 2 encountered delays because of (1) design changes arising from design reviews, (2) the inability of contractors to obtain materials in a timely manner, and (3) changes in JPL specifications directed toward improving modules' design or performance capability.

# SECTION III

# PROJECT ANALYSIS AND INTEGRATION TASK

The Project Analysis and Integration (PA&I) Task supports the planning, integration, and decision-making activities of the Project. To provide this support, the PA&I Task is organized into three highly interrelated functional areas: planning and integration; array technology cost analysis; and economics and industrialization. Most of the PA&I activities are backed up by analytical tools developed for those activities.

## A. PLANNING AND INTEGRATION SUBTASK

During the quarter, the Planning and Integration Subtask focused on internal LSSA Project planning activities, e.g., the Project Implementation Plan and Annual Operating Plan revisions. In addition, at the request of ERDA Headquarters, support was given to several planning tasks. The Program Planning Group* continued work on writing a National Photovoltaic Energy Conversion Plan.

Integration efforts to improve internal LSSA technical task communications continued. These included supporting the quarterly Project Integration Meeting and various other technical task meetings, some of which involved non-Project personnel.

## B. ARRAY TECHNOLOGY COST ANALYSIS SUBTASK

Progress under the Array Technology Cost Analysis Subtask was made in three related areas:

(1) Uniform Costing Methodology. Development of the Solar Array Manufacturing Industry Costing Standards (SAMICS) continued during the quarter. The methodology was described at the Photovoltaic Specialists' Conference in November 1977. The need for a worksheet to clarify the calculation procedure was identified, and its preparation was begun. It soon became clear that the "worksheet" should be a "workbook" to facilitate explanation of the steps to be performed. Preparation of the SAMICS Workbook was accompanied by further development of detailed submodels within that methodology. The workbook is now about 75% complete.

---

*ERDA Headquarters established a Program Planning Group consisting of representatives from all the Photovoltaic Program elements, including JPL. The purpose of the group is to write the National Photovoltaic Energy Conversion Plan.

The kind of firm that would be a suitable support contractor to assist in the development of standardized data has been identified, and initial efforts to obtain such a contractor have been made. The JPL Facilities Engineering and Construction Section is helping in the selection process.

(2) Industry Simulation. The Solar Array Manufacturing Industry Simulation (SAMIS) activity also continued during the quarter. The methodology is identical with, but slightly more general than, that of SAMICS. The SAMIS/SAMICS methodology is well understood. The SAMIS III computer program design team is in existence, as is the design document. Program design, based on the SAMICS Workbook, is under way.

(3) Price Goal Allocations. The allocation of manufacturing price goals for each of the technology development tasks at two-year intervals throughout the life of the Project was reviewed and updated. Updated price goal allocations were presented at the October Project Integration Meeting; further updates are being prepared for the January Project Integration Meeting.

## C. ECONOMICS AND INDUSTRIALIZATION SUBTASK

The Economics and Industrialization Subtask made progress in three related areas:

(1) Life-Cycle Cost of Energy Systems. Attention in this area centered on the development and testing of small, exportable computer programs for the analysis of energy systems, with particular emphasis on break-even analysis and the effects of incentives. The USES methodology, which forms the conceptual basis of this effort, was described at the Photovoltaic Specialists' Conference in November 1977.

The file of correspondence on the USES methodology has grown quite large, and considerable user interest has been expressed in broadening its scope. A companion document to USES, describing and demonstrating computerized capabilities based on USES, is being designed.

(2) Price/Quantity Relationships. An analysis was conducted of the capital requirements implied in the Program's quantity goals for 1986 and 2000. The analysis utilized currently available process information from the manufacturing process contracts being performed under the Automated Array Assembly Task. A PA&I report was issued describing methodology and results of this analysis.

An effort is under way to calibrate the capital requirements analysis against the SAMIS modeling effort. A critical need remains for rapid and accurate access to technical informa-

tion on changes in process equipment and/or parameters. This need is shared with the SAMIS effort.

(3) Industry Modeling and Program Planning. The Economics and Industrialization Subtask continued its heavy involvement in program planning activities based on economic models of the growth of an energy industry using new technology. The major activity in the quarter involved interfacing with the staff of the MIT Lincoln Laboratory, newly added to the Program, to determine roles and missions for an effective division of analytical effort.

The industry modeling and program planning effort is being considerably strengthened, and is expected to become the major emphasis of the Task. Another economist has been hired to assist in industry modeling, and will start in January. The developing interface with economists at MIT is considered a high priority, as is the definition of a production analytical interface to support the Program Planning Group economics effort. The Planning Group has resumed meetings, and a plan is under way to produce a complete National Photovoltaic Conversion Program by July 1977.

# SECTION IV

# SILICON MATERIAL TASK

The objective of the Silicon Material Task is to establish by 1986, an installed plant capability for producing silicon suitable for solar cells at a rate equivalent to 500 megawatts (peak) of solar arrays per year at a price of less than $10 per kilogram. The program formulated to achieve this objective is based on the conclusion that the price goal can not be reached if the process used is essentially the same as the present commercial process for producing semiconductor-grade silicon. Consequently, it is necessary that either a different process be developed for producing semiconductor-grade silicon or a less pure and less costly silicon material (i.e., a solar-cell-grade silicon) be shown to be utilizable.

## A. TECHNICAL BACKGROUND

Solar cells are presently fabricated from semiconductor-grade silicon, which has a market price of about $65 per kilogram. A drastic reduction in price of material is necessary to meet the economic objectives of the LSSA Project. One means for meeting this requirement is to devise a process for producing a silicon material which is significantly less pure than semiconductor-grade silicon; the price goal for this material is less than $10 per kilogram. However, the allowance for the cost of silicon material in the overall economics of the solar arrays for LSSA is dependent on optimization trade-offs, which concomitantly treat the effects of the price of silicon material and the effects of material properties on the performance of solar cells. Accordingly, the program of the Silicon Material Task is structured to provide information for the optimization trade-offs concurrently with the development of high volume and low cost processes for producing different impurity-grades of silicon.

## B. ORGANIZATION AND COORDINATION OF THE SILICON MATERIAL TASK EFFORT

The Silicon Material Task effort is organized into five phases. As Table 4-1 indicates, Phase I is divided into four parts. In Part I the technical feasibility and practicality of processes for producing semiconductor-grade silicon will be demonstrated. In Part II the effects of impurities and of various processing procedures on the properties of of single-crystal silicon material and the performance characteristics of solar cells will be investigated. This body of information will serve as a guide in developing processes (in Part III) for the production of solar-cell-grade silicon. The process developments in Parts I and III will be accomplished through chemical reaction, chemical engineering, energy-use, and economic studies. In Part IV of Phase I, the relative commercial potentials of the various silicon-production processes developed under Parts I and III will be evaluated. Thus, at the end of Phase I a body of information will have been obtained for optimization trade-off studies and the most promising processes will have been selected.

Table 4-1. Organization of the Silicon Material Task Effort

| Phase/Part | Objective |
|---|---|
| Phase I | Demonstrate the technical feasibility and practicality of processes for producing silicon. |
| Part I | Establish the practicality of a process capable of high volume production of semiconductor-grade silicon at a markedly reduced cost. |
| Part II | Investigate the effects of impurities and of various processing procedures on the properties of single-crystal silicon material and the performance characteristics of solar cells. |
| Part III | Establish the practicality of a process capable of high volume production of solar-cell-grade silicon at a price of less than $10 per kilogram. |
| Part IV | Evaluate the relative commercial potential of the silicon-production processes developed under Phase I. |
| Phase II | Obtain process scale-up information. |
| Phase III | Conduct experimental plant operations to obtain technical and economic evidence of large-scale production potential. |
| Phase IV | Design, install, and operate a full-scale commercial plant capable of meeting the production objective. |

Phase II will be initiated to obtain scale-up information. This will be derived from experiments and analyses involving mass and energy balances, process flows, kinetics, mass transfer, temperature and pressure effects, and operating controls. The basic approach will be to provide fundamental scientific and engineering information from which valid extrapolations usable for plant design can be made; applicable scale-up correlations will also be used. This body of scale-up information will then provide the necessary basis for the design, construction, and operation of a large-scale production plant.

Since the installation and operation of a commercial chemical process plant that incorporates a new process involves high risks,

experimental plants will be used to obtain technical and economic evidence of large-scale production potential. In the experimental plant phase (i.e., Phase III) there will be opportunities to correct design errors; to determine energy consumption; to establish practical operating procedures and production conditions; and to more realistically evaluate the requirements for instrumentation, controls, and on-line analyses.

In the final phase of the Silicon Material Task (i.e., Phase IV), a full-scale commercial plant capable of meeting the production objective will be designed, installed, and operated. The experimental plant and the commercial plant will be operated concurrently so as to permit the use of the experimental plant for investigations of plant operations, i.e., for problem solving and for studies of process optimization.

Additional basic chemical and engineering investigations to respond to problem-solving needs of the Silicon Material Task will be conducted in supporting efforts. These supporting subtasks will be accomplished under contract and by an in-house JPL program.

## C. SILICON MATERIAL TASK CONTRACTS

Eleven contracts are in progress: three for Part I, two for Part II, five for Part III, and one for Part IV. These contracts were negotiated after careful evaluations of responses to a Request for Proposal (RFP) and of unsolicited proposals. The contracts are listed in Table 4-2. Additional contractors for subsequent phases will be selected from unsolicited proposals and from future RFPs.

Two contractors (Monsanto, in Part II, and Texas Instruments, in Part III) have completed their technical programs and are processing final reports.

Table 4-2. Silicon Material Task Contractors

| Contractor | Technology Area |
|---|---|
| **SEMICONDUCTOR-GRADE PRODUCTION PROCESSES (Part I of Phase I)** | |
| Battelle Memorial Institute, Columbus, Ohio (JPL Contract No. 954339) | Si from $SiCl_4$ reduction by Zn |
| Union Carbide, Sistersville, W. Virginia (JPL Contract No. 954334) | Si from $SiH_4$ derived by redistribution process |
| Motorola, Phoenix, Arizona (JPL Contract No. 954442) | Si using $SiF_4$ reaction with metallurgical grade Si and $SiF_2$ transfer |
| **SOLAR-CELL-GRADE SPECIFICATIONS (Part II of Phase I)** | |
| Westinghouse Electric, Pittsburgh, Pennsylvania (JPL Contract No. 954331) | Investigation of effects of impurities on solar cell performance |
| Monsanto Research, St. Louis, Missouri (JPL Contract No. 954338) | Investigation of effects of impurities on solar cell performance |
| **SOLAR-CELL-GRADE PRODUCTION PROCESSES (Part III of Phase I)** | |
| Dow Corning, Hemlock, Michigan (JPL Contract No. 954559) | Si from purer source materials using arc furnace processing |
| Stanford Research Institute Menlo Park, California (JPL Contract No. 954471) | Si by Na reduction of $SiF_4$ |
| Westinghouse Electric Pittsburgh, Pennsylvania (JPL Contract No. 954589) | Si by plasma-arc-heater reduction of $SiCl_4$ with $H_2$ and alkali metals as reducing agents |

Table 4-2. Silicon Material Task Contractors
(Continuation 1)

| Contractor | Technology Area |
|---|---|
| AeroChem Research Laboratories, Princeton, New Jersey (JPL Contract No. 954560) | Si by use of a nonequilibrium plasma jet |
| Texas Instruments, Dallas, Texas (JPL Contract No. 954412) | Si from C reduction of $SiO_2$ using plasma processing |
| COMMERCIAL POTENTIAL OF PROCESSES (Part IV of Phase I) | |
| Lamar University, Beaumont, Texas (JPL Contract No. 954343) | Evaluate relative commercial potentials of Si-production processes developed under the Silicon Material Task |

D. SILICON MATERIAL TASK TECHNICAL ACTIVITY

The objectives of Phase I of the Silicon Material Task are as follows:

- Part I - Establish the practicality of a process capable of the high volume production of semiconductor-grade silicon at a markedly reduced cost.
- Part II - Investigate the effects of impurities and process-steps on the properties of single-crystal silicon material and the performance characteristics of solar cells.
- Part III - Establish the practicality of a process capable of the high volume production of solar-cell-grade silicon at a price of less than $10 per kilogram.
- Part IV - Evaluate the relative commercial practicality of the silicon-production processes developed under Phase I of the Silicon Material Task.

1. Processes for Producing Semiconductor-Grade Silicon

The approach for Part I incorporates theoretical studies involving thermodynamics, reaction chemistry, and chemical engineering; chemical

reaction investigations consisting of the experimental determinations of reaction kinetics yields, and suitable process conditions; a chemical engineering effort for securing an experimental data base for preliminary process modeling; and energy-use and economic calculations for preliminary process models. In each case the contract requires a demonstration of technical feasibility and a projection of commercial practicality, involving the preliminary analysis of suitability for a scale-up study. The processes for the Phase II scale-up studies will be selected over a period of time, the decision point for each process-development being dependent upon the maturity of that process. The scale-up studies for the most mature processes will begin in early FY 1977.

a. Semiconductor-Grade Si Production by Zn Reduction of $SiCl_4$ - Battelle Memorial Institute. The contract with Battelle Memorial Institute is for the development of the reaction for the Zn reduction of $SiCl_4$ using a fluidized bed reactor as an economical means for producing Si. Calculations based on a well-developed flow diagram have indicated a total product cost between $9.12 and $9.60/kg for a 1000 metric tons/year plant and an energy consumption equivalent to a 2.2 month payback period.

A miniplant was operated to obtain parametric data. Si was deposited in dense coating on seed particles at rates of about 130 g/hr and with a net efficiency of about 73%, taking into account inadvertent blow-over caused by the peculiar operation of the reactor. Examination of the $Zn/ZnCl_2$ condenser revealed clean surfaces, indicating no interference with heat transfer. Thus, the earlier problem of depositions of Si in this unit has been solved by the changes in positioning the unit. A multiple-inlet design was shown to operate with greater mass-flow capacity short of slugging. This design will be refined to insure reactant mixing within the bed rather than at the inlet orifices.

In addition, a preliminary flow diagram for a 25 metric tons/year experimental production facility was drawn; features of process outlines from Battelle and Lamar were used; the process concept will be refined using the data from the miniplant.

b. Production of $SiH_4$ by Redistribution of Chlorinated Silanes - Union Carbide Corporation. The Union Carbide contract is for the development of processes for the production of $SiH_4$ and for the deposition of Si from $SiH_4$. The $SiH_4$ process includes systems for the redistribution of chlorohydrosilanes and the hydrogenation of $SiCl_4$. Techniques incorporating a free space reactor or a fluidized bed reactor are being investigated as the means for Si deposition.

The redistributions of chlorohydrosilanes are described by the following equations:

$$2\ SiHCl_3 = SiH_2Cl_2 + SiCl_4$$

$$3\ SiH_2Cl_2 = 2\ SiHCl_3 + SiH_4,$$

the overall reaction being

$$4\ SiHCL_3 = SiH_4 + 3\ SiCl_4.$$

The general characteristics of the reactions have been studied using $SiH_2Cl_2$ as the feedstock. A recent concern was the potential for a decreased catalyst activity with extensive operation. In a series of runs it was shown that the activity decrease of about 5.5%, which occurred in the first 9 hours of use, was due to the evaporative loss of physically absorbed active tertiary amines, and that the remaining chemically bonded active tertiary amines yielded essentially constant productivity of 70% of the original over extended operations; and that there was no evidence of activity loss due to surface poisoning. Calculations based on the experimental data, which are not for optimized conditions, led to the description of a resin bed 2 feet in diameter and 15 feet tall capable of producing 222 kg of $SiH_4$ per hour; this production rate is roughly equivalent to 1000 metric tons per year at 60% efficiency.

A study of the effects of extended reaction times on the reactivity of the Cu/Si contact mass for the fluidized bed reaction for the hydrogenation of $SiCl_4$ ($3\ SiCl_4 + 2\ H_2 + Si \overset{Cu}{=} 4\ SiHCl_3$) was conducted for a total of 40 hours. The conversion yield was about 14% per pass and remained nearly constant for several runs, indicating the maintenance of catalytic activity under a $H_2/SiCl_4$ atmosphere during shutdowns. A good agreement of 91% was obtained for a comparison of the reaction stoichiometry and a mass balance calculated from experimental data.

The reaction for the direct synthesis of $SiH_2Cl_2$ in a fluidized bed reactor using a Cu/Si mass was investigated in a series of experiments. The reactor temperatures were low ($< 270^{o}C$), to avoid hot spots which might result from the highly exothermic reaction; in addition, the decomposition of the $SiH_2Cl_2$ product would be low at these temperatures. Discouragingly low yields of 1 to 1.5% of $SiH_2Cl_2$ were obtained; the concentration of heavies increased markedly under these conditions. Thus, there is strong evidence against continuing to develop this reaction for use in the overall process.

The construction and initial checkout of the miniplant, which is to be used for the studies of steady-state operation of the overall process using $SiH_2Cl_2$ as the feed material, was completed. A critique of the installation, operating procedures, and safety considerations was made by a Union Carbide Pre-Startup Safety Review Team. The team has approved the corrective actions for problem areas, including a flameless method for venting $SiH_4$.

A computer program was written to aid in data reduction and in the analysis of unit operation. Data will be converted to a standard base, and overall material balances, as well as component material balances around the main distillation column, will be calculated.

c. Semiconductor-Grade Si Production by $SiF_4/SiF_2$ Transport - Motorola Corporation. The Motorola contract is for the development of a process for the conversion of metallurgical-grade Si into semiconductor-grade Si using three $SiF_2$ transport purification reaction steps. The effort for this quarter involved five areas: equipment modifications, kinetic experiments, thermal decompositions of polymers, Si product analyses, and an economic assessment of the overall process.

Investigations of modifications of apparatus to prevent contamination of the Si product progressed. The feasibility of a high vacuum seal between conical quartz and Mullite flanges using a Teflon sealant was shown, but the adaptability for scale-up apparatus is yet to be demonstrated. The construction costs were estimated to be within the costs of other typical chemical processing equipment.

Experiments were conducted to determine the temperature and other conditions at which the $SiF_2$ polymer decomposes and to evaluate the products of the reaction; Si, $SiF_4$, and higher homologues of $SiF_2$ were expected to result from the thermal decomposition. The decomposition was found to occur in stages at three temperature ranges, 100 to 200°C, about 350°C, and 800 to 900°C. Although only $SiF_4$ was observed at 350°C, the products at the other temperatures have not been defined. There was no evidence that the rapid decomposition of the polymer would cause an explosion.

A Figure of Merit, defined as

$$FM = \log \frac{\text{concentration in metallic grade Si}}{\text{concentration in product Si}}$$

was used to evaluate purity. The calculated values ultimately depend entirely on measured values. There is concern about the reliability of the data from a commercial laboratory. An economic analysis was performed to estimate the total product cost and the capital expenditure for a 2000 metric tons per year plant. The major assumptions were (1) the product Si is 85% of the input Si; (2) input $SiF_4$ is generated from HF and metallurgical grade Si; and (3) 80% of the waste fluorides are reconverted to $SiF_4$. The estimate, based on the use of January 1975 dollars, is as follows:

| | |
|---|---|
| Installed Equipment | $10,300,000 |
| Fixed Capital | 31,750,000 |
| Working Capital | 3,850,000 |
| Total Capital | $36,600,000 |
| Materials | $1.30/kg Si |
| Direct Expenses | 2.80/kg Si |
| Indirect Expenses | 2.33/kg Si |
| Total Manufacturing Cost | $6.43/kg Si |
| Administration and Selling Expenses | 0.57/kg Si |
| Total Product Cost | $7.00/kg Si |

2. Determination of the Effects of Impurities and Process-Step on Properties of Silicon and the Performance of Solar Cells - Westinghouse Electric Corporation

The Phase I approach for Part II involves setting up a matrix of impurities and concentrations; preparing crystals, using techniques for Czochralski, float zone, and dendritic-web crystals, which contain the baseline dopant B and selected concentrations of specific elements; performing a series of chemical, microstructural, and electrical tests; and analyzing the data for the purpose of correlating the impurities and concentrations with material properties and solar cell performance. The conclusions from the Phase I investigations will form a preliminary description upon which the more comprehensive, detailed plan for Phase II will be structured.

Phase I of the contractual effort by Westinghouse to determine the effects of impurities on the performance of solar cells has been completed. In this phase 52 Czochralski ingots and 44 dendritic web specimens were prepared. The inpurities incorporated in these were Cr, Cu, Fe, Mn, Ni, Ti, V, Zr, Zn, Mg and Al; these are the elements usually found in metallurgical grade Si, a raw material for most of the polycrystal Si process developments. The concentrations were measured using Spark Source Mass Spectroscopy and Neutron Activation Analysis methods, with the values ranging between 0.6 and 200 ppba and the measurement sensitivity being dependent upon the specific element as well as the method of measurement. Estimates of the composition below this concentration range were calculated using segregation coefficients. The concentrations of unintentionally added impurities in the base material were determined to be below 0.02 to 0.2 ppba, the level of detection by NAA.

Based upon the concept that the minority carrier recombination lifetime could be used to assess the suitability of metal doped ingots for the fabrication of solar cells having satisfactory performance, a concerted effort was made to determine the relationship and applicability of lifetime measurements to cell characteristics. The development of a theoretical model for relating $I_{sc}$ and $\tau_r$ was performed to describe the experimental data and to provide the capability for extrapolating values beyond the range of unreliable experimental data. A reasonable correlation between $I_{sc}$ and $\tau_r$ was found for diffused material whereas no such correlation was obtained when $\tau_r$ was measured before diffusion. This observation means that the lifetime of the Si in a fabricated solar cell cannot be predicted by measurements of the lifetime of the as-grown ingot owing to the dominance of processing effects. Consequently, correlations with $I_{sc}$ for finished cells can only be made under controlled conditions of calibrated processing steps from the ingot through the completed cell.

A preliminary model was developed for lifetimes of multiply doped materials using the assumption of independent recombination centers, i.e., that there are no interactions between impurity atoms which affect energy levels, capture cross-sections, or recombination rates. This model was derived after the conclusion that although upper limits in the concentrations of single impurities could be obtained, the large number of permutations of concentrations and impurities for multiply doped materials made the extrapolations in these cases impractical if not impossible. The model was evaluated by comparing the calculated and measured lifetimes for several multiply doped ingots. A reasonable agreement of values was obtained except in a few cases; additional data will be secured to examine the deviations and to increase confidence in the correlations.

The effects of impurities on solar cells were determined from measurements using wafers comprised of 1 $cm^2$ solar cells, 6 van der Pauw (for measuring diffused layer sheet resistance), 6 small test diodes, 4 small cells (0.0576 $cm^2$), and a test pattern for measuring specific contact resistance. Based on data from more than 60 experimental runs, baseline cell (without AR coatings) efficiencies averaged $10.26 \pm 0.24\%$ and yields were between 80 and 90%. The application of SiO AR coatings resulted in an average increase of 36% in $I_{sc}$ and in cell efficiencies between 13 and 14%.

The I-V data for the cells were analyzed using a double expotential model to describe the cell. The conclusions were that (1) the shunt resistance term is negligible except where processing faults occur; (2) the saturation current and the n-factors increase, as expected, with the addition of impurities but the changes are not sensibly correlatable with concentrations or with other cell parameters, and (3) the most effective parameters for the characterization of the effects of impurities are $I_{sc}$, $V_{oc}$, peak power, and efficiency.

The reduction of the cell conversion efficiency was shown to be measurable by the decrease in the minority lifetime values. The functional relationship between $I_{sc}$ and the effective cell lifetime was obtained by solving the carrier transport equations using appropriate

boundary conditions and material and spectral parameters. The plot of relative $I_{SC}$ as a function of corrected (open circuit voltage decay) lifetime showed that the data are described quite well by the derived equation.

The mathematical model was continued to describe the dependence of $I_{SC}$ in multiply doped cells. The calculated values of $I_{SC}$ were in fairly good agreement with the measured values, despite the uncertainties of some of the concentrations. The equation contains constants which are very sensitive to the effects of cell processing; the dependence of the model predictions on a well-controlled process was emphasized.

The mathematical treatment was extended to derive a relationship between the normalized $V_{OC}$ and $I_{SC}$ for doped cells. The functional relationship was in good agreement with the data. However, an inconsistency, which arose between the measured open circuit voltage decay lifetime and the implied lifetime deduced from $V_{OC}$ data, may indicate a limitation of the model used.

Some preliminary conclusions were derived from experiments to determine the effects of cell processing using impurity doped material on cell performance. High temperature P-gettering at 1200°C was found to reduce the lifetimes of baseline and Mn-containing cells but to improve the lifetimes of cells containing Ti or V. Sustantial improvement in the lifetimes of all of the impurity doped cells were obtained for damage-gettering using 60-μm grit as the lapping agent. The salient conclusion from this work is that further systematic studies of the effects of cell processing steps on cell performance need to be done and that the processing of cells must be defined and well controlled to assure uniform cells.

A first step was taken in the evaluation of the impact of impurities on overall economics, involving aspects of crystal growth technique, cell fabrication processes, and cell performance criteria. Two interactions arising in crystal growth were considered: the relationship between crystal growth feedstock and solar cell performance and the effect of feedstock impurity on the yield of the crystal growth process. The analysis was applied to the Czochralski ingot growth and the paramount parameter was the effective distribution coefficient for each impurity. The conditions of normal freeze without replenishment of the melt, sequential melt replenishment, and continuous melt replenishment were used. Equations were derived for each case and then modified for the further condition of very small distribution coefficients. Families of curves can be constructed relating impurity concentration increases in the melt or crystal as functions of volumes of crystal grown by the sequential or continuous melt replenishment procedures. The compositions of the Czochralski crystal ingot were shown to be strongly dependent on the method of melt replenishment. Different dependencies would, in general, be obtained for crystal growth processes in which other physical considerations governed the impurity distributions. Thus, the economic analysis is a function of the conditions for a particular process, the feedstock composition, and the strategy for melt replenishment.

The calculations for the compositions of crystal ingots were then coupled with the data for the effects of various impurities on cell performance to derive maximum tolerable specific element concentrations in the melt for the production of solar cells, which are 90% as efficient as baseline cells. Obviously, the calculated values depend on the choices of the crystal growth process, the melt replenishment, and the acceptable cell efficiency.

A further consideration was the derivation of an equation describing the dependence of the critical impurity concentration in the melt (the limiting concentration for maintaining single crystal growth) on the rate of growth for Czochralski ingots. The critical impurity concentration for crystal breakdown was shown to vary inversely with the growth rate at low rates and to decrease rapidly as the maximum rate is approached. A reasonable agreement was obtained between experimental data for breakdown concentrations and values calculated from the equation. The conclusions were (1) that the critical impurity concentrations are strongly dependent on growth rate but rather insensitive to the crystal radius magnitude; (2) that, since it appears from this emphasis that total impurity concentrations over $10^{19}$ atoms/cc can be tolerated for steady-state Czochralski growth, concentration limits will be determined by the degrees of the effects of impurities on cell performance (it has been shown that cells with efficiencies 90% of baseline can be fabricated from Czochralski ingots, which are prepared from feedstock material containing $10^{18}$ to $10^{19}$ atoms/cc of most impurities but not greater than about $6 \times 10^{17}$ atoms/cc for Ti or V); and (3) that the costs of discarding feedstock material rendered unusable by the buildup of impurity concentrations are important factors in defining tolerable feedstock compositions.

## 3. Processes for Producing Solar-Cell-Grade Silicon

The approach used for Part III of Phase I (see Table 4-1) incorporates theoretical studies involving thermodynamics, reaction chemistry, and chemical engineering; chemical reaction investigations consisting of experimental determinations of reaction kinetics, yields, and suitable process conditions; a chemical engineering effort for securing an experimental data base for preliminary process modeling; and energy-use and economic calculations for preliminary process models. In each case the contract requires a demonstration of technical feasibility and a projection of commercial practicality, involving the preliminary analysis of the suitability for a scale-up study. Each process candidate will be evaluated on a separate milestone schedule. Selections for the next phase of scale-up studies will be made at times which are appropriate for individual or collective assessments.

a. Solar-Cell-Grade Si Production Using Submerged Arc Furnace, Vacuum Evaporation, and Unidirectional Solidification Processes - Dow Corning Corporation. The contract at Dow Corning involves improving metallurgical grade Si, the use of purer raw materials, and the further purification of Si by unidirectional solidification to yield solar-cell-grade Si. In this quarter there was progress in efforts for raw

materials, identification and selection, arc furnace studies, vacuum evaporation studies, unidirectional solidification studies, Si analyses, and in energy analysis.

Sources for high purity raw materials were identified in surveys of resources in the U.S. and worldwide. Large differences in the concentrations of the elements were found in comparisons of quartz and carbon supplies for the commercial process with experimental raw materials. The C-reductant can be charcoal, which can be purified by various processes to different levels of purity. The graphite electrodes can be similarly purified. Quartz with significantly lower concentrations of B and P was found to be available within the U.S.

The experimental electric arc furnace is 40 kW; it was modified to decrease the likelihood of contamination from materials of construction. Three experiments were run to show the feasibility of using charcoal and to determine an impurity balance. The energy use in these cases was about 60 to 85% greater (30 kWh/kg Si versus 13 kWh/kg Si) than for smelting quartzite with the usual reductants of coal, coke, and wood chips. Reduction by charcoal was successful. Some decreases in impurity content were found, although no marked improvements were made. Charcoal is believed to be the source for B, Ca, and P contamination in these runs.

Experiments for the purification of metallurgical grade Si by vacuum evaporation gave no evidence of measurable success. No further work will be done in this area.

Semiconductor-grade polycrystalline Si backdoped with impurities is being used to simulate the type of material which would be subjected to purification by unidirectional freezing. This choice followed the conclusions derived from the work under the contract with Westinghouse (with Dow Corning as a subcontractor) for the determination of the effects of impurities on the properties of Si materials and solar cells. In that contract the maximum melt impurity concentrations at breakdown of growth interface due to constitutional supercooling were derived for a series of elements. The loss of crystal structure occurred in the concentration range of 0.31 to 0.73 percent atomic. The conclusion was that the relatively high impurity concentrations in metallurgical grade Si severely limit the conditions, and therefore the information, which could be obtained by a study of unidirectional freezing of arc-furnace-produced Si.

The initial experiments were conducted to verify predictions of growth rate and the onset of constitutional supercooling. Mn and Cu backdoped Si ingots were used since their effective segregation coefficients span the range. Czochralski pulls at three rates have been done. The onset of constitutional supercooling with attendant polycrystalline growth was shown to be proportional to the rate. For these data, there are significant differences between the experimental and calculated values at high melt impurity concentrations. The effective segregation coefficients as a function of growth rate were also determined; the data for 2.5 cm/hr are only slightly different from those at 6.8 cm/hr. The loss of crystal structure results in large increases in concentrations and

increases in the values of the effective segregation coefficients of several orders of magnitude. The conclusions derived were (1) as long as constitutional supercooling does not occur, single crystal growth is achievable with only minor growth-rate-dependent variations in effective segregation coefficients and (2) a simple thermal model describes the onset of constitutional supercooling at melt concentrations less than $10^{20}$ atoms/cc. Czochralski pull experiments using Si having total impurity concentrations $10^2$ lower than metallurgical grade Si showed that a multigrained ingot was attained and that, at the 40% of melt pulled point, the impurities, except for Al, were below the detection limits by spark source mass spectroscopy.

b. Solar-Cell-Grade Si Production From $Na_2SiF_6$ Source Material Using Na Reduction of $SiF_4$ and the $SiF_4/SiF_2$ Transport Process - Stanford Research Institute. The contract with Stanford Research Institute is for the development of a two-step process for the production of solar-cell-grade Si. The steps are: (1) the reduction of $SiF_4$ with Na to produce high purity Si and (2) the further purification of this product by reaction with $SiF_4$ to form $SiF_2$ followed by the disproportionation of the $SiF_2$ to yield solar-cell-grade Si with the regeneration of $SiF_4$. The work to date has dealt entirely with the first reaction.

The reduction reaction was studied in a series of experiments under controlled conditions to permit $SiF_4$ purification and transfer into the reactor as well as a parametric investigation with temperature, mole ratio of reactants, and pressure as the variables. NaF, $Na_2SiF_6$, and Si were detected as reaction products. Emission spectrographic analyses of the product Si revealed a high residual content of Na; with the exceptions of Cu, Mg, and Al, the other elements of interest, Ba, Cu, Fe, Ti, V, Cr, and Zr, were not detected; in most of these cases the limit of detectability ranges between 10 to 50 ppmw.

The following observations were made: (1) the reduction reaction is initiated below 175°C, is exothermic, and goes to completion; (2) the Si product is a fine powder; (3) the reaction rate and the form of the Si are dependent upon the partial pressure of $SiF_4$; (4) the preliminary conversion efficiency is about 90%; (5) the separation of the products is a major problem; and (6) experimental conditions must be carefully controlled to react the Na completely. An atomic absorption technique is being explored for the measurements of impurities in the product at concentrations less than 1 ppma.

c. Solar-Cell-Grade Si Production Using an Arc Heater Plasma Process for the Reduction of $SiCl_4$ with Na, Mg, or $H_2$ - Westinghouse Electric Corporation. This contract with Westinghouse is for the development of an electric arc heater for the production of Si using reactions for the reduction of $SiCl_4$ by either Na, Mg, H or Zn. The first phase consists of a review of the chemical and engineering feasibility and the designing of a system for experimental verification; it includes four subtasks: reaction analysis, plasma reactor, reactor storage and injection, and product collection and effluent disposal.

In the subtask for reaction analysis, thermochemical analyses for each reaction system were completed. Theoretical reaction yields, energy requirements. and reactant feed ratios were determined. A comparison of these results led to the conclusion that Zn should be eliminated as a candidate reductant. The assessment procedure was continued using a set of economic and technical criteria, and Na was selected as the primary reductant, although Mg was calculated to be very advantageous based on total cost/kg Si and energy requirement considerations. The choice of Na was based in part on the judgment that the technology for controlling and using Na is much better established than that for Mg; $H_2$ remains as a backup, also.

The problems of the vaporization of molten Si droplets, Si particle growth, reactor wall analysis, cyclone separation design, and materials compatibility were investigated in the subtask for the plasma reactor. The critical requirement for a high degree of vaporization of the metal reductant prior to the introduction of $SiCl_4$ was recognized. A model was formulated to determine the velocity, temperature, and radius of the metal droplet as well as the velocity, temperature, and composition of the gas as functions of axial distance along the reactor. The dependence of reactor length for various degrees of Na vaporization on reactor diameters, droplet diameters, and Na flow rates will be calculated using a computer program. The analysis of the reactor wall makes use of the assumption of a cross-section of solid Si with an inner wall of liquid Si to minimize contamination. A heat transfer model was developed, and values were calculated for the outer wall heat flux, the ratio of radiation to convective haat transfer at the inner wall, the gas/particle temperature, and the equilibrium inside diameter as a function of the axial position. The conclusions were that (1) radiation remains the dominant heat transport over most of the reactor length, (2) a higher Si flow rate significantly reduces the necessary wall thickness, and (3) the wall thickness decreases markedly with Si temperature entering the growth section.

A simplified analysis was conducted to estimate particle growth rates as the first step in dealing with the extremely complicated situation of the formation of particles in the reaction system of a plasma reactor. It was shown that under quiescent conditions the main particle growth is dependent upon the coagulation process and that, in the flow time assumed to be available, the particle growth is entirely too slow. Effects induced by the reactor operation are expected to increase the rate to practical values.

The arc heater reaction environment of high temperature, very reactant vapors, liquid Si and possible reactant by-products necessitates that the materials of construction for each subsystem be analytically and experimentally studied. The selection of materials will be based upon the criteria of chemical stability at temperatures of about 2400°K in the presence of corrosive Si compounds, impurity content, cost, and availability. The potentially suitable materials primarily being considered are refractory metals, ceramics, and graphites. In general, the refractory metals are costly; impurity content and reactivity are other drawbacks, although the use of a protective skin is possible. Most ceramics also could potentially contaminate the Si

product; SiC may be usable as a liner material. Purified graphite is also a candidate as a liner material. Thus, the analysis has shown that the prime candidates for the metal containment are two Mo alloys (HT and $T_2M$) and that a liner made from SiC or graphite may be necessary.

Preliminary designs were completed for the $SiCl_4$ and Na storage and feed subsystems. Flow diagrams were reviewed, and the comparisons of the reactants were assessed. Techniques for handling reactants; monitoring purity; controlling injection; and instrumenting storage, injection, and containment were analyzed; the requirements of these subsystems are being defined.

In the subsystem for product collection and effluent disposal, conceptual designs were formulated and preliminary flow diagrams were devised. The Si collection consists of a separator, which may be a cyclone chamber, to aggregate the Si and boil off the by-products, and an ingot caster. The Si container is to be designed to hold about 100 kg. It will have a ceramic valve gate, which has the advantages of proven design, economy, and ease of replacement, and allows an isolation interface between the reactor and the caster. A carousel mold is envisioned for the solidification assembly. The schemes for by-product collection being evaluated are a water spray collection tank and a series-connected secondary condenser with a scraper.

d. Production of $SiH_4$ or Si Using a Nonequilibrium Plasma Jet for the Reduction of $SiCl_4$ - AeroChem Research Corporation. The objective of the contract with AeroChem is to determine the feasibility of using a nonequilibrium plasma jet to produce $SiH_4$ or Si. This process, which involves a glow discharge in $H_2$ to create the hydrogen atoms, seems feasible based upon thermodynamic and kinetic agreements. Preliminary estimates indicate a suitability for low-cost, high-volume production.

The first phase is a study to ascertain whether hydrogen atoms can be produced at sufficient concentrations and at a reasonable energy yield to indicate the process can be economically practical. Some exploratory experiments of the reaction of the $H/H_2$ stream with $SiCl_4$ were carried out. In following phases the reaction paths to $SiH_4$ or Si and the adjustment of the plasma jet conditions for optimizing yields will be investigated.

As a part of the hydrogen atom study the conditions for discharge stability were examined by first considering various nozzle sizes. This will be extended to consider nozzle geometry and material effects.

Complete energy balance data were obtained for the discharges at various $H_2$ pressures. The energy to heat the gas was calculated from enthalpy differences at two temperatures, assuming that the flow is isentropic, no heat is lost to the nozzle, and all of the energy is added upstream of the nozzle entrances; considerable deviations from these assumptions may occur. The preliminary calculations indicate H atom concentrations of 2.7% by volume with 30% energy conversion into H atoms. For this case, assuming isentropic expansion and a downstream pressure of 30 Torr, the gas temperature would be $420^{\circ}K$; to achieve

an equivalent H atom concentration, an equilibrium temperature of about 2200°K is required. This comparison illustrates the nonequilibrium characteristic of the jet. Initial studies of the reaction of the H atoms with $SiCl_4$ yielded small amounts of deposits. The characteristics and masses depended on the mode of operation. Qualitative tests of a powdery deposit indicated it to be amorphous Si.

e. Solar-Cell-Grade Si Production by C Reduction of $SiO_2$ Using an Induction Plasma - Texas Instruments Corporation. This investigation of the technical feasibility of a process for the C reduction of $SiO_2$ using a laboratory-scale plasma reactor has been completed. In a series of experiments which explored the optimization of reaction conditions, a maximum yield of 33% Si was obtained and impurity concentrations were found to be decreased by two orders of magnitudes. Because of the very inefficient energy utilization and low Si yields, it was concluded that the process is economically unsatisfactory as an approach to the production of solar-cell-grade Si.

4. Evaluation of Silicon Production Processes - Lamar University

The objective of this contract is to evaluate the potentials of the processes being developed in the Silicon Material Task program. The economic evaluations will be based upon analyses of process-system properties, chemical engineering characteristics, and costing-economics. The evaluations will be performed for each stage of the Silicon Material Task - technical feasibility, scale-up, experimental plants, and commercial plant - using information which becomes available from the various process development contracts.

Major activities during the report period were focused on process system properties, chemical engineering and economic analyses.

a. Process System Properties. Analyses of process system properties were continued including investigation of estimation methods for critical constants of silicon source materials under consideration for solar-cell-grade silicon. Property values for critical temperature, pressure, volume, compressibility factor and density were estimated and presented for $SiF_4$ and $SiI_4$. The recommended values will be used in performing the preliminary plant design for these solar-cell-grade silicon processes.

In additional analyses, correlation activities were initiated for process system properties of silicon source materials. Initial correlation efforts focused on vapor pressure data, which are extremely important in phase equilibria in a chemical plant processing silicon source materials. The vapor pressure of silane as a function of temperature was correlated by the reaction

$$\log P_V = A + \frac{B}{T} + C \log T + DT + ET^2$$

The versatile correlation covers both low and high pressure regions and is applicable over the complete range from the triple point to the critical point. The agreement of correlation and data values is good. These results--vapor pressure correlation--will be utilized in performance of the chemical engineering analysis for the $SiH_4$ process (Union Carbide).

In the investigation for $SiF_4$ generation from the relatively inexpensive fertilizer industry by-product hydrofluosilic acid, the conditions for precipitation of $BaSiF_6$ (precursor to $SiF_4$) were determined. It was found that $BaSiF_6$ could be obtained in good yields by the reactions of $BaCl_2$ and $BaF_2$ solutions with $H_2SiF_6$. Slightly more efficient results were obtained using $BaCl_2$.

The thermal decomposition of $BaSiF_6$ to generate $SiF_4$ was also investigated. Parameters such as temperature and reaction time were studied and it was determined that the reaction proceeds readily above 400°C. Essentially quantitative yields of $SiF_4$ can be obtained by heating $BaSiF_6$ to 500°C for 5 to 10 minutes.

b. Chemical Engineering. Major chemical engineering analysis activities were devoted to preliminary process design for a 1000 metric ton/year plant for solar-cell-grade silicon utilizing $SiI_4$ decomposition technology developed by Battelle. The process flow diagram, material balance, energy balance, and equipment design are essentially complete. Results are presented for the reaction chemistry, raw materials, utilities, major process equipment and production labor requirements.

In additional solar-cell-grade silicon processes, technology developed by Union Carbide for the production of $SiH_4$ using hydrogen and metallurgical-grade silicon as raw materials is being investigated. The process flow diagram and material balance are presently being developed.

c. Economic Analysis. Economic analysis for the Battelle process for $SiI_4$ decomposition was completed. A plant investment cost (fixed capital) of $77,098,000 and total product cost of $48.08/kg for solar-cell-grade silicon were determined for the process. These cost economics exceed the target goal of $10/kg of silicon and confirm the Battelle results leading to the discarding of the iodination process. Also, the variation of total product cost (without profit) with plant investment (fixed capital) was determined for solar-cell-grade silicon via the $Zn/SiCl_4$ process (Battelle technology). The target goal of $10/kg of silicon is attained only when fixed capital plant investment does not exceed approximately $11,000,000.

5. JPL In-House Activities

Studies of fluidized bed reactor technology and silane pyrolysis make up a major section of the in-house program. The program plan consists of (1) theoretical thermodynamic and kinetic analyses of fluidized bed deposition and pyrolysis reactions using $SiH_4$, (2) formulation of practical models based on fluid mechanics and mass/heat transfer phenomena, and (3) experiments to determine operating characteristics to supplement and support the developments on JPL contracts. The contractual efforts at Union Carbide and the Battelle Memorial Institute will benefit directly from this work; an extension, using the more complex conditions of turbulence and the involvement of chlorosilanes as reactants, will be undertaken to support other contracts.

Two technical reports have been written to describe the results of the analyses. A JPL technical memorandum, "Modeling of Fluidized Bed Silicon Deposition Process," initiated by Dr. Kibong Kim, was reviewed by Dr. Ananda Praturi and is being edited for publication. The memorandum "Chemical Vapor Deposition from Silane Pyrolysis" was authored by Dr. Praturi. This report, which covers mass transport, homogeneous reaction and nucleation, adsorption of silane, surface reactions and desorption of hydrogen, and heterogeneous nucleation, is being reviewed.

Apparatuses for the $SiH_4$ pyrolysis and the fluidized bed experiments were assembled and checked out. The $SiH_4$ pyrolysis system includes (1) a multifunctional pyrolysis reactor, (2) a porous wall $H_2$ film thermowall, (3) a four-nozzle gas manifold with particulate inlet, (4) a Si dust hopper, and (5) an electrostatic precipitator. Modifications were made to eliminate leaks. The experimental plan will proceed with determinations of the effects of pressure and temperature. The fluidization reactor is being modified to correct functional problems. Bed voidage measurement techniques suggested by Professor T. Fitzgerald, a consultant to the Silicon Material Task, will be explored to ensure the incorporation of instrumentation which will provide satisfactory data. The two experimental programs will be altered as needed to allow cooperative efforts which closely track the JPL contracts.

# SECTION V

# LARGE-AREA SILICON SHEETS

The objective of the Large-Area Silicon Sheet Task is to develop and demonstrate the feasibility of several alternative processes for producing large areas of silicon sheet material suitable for low-cost, high efficiency solar photovoltaic energy conversion. To meet the objective of the LSSA Project, sufficient research and development must be performed on a number of processes to determine the capability of each for producing large areas of crystallized silicon. The final sheet-growth configurations must be suitable for direct incorporation into an automated solar-array processing scheme.

## A. TECHNICAL BACKGROUND

Current solar cell technology is based on the use of silicon wafers obtained by slicing large Czochralski or float-zone ingots (up to 12.5 cm in diameter), using single-blade inner-diameter (ID) diamond saws. This method of obtaining single crystalline silicon wafers is tailored to the needs of large volume semiconductor products (i.e., integrated circuits plus discrete power and control devices other than solar cells). Indeed, the small market offered by present solar cell users does not justify the development of silicon "real estate" production techniques which would result in low-cost electrical energy.

Growth of silicon crystalline material in a geometry which does not require cutting to achieve proper thickness is an obvious way to eliminate costly processing and material waste. Growth techniques such as edge-defined film-fed growth (EFG), web-dendritic growth, chemical vapor deposition (CVD), etc., are possible candidates for the growing of solar cell material. The growing of large ingots with optimum shapes for solar cell needs (e.g., hexagonal cross-sections), requiring very little manpower and machinery, would also appear plausible. However, it appears that the cutting of the large ingots into wafers must be done using multiple rather than single blades in order to be cost-effective.

Research and development on ribbon, sheet, and ingot growth plus multiple-blade and multiple-wire cutting, initiated in 1975-1976, is in progress.

## B. ORGANIZATION AND COORDINATION OF THE LARGE-AREA SILICON SHEET TASK EFFORT

At the time the LSSA Project was initiated (January 1975) a number of methods potentially suitable for growing silicon crystals for solar cell manufacture were known. Some of these were under development; others existed only in concept. Development work on the most promising methods is now being funded. After a period of accelerated development, the various methods will be evaluated and the best selected

for advanced development. As the growth methods are refined, manufacturing plants will be developed from which the most cost-effective solar cells can be manufactured.

The Large-Area Silicon Sheet Task effort is organized into four phases: research and development on sheet growth methods (1975-77); advanced development of selected growth methods (1977-80); prototype production development (1981-82); development, fabrication, and operation of production growth plants (1983-86).

## C. LARGE-AREA SILICON SHEET TASK CONTRACTS

The pursuit of optimal techniques for growing silicon crystalline material for solar cell production has led to the awarding of R&D contracts to 11 organizations. The processes being developed by the Phase 2 contractors are shown in Table 5-1. Figure 5-1 shows the schedule for each contract as it was initially negotiated. Follow-on work anticipated for each contract is indicated by the cross-hatched horizontal bars. During the report period most of the manufacturers' contracts were extended. Research and development work will continue through the end of FY 1977, by which time it is expected that technical feasibility will have been demonstrated. Selection of "preferred" growth methods for further development during FY 1978-80 is planned for late FY 1977 or early FY 1978. By 1980, both technical and economic feasibility should be demonstrated by individual growth methods.

Figure 5-1 also indicates the receipt of silicon "sheet" samples and solar cells from the various growth-process R&D programs. Sheet samples are now being characterized at JPL, with solar cell evaluation to follow.

## D. LARGE-AREA SILICON SHEET TASK TECHNICAL ACTIVITY

### 1. Silicon Ribbon Growth: EFG Method - Mobil-Tyco Solar Energy Corporation

The edge-defined film-fed growth (EFG) technique is based on feeding molten silicon through a slotted die (as illustrated in Figure 5-2). In this technique, the shape of the ribbon is determined by the contact of molten silicon with the outer edge of the die. The die is constructed from material which is wetted by molten silicon (e. g., graphite). Efforts under this contract are directed toward extending the capacity of the EFG process to a speed of 7.5 cm/min and a width of 7.5 cm. In addition to the development of EFG machines and the growing of ribbons, the program includes economic analysis, characterization of the ribbon, production and analysis of solar cells, and theoretical analysis of thermal and stress conditions.

During this quarter Mobil-Tyco achieved routine growth of 50 mm wide ribbons at a 50 mm/min rate. Substantial stress reductions were

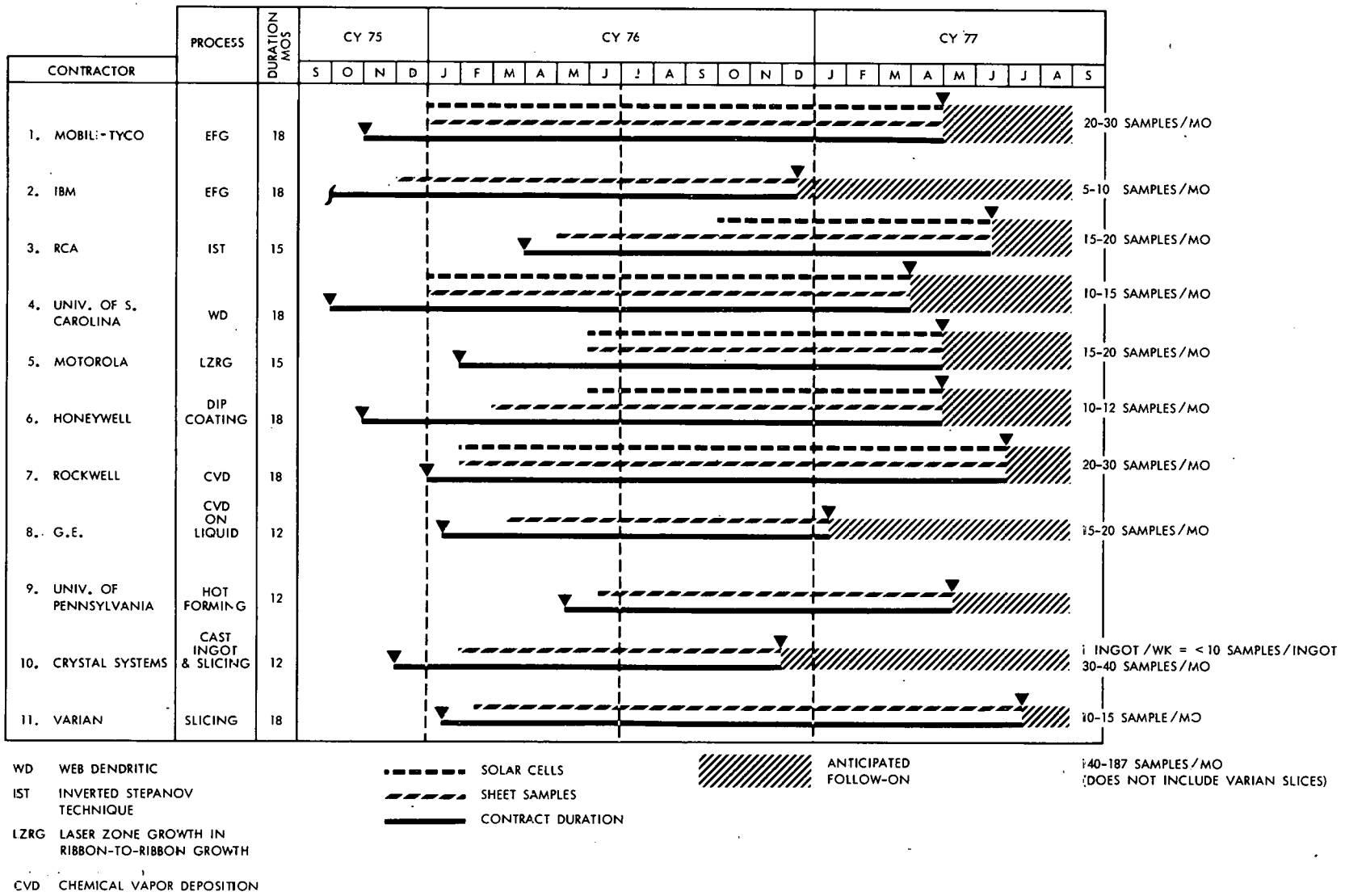


Figure 5-1. Large-Area Silicon Sheet Task Schedule

Table 5-1. Large-Area Silicon Sheet Task Contractors

| Contractor | Technology Area |
|---|---|
| **RIBBON GROWTH PROCESSES** | |
| Mobil-Tyco, Waltham, Massachusetts (JPL Contract No. 954355) | Edge-defined, film-fed growth |
| IBM, Hopewell Junction, New York (JPL Contract No. 954144) | Edge-defined, film-fed growth |
| RCA, Princeton, New Jersey (JPL Contract No. 954465) | Inverted Stepanov growth |
| Univ. of So. Carolina, Columbia, So. Carolina (JPL Contract No. 954344) | Web-dendritic growth |
| Motorola, Phoenix, Arizona (JPL Contract No. 954376) | Laser zone ribbon growth |
| **SHEET GROWTH PROCESSES** | |
| Honeywell, Bloomington, Minnesota (JPL Contract No. 954356) | Dip-coating of low-cost substrates |
| Rockwell, Anaheim, California (JPL Contract No. 954372) | Chemical vapor deposition on low-cost substrates |
| General Electric, Schenectady, New York (JPL Contract No. 954350) | Chemical vapor deposition on floating silicon substrate |
| Univ. of Pennsylvania, Philadelphia, Pennsylvania (JPL Contract No. 954506) | Hot-forming of silicon sheet |
| **INGOT GROWTH PROCESS** | |
| Crystal Systems, Salem, Massachusetts (JPL Contract No. 954373) | Heat-exchanger ingot casting* |

Table 5-1. Large-Area Silicon Sheet Task Contractors
(Continuation 1)

| Contractor | Technology Area |
|---|---|
| INGOT CUTTING | |
| Crystal Systems, Salem, Massachusetts (JPL Contract No. 954373) | Multiple wire sawing* |
| Varian, Lexington, Massachusetts (JPL Contract No. 954374) | Breadknife sawing |

*Single contract provides for both ingot casting and multiple wire sawing.

accomplished by including afterheaters in the growth process. Difficulties have arisen from the incorporation of metallic impurities into the melt. The source has been identified as the resistance heater. When an RF heater was used, the contractor noted a substantial change in ribbon quality, as indicated by electrical performance.

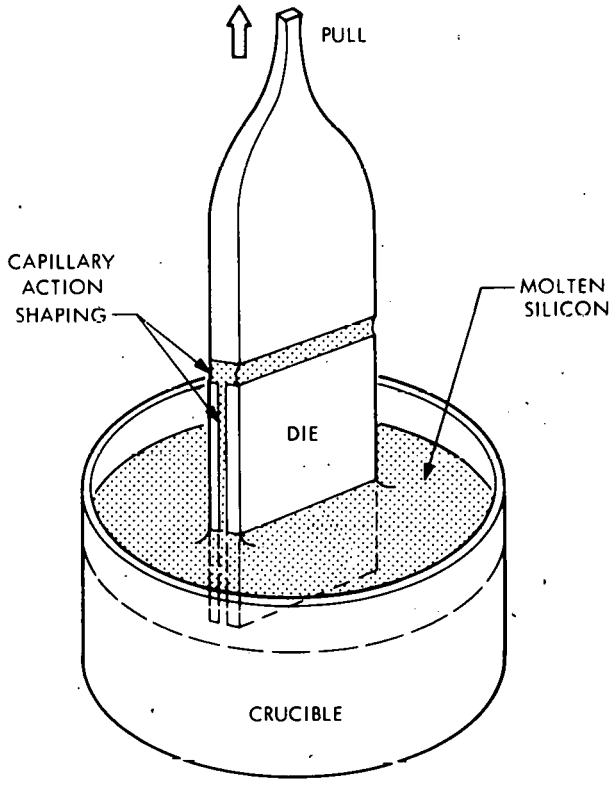


Figure 5-2. Capillary Die Growth (EFG and CAST) - Mobil-Tyco and IBM

## 2. Silicon Ribbon Growth: CAST Method - IBM

The capillary action shaping technique (CAST) is based on the same principle as EFG growth (Figure 5-2); i.e., it utilizes a die constructed from material which is wetted by molten silicon. Work under this contract is directed toward evaluation of the technical and economic potential of CAST for the preparation of silicon ribbon. The effort concentrates on (1) understanding and extrapolating the effects of growth conditions; (2) characterization of the ribbon, with special emphasis on the correlation of structure and electrical performance; and (3) economic analysis of silicon growth by this and other growth techniques.

The IBM investigators have been able to grow 50 mm wide ribbons. During the quarter they developed a process for routinely growing 38 mm wide ribbons at 3 cm/min with almost no stresses. The scale-up to a 50 mm dimension was delayed because of failures of furnace parts and the unavailability of replacements. Characterization of the ribbons continues to indicate the adverse effects of dislocations, grain boundaries, and incoherent twins, and the relative unimportance of the coherent twins.

## 3. Silicon Ribbon Growth: Inverted Stepanov Technique - RCA

In this program emphasis is placed on developing a technique for growing ribbon-shaped silicon using a "nonwetted" die (Figure 5-3). The use of the "nonwetted" die provides the possibility of minimizing the reaction between the molten silicon and the die material. Reaction between molten silicon and wetted dies is one source of degradation in the crystallographic quality of silicon grown using a wetted die (i.e., the edge-defined film-fed growth method). The introduction of the feed from above and the growth of the single crystal in a downward direction (the inverted Stepanov technique) in part compensates for the hydrodynamic drag in the slot and for the lack of capillary rise. (The capillary rise feeds the material to the die edge in the EFG method.) The inverted geometry also leads to considerable flexibility in the growth configuration when the feed is introduced from a molten zone at the end of a solid silicon rod.

The primary objective of the program is to investigate the basic seeding and growth processes involved in the growth of silicon sheet from "nonwetted" dies. The goal is to establish whether or not significant improvement in the crystallographic properties of the silicon can be realized by the use of "nonwetted" rather than "wetted" shaping dies. Silica and boron nitride shaping dies will be used. Methods will be sought to compensate for the lack of mechanical strength of silica at the growth temperature. Although boron nitride leads to unacceptable doping of the grown silicon ribbon, it is more rigid than silica and is therefore useful in the identification of fundamental limiting factors in the Stepanov growth method.

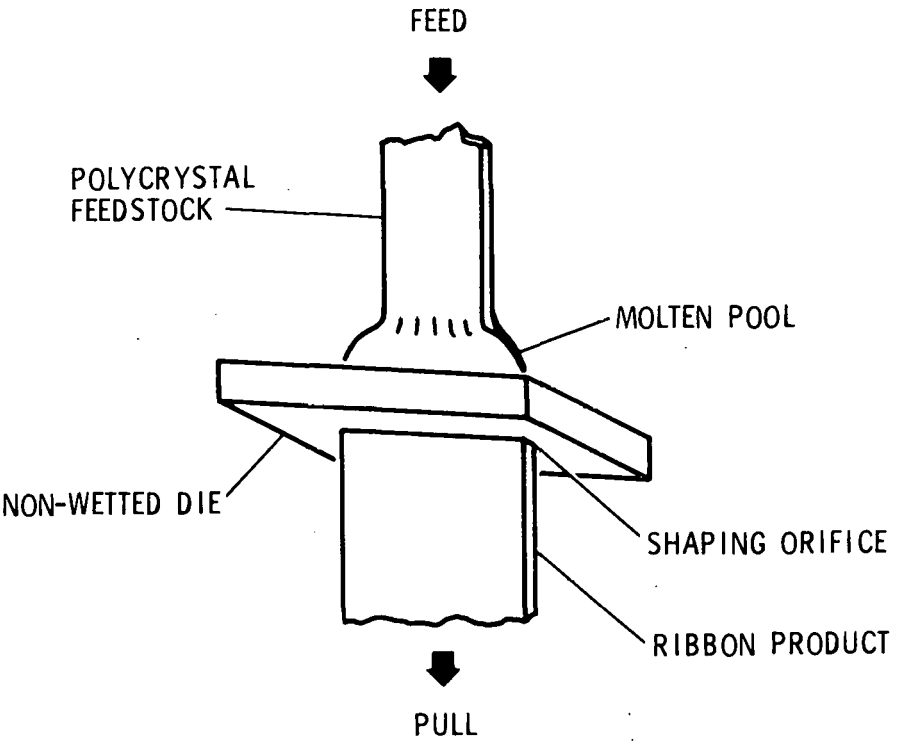


Figure 5-3. Inverted Stepanov Technique - RCA

During the quarter RCA experienced great difficulty using the $SiO_2$ die (Figure 5-4). This was associated with the evolution of gases as the result of reaction between silica amd molten silicon, yielding mechanical vibration of the melt and erratic wetting behavior. RCA has also tried applying a mechanical pressure differential to force the molten silicon through the die. Efforts are being made to minimize overheating of the liquid silicon and $SiO_2$ die. A program plan change was initiated with RCA to consider different die materials, especially those involving coating the dies with CVD nitride or CVD oxy-nitride, to avoid the Si-$SiO_2$ interface and reaction producing SiO gas. A great deal of work was done to model the thermal environment of the die.

4. Silicon Ribbon Growth: Web-Dendritic Method - University of South Carolina

Web-dendritic growth makes its own guides of silicon, whereas most other ribbon processes must rely on materials other than silicon for the guides (i.e., dies) (Figure 5-5). The guides are thin dendrites that grow ahead of the sheet and support the molten silicon between them to form the sheet. The dendrite guides grow in a very precise orientation dictated by their unique growth habit. Thus the orientation of the sheet which grows between them takes on this precise orientation. The twin plane reentrant edge mechanism (TPREM) controls the growth

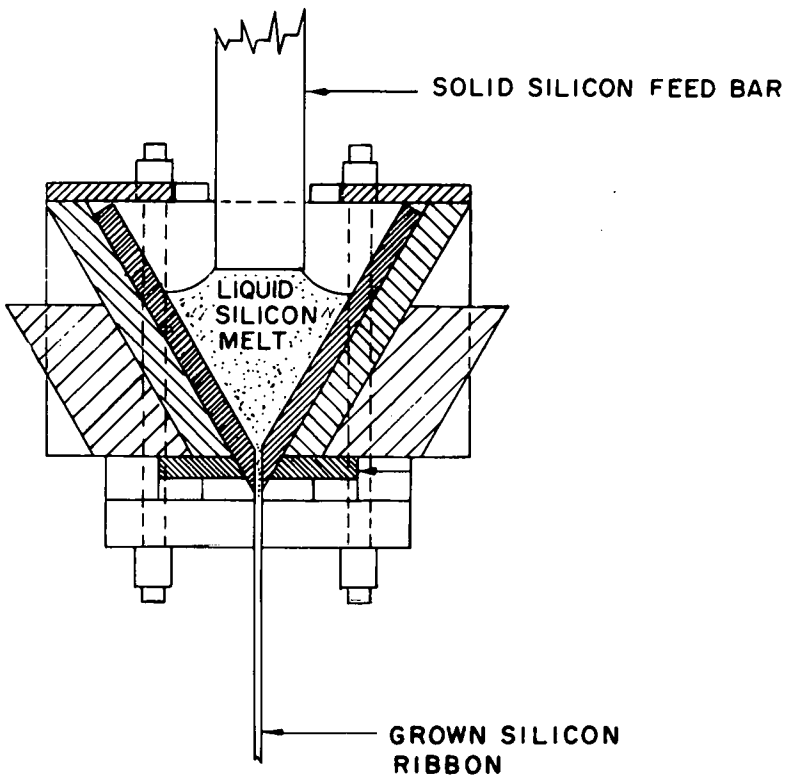


Figure 5-4. Model 1 IST Growth Apparatus - University of South Carolina

of the edge dendrites, giving them their unique and internally-controlled growth direction, allowing them to grow ahead of the sheet and thus act as guides.

The basic steps, then, in web sheet growth are (1) dip a seed of the proper orientation into a slightly undercooled melt, (2) hold the seed stationary while growth takes place laterally on the surface of the melt, forming what is termed the "button", and (3) when the lateral growth has proceeded to the desired width, start the pulling. As the pulling proceeds, two coplanar dendrites grow downward from each end of the button, propagating to a depth of 1-3 mm beneath the surface of the melt. As the button and its dendrites emerge from the melt, silicon is pulled up between them by surface tension, and the resulting sheet solidifies just above the melt surface. The unique orientation and slight undercooling to insure faceted growth give the sheet its almost mirror-flat surface finish. The overall goal of this contract is to develop a better understanding of the web-dendrite process and define in greater detail the basic limitations to the process (especially the maximum growth rate and width).

During this quarter, the University of South Carolina investigators introduced a major change in furnace geometry in the form of an aluminum pedestal and improved heat shielding. Thermal profile measurements were made for different positions of the heating coil relative to the

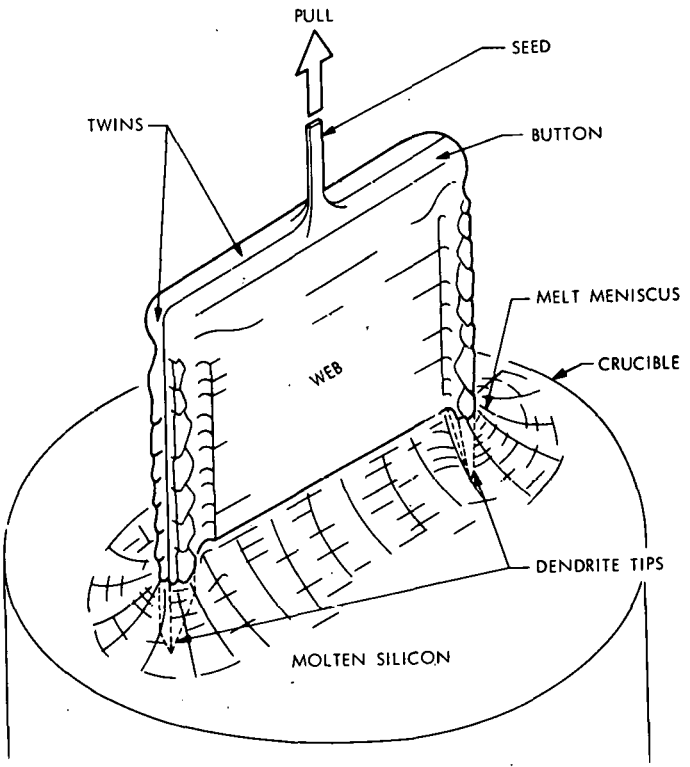


Figure 5-5. Web-Dendritic Growth - University of South Carolina

susceptor, and growth runs were attempted at each of these positions. Thermal measurements indicated greater control than previous thermal profiles in the melt. In growth studies, the furnace was found to be unreliable because of a current-limiting resistor. When this was corrected, the contractor was able to grow web-dendritic ribbons containing only two dendrites, up to 1 cm wide and 38 cm in length. This was accomplished by modifying the position of the work coil with respect to the susceptor and liner.

5. Silicon Ribbon Growth: Laser Zone Growth in a Ribbon-to-Ribbon Process - Motorola

The ribbon-to-ribbon process is basically a float-zone crystal growth method in which the feedstock is a polycrystalline silicon ribbon (Figure 5-6). The polysilicon ribbon is fed into a preheated region which is additionally heated by a focused laser beam, melted, and crystallized. The liquid silicon is held in place by its own surface tension. The shape of the resulting crystal is defined by the shape of the feedstock and the orientation is determined by that of a seed single-crystal ribbon.

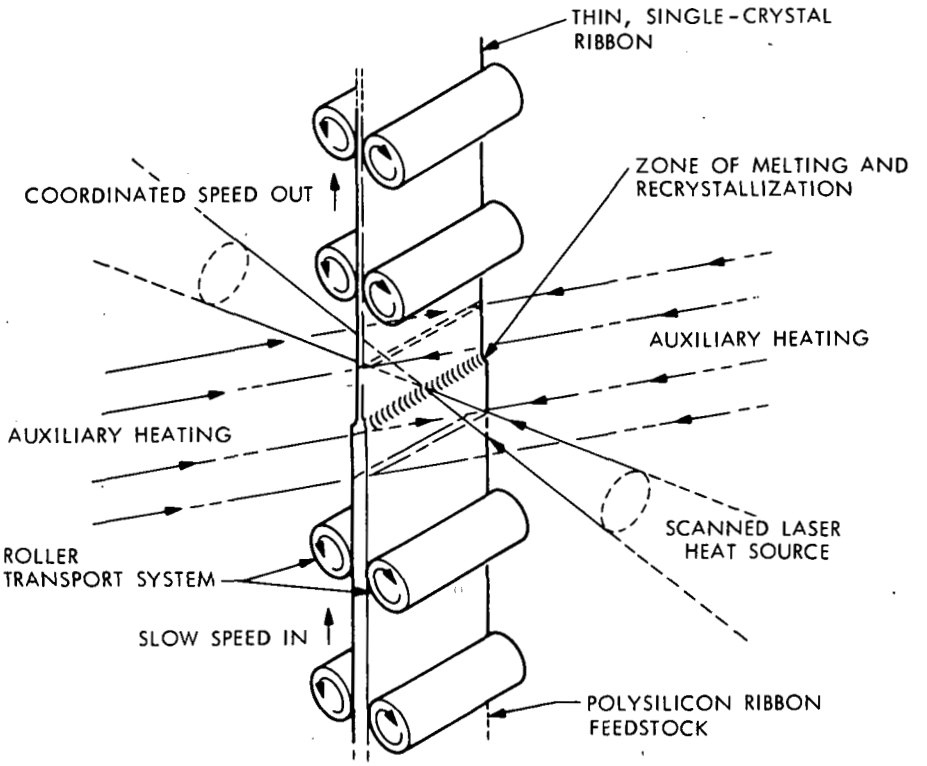


Figure 5-6. Laser Zone Crystallization - Motorola

Motorola has established a routine process for producing 2.5 cm wide ribbons at a 22.5 mm/min rate. The production of wider ribbons is limited by laser power and scanning frequency. JPL's characterization of the ribbons is proceeding on schedule.

6. Silicon Sheet Growth: Dip-Coating on Low-Cost Substrates - Honeywell

This program is directed toward the formation of thin silicon films by withdrawing suitably prepared ceramic substrates from a pool of molten silicon (Figure 5-7). Ceramics were selected because of their superior thermal expansion match with silicon and the greater ease with which this expansion may be adjusted. The ceramics are coated with a film of carbon or silicon carbide to enhance adhesion. The concept has been demonstrated previously. The total program includes construction of a dipping facility, selection and evaluation of substrates and associated coatings, production of dip films and their characterization by various structural, chemical, and solar cell performance methods. The solar cells will require some specialized techniques because of the nonconductive nature of the substrate.

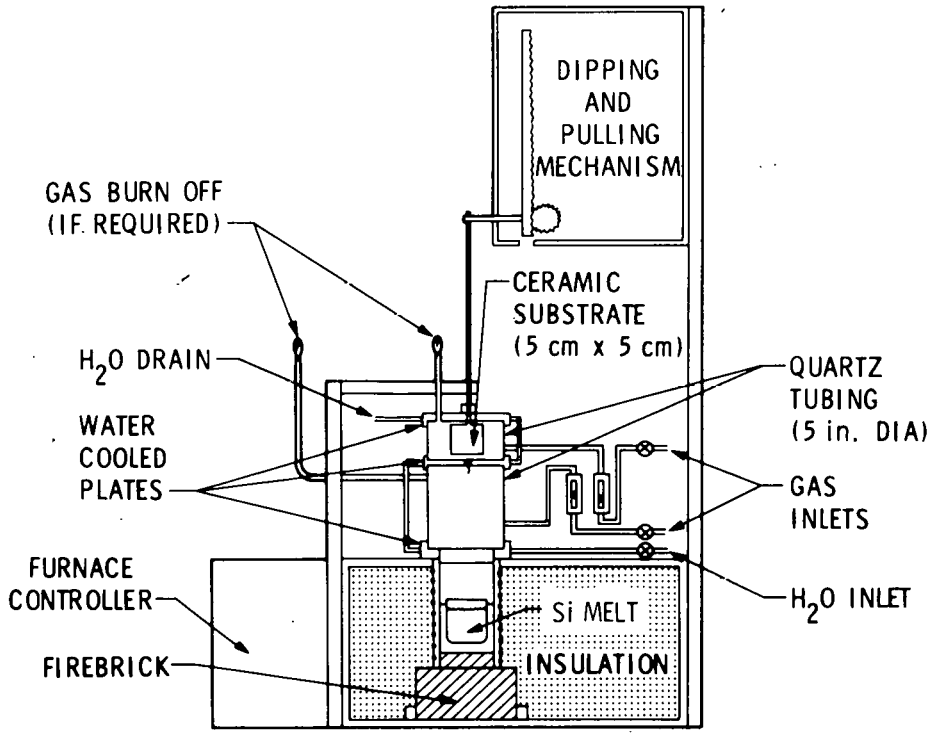


Figure 5-7. Cross-Sectional Sketch of Basic Sheet Dip Coating Growth Facility - Honeywell

Various substrates have been used to date, including mullite ($2SiO_2 \cdot 3Al_2O_3$), aluminum oxide, zirconium silicate, calcium aluminate, carbon-sintered $SiO_2$, and pressed fibrous insulation. The mullite substrates have proved to be the most satisfactory and, since this material offers the additional advantage of being low in cost, emphasis has been placed on its use.

Honeywell's studies to define the process parameters for film formation indicate that 50-micron-thick layers are available at 8°C above the melting point, at a pulling rate of 6 cm/min. Higher temperatures or pull rates tend to reduce the film thickness, and lower temperatures produce dendritic growth. Thermal trimming was not evaluated. Contamination of silicon by the mullite substrate is substantially reduced when a glass carbon coating is used on the mullite. Initial efforts have been directed toward improving solar cell preparation and characterization consistent with a recently-issued contract modification in that area. Data on small mesa-construction cells indicated raw data between 4% and 5% with corrected data at about 6% conversion efficiency. A proposal to expand and extend this program was received and reviewed. It is expected that agreement on this additional work will be reached in January.

7. Silicon Sheet Growth: Chemical Vapor Deposition on Low-Cost Substrates - Rockwell International

The purpose of this contract is to explore the chemical vapor deposition (CVD) method for the growth of silicon sheet on inexpensive substrate materials (Figure 5-8). As applied to silicon sheet growth, the method involves pyrolysis, or reduction, of a suitable silicon compound at elevated temperature and approximately atmospheric pressure. A laboratory-type CVD reactor system with a flow-through (open-tube) vertical deposition chamber is used for these investigations. The substrate is mounted on a silicon carbide-coated carbon pedestal heated by an RF coil external to the chamber. The reactor system has been extensively modified by installation of mass flow controllers, automatic process sequence timers, and special bellows-sealed air-operated valves. This system, which has a capacity of 30 $cm^2$, is used as a research vehicle in an attempt to reach the goals of 100 $\mu m$ grains deposited 20 to 100 $\mu m$ thick on inexpensive substrates at rates up to 5 $\mu m$ per minute.

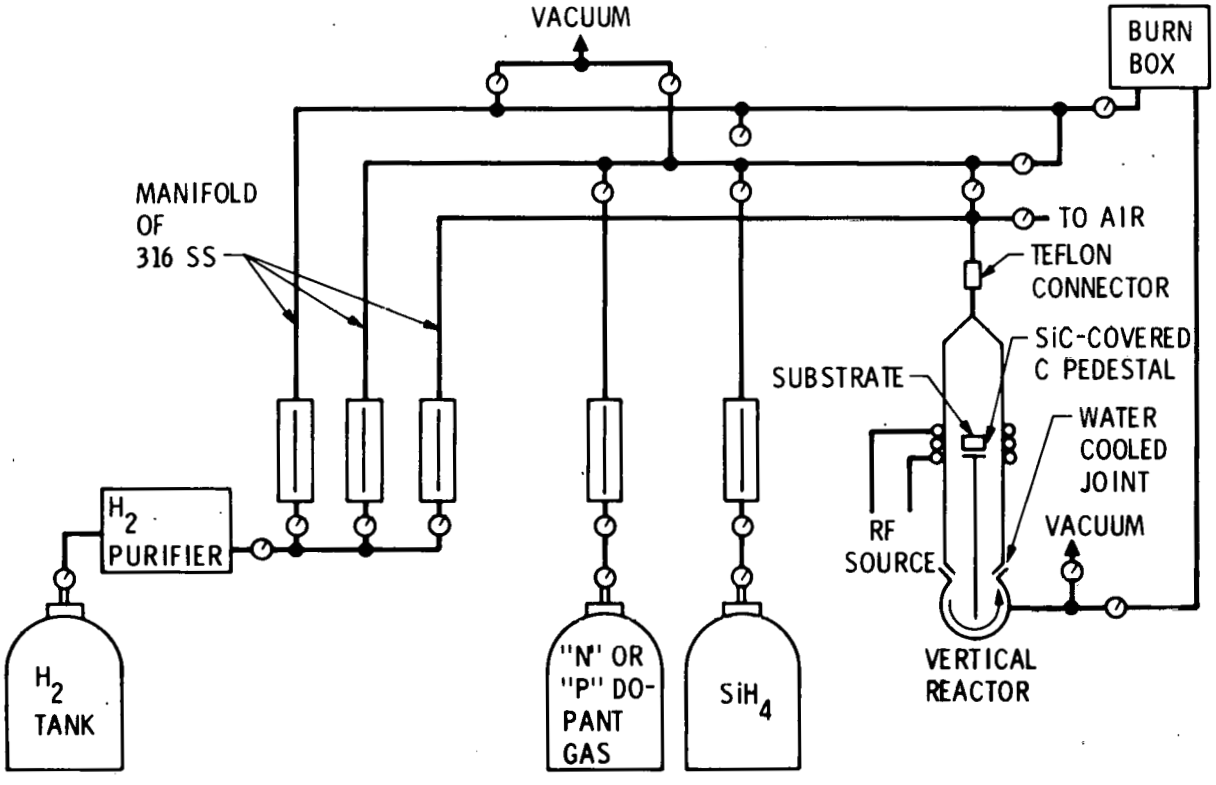


Figure 5-8. Chemical Vapor Deposition on Low-Cost Substrates - Rockwell International

The properties of the silicon sheet are determined by deposition temperature, reactant concentrations, the nature of the carrier gas, the silicon source compound used, growth rate, doping impurities (added by introduction of appropriate compounds into the carrier gas stream), and the properties of the substrate.

A number of two-step processes have been proposed in which the nucleation and growth are done under different conditions in hopes of achieving larger grain size. The first of these involved depositing a thin full-coverage layer from $SiH_4$ and then adding HCl to the stream to preferentially etch the smaller grains, but no dramatic improvement was seen.

During this quarter Rockwell began experiments using the second two-step process, in which a partial-coverage layer of silicon is deposited and hydrochloric acid is then added to prevent new nucleation. Under the usual conditions used for alumina substrates, that is, 1025°C in hydrogen, partial coverage took less than 1 second of exposure; consequently, the process conditions will be changed to allow for more control. Nucleation is more controllable under the conditions used for glass, that is, 850°C in helium. Partial coverage was therefore easily achieved, but glass may not survive the subsequent HCl treatment. The problem of the contamination introduced by some of the glasses will be addressed. New cleaning procedures may solve it. Nucleation studies of large-grain alumina show nuclei evenly distributed on each grain. Annealing and HCl etching will now be used in an attempt to get bigger nuclei, further apart. An experimental curve of carrier concentration vs. doping level to polycrystalline films shows a sharp, nonlinear increase in carriers as doping goes from $10^{16}$ to $10^{18}$ atoms/cm$^3$. This data makes it possible to predict the required $B_2H_6$ flow rates for desired solar cell base layer resistivities.

8. Silicon Sheet Growth: Chemical Vapor Deposition on a Floating Silicon Substrate - General Electric

The purpose of this contract is to demonstrate the feasibility of growing silicon sheet on a floating silicon substrate (Figure 5-9). In the process single crystal silicon is formed by direct epitaxial conversion from gaseous silane. In an appropriate reactor, silane is passed over silicon substrate which is supported on a thin film of molten tin. Single crystal silicon grows to the desired thickness by vapor phase epitaxy. Nucleation of fresh substrate silicon takes place at one end of the reactor where the edge of the growing sheet is in contact with a region of the tin which is supersaturated with silicon. The process lends itself to continuous operation, with the finished sheet being withdrawn from the opposite end of the growth zone. The major portion of the program will focus on nucleation studies and the rapid growth of silicon substrate from supercooled melts. These efforts should lead to a sheet growth demonstration by the end of the first contract year and a design and cost analysis for a prototype sheet growth apparatus by contract close.

Sessile drop experiments by GE to determine the capabilities of various tray materials for the molybdenum susceptor were begun in a horizontal furnace. Preliminary experiments with tin drops on a silicon substrate in a "clean" atmosphere show indications of surface contamination associated with the silicon and/or the tin. The first serial growth experiment with the new molybdenum susceptor was attempted using a quartz liner. The tin surface, under a hydrogen atmosphere, appeared very clean. A seed was introduced and growth was sustained

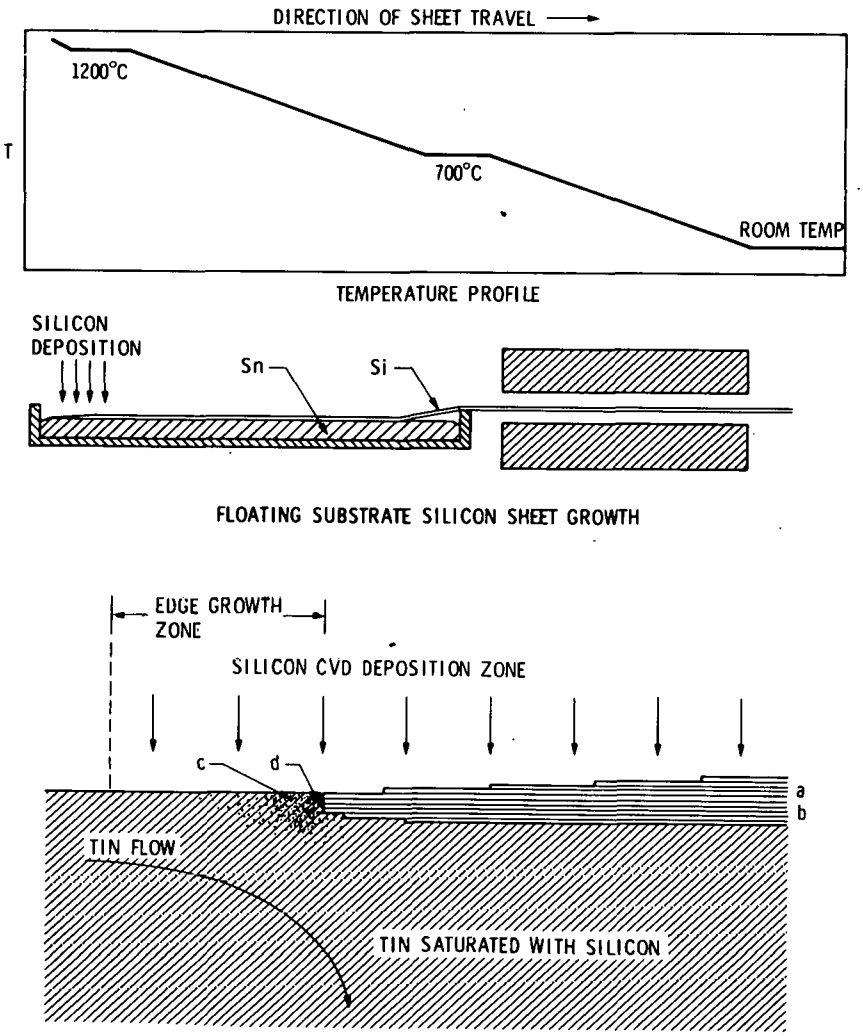


Figure 5-9. Silicon Sheet Growth Through Chemical Vapor Deposition on Floating Silicon Substrate - General Electric

to about 11 mm. Advance efforts were directed at selecting several materials for use as susceptor liners. For each of the materials selected, serial growth with hydrogen ambient will be attempted. Sessile drop experiments with tin on silicon, sapphire, and spinel substrates were continuing. There was definite evidence of a film on the tin drop both in the hydrogen atmosphere and in vacuum. The film is stable at temperatures up to about 800°C and prevents normal interaction of the molten tin with the substrate. At 800° to 900°C the film breaks up and, in the case of the silicon substrate, wetting occurs. The origin and nature of the film was not determined.

9. Silicon Sheet Growth: Hot-Forming of Silicon - University of Pennsylvania

This contract is designed to determine the feasibility of hot-forming silicon in a cost-effective manner. The procedure to be followed is high-strain-rate ($\dot{\epsilon}>1$), high-compression deformation of silicon. From this information, one can construct the hot-forming diagram for silicon and make some extrapolations of the economics of the process. The program also includes evaluations of metallurgical properties such as hot-forming texture, recrystallization texture and grain size, and of electrical properties.

During the quarter, the University of Pennsylvania investigators performed stress/strain rate measurements, extending the measurements to a strain rate of 13 cm/sec in a temperature interval of 1300°C to 1380°C. They observed crystallite sizes up to 1 mm in recrystallization studies of samples deformed at 1250°C. Based on the preliminary rolling schedule, an economic analysis was made. Discussions are now under way with a rolling mill manufacturer to obtain further economic data. Enough data was obtained to plot the final forming limit diagram. The data indicate that silicon can be deformed. The recrystallization studies have progressed, but the data obtained thus far are inconclusive.

10. Ingot Growth: Heat Exchanger Method - Crystal Systems

The Schmid-Vicchnicki technique (heat-exchanger method) has been developed to grow large single-crystal sapphire (Figure 5-10). Heat is removed from the crystal by means of a high-temperature heat exchanger. The heat removal is controlled by the flow of helium gas (the cooling medium) through the heat exchanger. This eliminates the need for motion of the crystal, crucible, or heat zone. In essence this method involves directional solidification from the melt where the temperature gradient in the solid might be controlled by the heat exchanger and the gradient in the liquid controlled by the furnace temperature.

The overall goal of this program is to determine if the heat-exchanger ingot casting method can grow large silicon crystals (6 inches in diameter by 4 inches in height) in a form suitable for the eventual fabrication of solar cells. This goal is to be accomplished by the

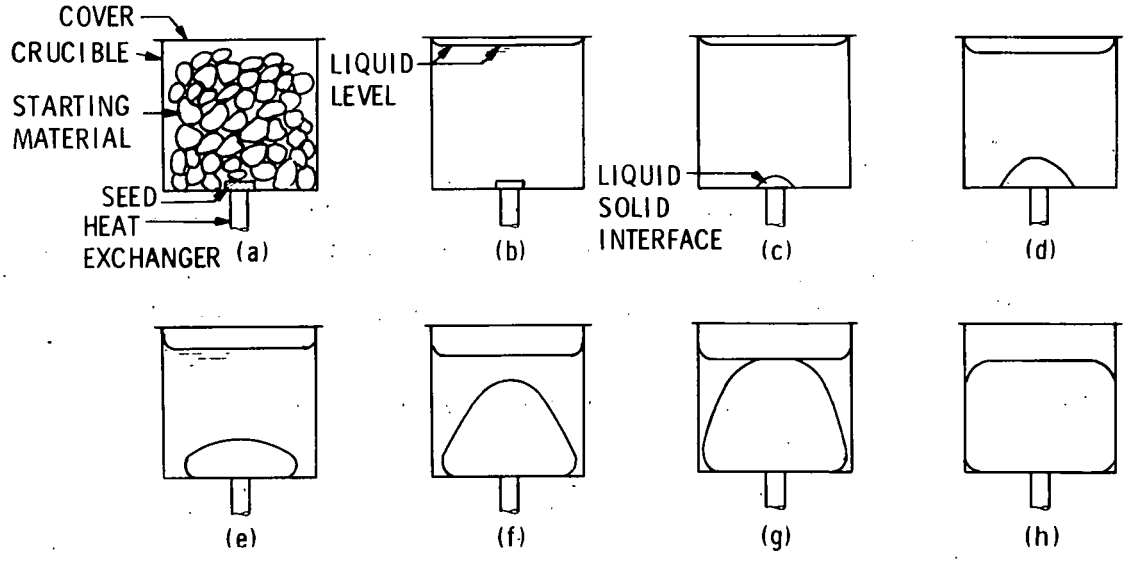


Growth of a crystal by the heat exchanger method:
(a) Crucible, cover, starting material, and seed prior to melting.
(b) Starting material melted.
(c) Seed partially melted to insure good nucleation.
(d) Growth of crystal commences.
(e) Growth of crystal covers crucible bottom.
(f) Liquid-solid interface expands in nearly ellipsoidal fashion.
(g) Liquid-solid interface breaks liquid surface.
(h) Crystal growth completed.

Figure 5-10. Crystal Growth Using the Heat Exchanger Method - Crystal Systems

transfer of sapphire growth technology (50-pound ingots have already been grown), and theoretical considerations of seeding, crystallization kinetics, fluid dynamics, and heat flow for silicon.

During the quarter Crystal Systems experienced cracking of crucibles because of the thermal expansion mismatch between the silicon and the silica crucible. Preliminary experiments utilizing silica coatings and 1.5-inch-diameter silica crucibles permitted separation of the silicon and the silica without cracking the silicon during cool-down. For large diameter ingots, single crystallinity has been extended laterally to the walls. Work is progressing toward (1) obtaining single crystal growth and (2) eliminating the cracking problem. Increased solidification rates for ingots weighing up to 2.5 kg yielded larger areas of single crystalline material compared to the lower solidification rates previously used.

11. Ingot Cutting: Multiple Wiring Sawing - Crystal Systems

Today most silicon is sliced into wafers with an inside diameter saw, one wafer at a time being cut from the crystal. This is a big cost factor in producing solar cells. The lesser-used multiblade slicer can be utilized to slice silicon. The multiblade slicer has not been developed for the semiconductor industry since this method produces bow and taper unacceptable for integrated-circuit applications.

The overall goal of the slicing program is to optimize multiblade (wire) silicon slicing, investigating the following parameters in particular:

(1) Rate of material removal and kerf removal.

(2) Slice thickness, wire blade dimensions, cutting forces, wire/blade tension, and other machine variables.

(3) Wires versus blades as a cutting tool.

(4) Variation of rocking motion.

(5) Introduction of abrasive during slicing operation.

(6) Effect of surface condition of tool, including consideration of hardness and method of plating.

(7) Effect of diamond abrasive particle size and type.

(8) Effect of cutting fluid composition.

The slicing operation employs a rocking motion and utilizes 50 8-mil wires. These are 6-mil steel wires surrounded by a 1-mil copper sheath, which is impregnated with diamond as an abrasive. The shape of the abrasives and their interaction with the copper and steel is an unknown variable and will be investigated. The individual wires within a multiple wire package are equitensioned by the use of a single jig in the form of a weaving machine.

The variables for slicing have been specifically identified. The independent variables are feed force, speed, rocking angle, and phase angle; the dependent variables are cutting rate, deflection, degradation of diamond, and cut profile of y versus x.

During the quarter, 12 slicing runs were completed with new wire guides and support system. Increasing the diamond concentrations by a factor of 2 has permitted a large increase in wire life. Copper-plated wires with increased diamond concentrations were also utilized, and improved blade life was apparent. Blade wander was identified as a major problem.

12. Ingot Cutting: Breadknife Sawing - Varian Corporation

The purpose of this contract is to develop a multiple-blade sawing process that will significantly reduce the cost of cutting wafers from ingots or blocks of single crystal silicon for solar cell fabrication and has the potential to be scaled up for eventual large production environments. The major portion of the program consists of a systematic experimental investigation of:

(1) Variation in cutting loads.

(2) Speed of slicing head.

(3) Blade dimensions.

(4) Abrasive, size, and concentrations.

(5) Blade material properties and costs.

(6) Lubricants.

(7) Specimen mountings.

During the report period, Varian ran 600-grit boron chloride cutting tests under standard conditions. Cutting time was reduced by about 30% but side losses were very high (approximately 0.008 cm). Slice accuracies were comparable to similar silicon carbide studies. When the slurry flow rate was increased by 5 liters/sec, the slicing typically resulted in <0.005 cm side loss, with fair slice accuracy. Experiments in which the sliding speed was reduced by one-half showed the cutting speed to be reduced by slightly more than one-half. However, slice accuracy and blade wear were the best yet attained. Cutting experiments with 4-mil blades continued to have difficulty.

13. JPL In-House Activities

a. JPL Refractory Materials Program. The objective of this program is to make a preliminary evaluation of the compatibility of selected high temperature refractory materials with molten silicon. The program involves the measurement of wetting angles of sessile drops of molten silicon on selected refractories. Approximately 50 sessile drop experiments will be conducted to provide a basic core of data, and to permit conclusions to be drawn concerning the influence of physical and chemical variables of the refractories.

The basic experiments being conducted involve measuring the contact angle of drops of molten silicon on solid substrates at a temperature just above the melting temperature of silicon. A photographic system is utilized to permit actual measurements to be made from a series of photographs depicting pre-selected time and temperature conditions. These photographs serve as permanent records and records for comparison where some modifications are made, such as a changed atmosphere, in otherwise identical test conditions.

During the quarter, JPL performed 10 sessile drop experiments with substrate materials of reaction-bonded silicon nitride, hot-pressed boron nitride, glassy carbon, mullite, and black glass. The black glass samples did not maintain a flat surface geometry at test temperatures of 1430 $\pm$ 15°C. Efforts to solve the problem are continuing. Excellent photographic results have been obtained for all other samples.

b. JPL Structural and Electrical Characterization. During the quarter considerable work was done in this area at JPL. A 37 mm wide CAST ribbon from IBM was evaluated for resistivity uniformity both on the surface and in a transverse section. A section of ribbon was evaluated that was formed by remelting CAST ribbon in the laser zone melting facility at Motorola. A detailed investigation of the structure of RTR ribbons grown with polysilicon feedstock was performed. Reports were prepared from evaluations of quantitative microscopy as a tool for characterizing silicon ribbon, and of the Bond technique for measuring stress in silicon ribbons.

c. Ingot Technology. It now appears, from an economic analysis performed by JPL, that ingot technology has excellent potential for producing low-cost silicon, provided that current efforts to reduce crucible and machine costs succeed, or, in other words, provided that the technology for continuous ingot growth is developed and the wafering goals presently set for multiblade and multiwire sawing are achieved.

# SECTION VI

# ENCAPSULATION TASK

The objective of the Encapsulation Task is to develop and qualify a solar array module encapsulation system that has a demonstrated high reliability and a 20-year lifetime expectancy in terrestrial environments, and is compatible with the low-cost objectives of the Project.

The scope of the Encapsulation Task includes developing the total system required to protect the optically and electrically active elements of the array from the degrading effects of terrestrial environments. The most difficult technical problem is expected to be developing the element of the encapsulation system for the sunlit side; this element must maintain high transparency for the 20-year lifetime, while also providing protection from adverse environments. In addition, significant technical problems are anticipated at interfaces between the parts of the encapsulation system, between the encapsulation system and the active array elements, and at points where the encapsulation system is penetrated for external electrical connections. Selection of the element for the rear side (i.e., the side opposite to the sunlit side) of the encapsulation system will be based primarily on cost, functional requirements, and compatibility with the other parts of the encapsulation system and with the solar cells.

Depending on the final solar array design implementation, the encapsulation system may also serve other functions, e.g., structural, electrical, etc. - in addition to providing the essential protection.

At present, options are being kept open as to what form the transparent element of the encapsulation system will take - glass or polymer sheet, polymer film, sprayable polymer, castable polymer, etc. The transparent element may contain more than one material and may be integral with the photovoltaic device, or be bonded to it, or installed as a window or lens remote from the device.

## A. TECHNICAL BACKGROUND

Photovoltaic devices (solar cells) and the associated electrical conductors which together constitute solar arrays must be protected from exposure to the environment. Exposure would cause severe degradation of electrical performance as a result of corrosion, contamination, and mechanical damage.

In the past, test experience by government organizations and industry has confirmed that spacecraft solar arrays are poorly designed to survive the earth environment. Arrays designed for terrestrial use have shown mixed results. These results, and analyses performed as part of this task, suggest that long-life, low-cost encapsulation is possible under terrestrial conditions; however, at present, successful protection from degradation by the environment is associated with encapsulation materials and processing costs which are excessive for

large-scale, low-cost use. Thus, an acceptable encapsulation system - one that possesses the required qualities and is compatible with low-cost, high-volume solar array processing - has yet to be developed.

## B. ORGANIZATION AND COORDINATION OF THE ENCAPSULATION TASK EFFORT

The approach being used to achieve the overall objective of the Encapsulation Task includes an appropriate combination of contractor and JPL in-house efforts. The contractor efforts will be carried out in two phases. Within each phase some parallel investigations will be conducted to assure timely accomplishment of objectives.

During Phase I the contractor and the JPL in-house efforts consist primarily of a systematic assessment and documentation of the following items:

(1) Potential candidate encapsulant materials based on past experience with the encapsulation of silicon and other semiconductor devices and on available information on the properties and stability of other potential encapsulant materials and processes.

(2) The environment which the encapsulation system must withstand.

(3) The properties, environmental stability, and potential improvement of potential encapsulant materials and processes.

(4) Test and analytical methods required to evaluate performance and predict and/or verify lifetime of encapsulant materials and encapsulation systems.

The results of this effort will then be used to specifically define additional research, development, and evaluation required during the subsequent phase.

Throughout the task atypical or unique approaches to solving the encapsulation system problem will be sought and evaluated. For example, Phase I will include an evaluation of the feasibility of utilizing electrostatically-bonded integral glass covers as part of the encapsulation system.

In Phase II, contractor and JPL in-house efforts will be conducted to identify and/or develop one or more potentially suitable encapsulation systems and then verify the expected lifetime and reliability of these systems. Depending on the results of Phase I, the contractor effort in this phase will include an appropriate combination of some of the following items:

(1) Evaluate, develop, and/or modify test and analytical methods and then validate these methods.

(2) Perform materials and interaction testing, using these methods to evaluate candidates and demonstrate the reliability of encapsulation systems.

(3) Modify materials and processes used in encapsulation systems to improve automation and cost potential.

(4) Modify potential encapsulation system materials to optimize mechanical, thermal and aging properties.

(5) Implement research and development on new encapsulant materials.

## C. ENCAPSULATION TASK CONTRACTS

Encapsulation Task contracts are shown in Table 6-1. In addition, Professor Charles Rogers, Department of Macromolecular Science, Case Western Reserve University, serves as a consultant to this task (JPL Contract No. 954738). Dr. Rogers is a specialist in polymer characteristics and aging as well as the field of diffusion through polymers. He serves as a technical specialist and also provides assistance in defining the overall scope and direction of the task activities. He will also implement selected supporting experimental investigations in the laboratories at Case.

Contractual negotiations in progress include follow-on contracts to the four major contractors, a contract with the Rockwell Science Center to study the surface characteristics of solar cells. a contract with the Motorola Solar Energy Department to investigate the feasibility of developing antireflectance coatings for glass, and a contract with Endurex of Mesquite, Texas, to study ion plating coating techniques. All of the above contracts are scheduled for execution in the third and fourth quarters of FY 1977.

In addition, considerable effort has been expended in preparing two Phase II statements of work. These are essentially complete, but may be held up pending release of the Battelle Study 4 report on life prediction methodology.

## D. ENCAPSULATION TASK TECHNICAL ACTIVITY

The sequence of Encapsulation Task technical activities is shown in Figure 6-1.

Table 6-1. Encapsulation Task Contractors

| Contractor | Technology Area |
|---|---|
| Battelle Memorial Institute<br>Columbus, Ohio<br>(JPL Contract No. 954328) | Study 1: Identification of candidate encapsulant materials based on a review of (a) worldwide experience with encapsulant systems for silicon solar cells and related devices and (b) the properties of other available materials.<br><br>Study 2: Definition of environmental conditions for qualifying encapsulant materials.<br><br>Study 3: Evaluation of encapsulant material properties and test methods.<br><br>Study 4: Analysis of accelerated/abbreviated encapsulant test methods. |
| Rockwell International<br>Anaheim, California<br>(JPL Contract No. 954458) | Experimental evaluation of accelerated/abbreviated encapsulant test methods. |
| Simulation Physics<br>Burlington, Massachusetts<br>(JPL Contract No. 954521) | Electrostatically-bonded glass covers. |
| Springborn Laboratories<br>(formerly DeBell and Richardson)<br>Enfield, Connecticut<br>(JPL Contract No. 954527) | Polymer properties and aging. |

1. Study 1: Identification of Candidate Encapsulant Materials: Worldwide Experience and Available Materials - Battelle

Work on this study was completed during the April-June 1976 quarter. The final report was distributed during the present report period (Review of World Experience and Properties of Materials for Encapsulation of Terrestrial Photovoltaic Arrays, Report No. ERDA/JPL-954328-76/4, Battelle Columbus Laboratories). In the course of the study over 1000 documents were reviewed, out of approximately 6000 identified in various literature searches. These documents relate primarily to worldwide experience in encapsulation in various kinds of

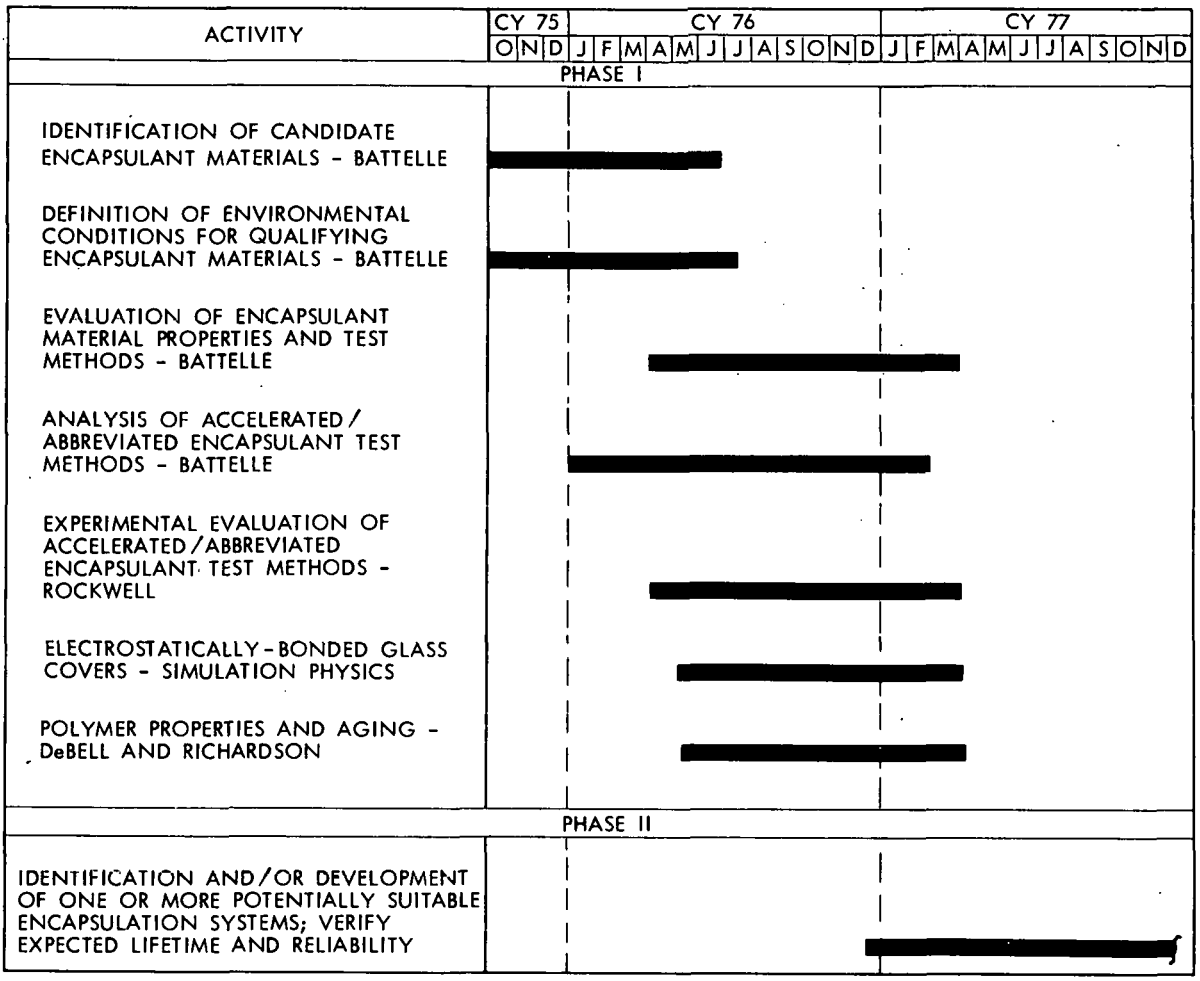


Figure 6-1. Encapsulation Task Schedule

devices and the terrestrial use of transparent materials. Specific references on appropriate materials and their properties were also included. No one or group of outstanding candidate encapsulant materials was identified from this effort. The lack of definition of module design implementation requirements precluded specific identification of leading candidates. The information gathered will provide the basis for candidate selection as module design requirements are defined.

2. Study 2: Definition of Environmental Conditions for Qualifying Encapsulant Materials - Battelle

Work on this study was completed during the April-June 1976 quarter. The final report was distributed during the present report period (Terrestrial Service Environments for Selected Geographic Locations, ERDA/JPL-954328-76/5, Battelle Columbus Laboratories). The study was concerned with developing an understanding of the environments which

the module must withstand. Real-time field testing to the 20-year lifetime is obviously impossible; testing in a wide variety of locations is impractical; and materials selection to unrealistic environmental requirements would prove excessively costly. The validity of extrapolating available aging data, laboratory test data, or field test data to 20 years in a particular environment depends on the relationship of the test environment to that of the longer period.

The decision as to whether to seek a single encapsulant suitable for all possible locations or several climate-unique designs depends on many factors including production, economics, etc. In either case, a knowledge of the various environments is essential to such a decision.

## 3. Study 3: Evaluation of Encapsulant Materials Properties and Test Methods - Battelle

Results of the analysis of the world experience with existing modules (Study 1) indicate that major problems have been encountered with materials interactions and interfaces, and these problems have been more important than changes in bulk properties of materials. Experience has shown that many module failures occur, for instance, at the seals attaching the bottom cover to the top cover and at interfaces forming the seal of the electrical leads to the protective covers. Further encapsulation system developments depend significantly on finding solutions to the seal and other interface problems. Thus. a substantial portion of the Study 3 effort during the quarter was directed toward investigating the materials properties involved in these problems. The environmental parameters of first concern are ultraviolet radiation, temperature (including temperature cycling), and relative humidity.

For purposes of reporting, the efforts of Study 3 are organized into studies of polymeric materials and studies of glass materials. This division is somewhat arbitrary because many of the encapsulation concepts employing glass (as the top cover) employ polymeric materials as well.

### a. Polymeric Materials Studies

#### Bond-Strength Measurements

The principal efforts have been directed toward screening adhesives and sealants for use with candidate encapsulants. To date, tests with several candidate adhesives have determined the effects on bond strength of exposures to ultraviolet radiation and temperature cycling. Teflon FEP and weatherable Mylar films (which were the first materials received) were used in the tests. Measurements of water permeation rates for adhesive/film composites were made.

Lap-shear specimens (2.54 X 12.7-cm strips) of the selected film materials were used in the bond-strength measurements. (Two of these strips are used for each lap-joint.) Bond-strength measurements were

made on lap-shearspecimens after they had been exposed to a potentially degrading environment (ultraviolet radiation or temperature cycling). The ultraviolet radiation was provided by a 6000-watt xenon lamp; the temperature-cycling was carried out in a commercial environmental chamber, in which the temperature was cycled in the range -40 to +90°C over a 4-hour cycle time.

Water Vapor Transmission Rate Measurements

Experience to date with the encapsulation of photovoltaic modules with polymeric materials indicates that water vapor is one of the important contaminants affecting the service life of the enclosed solar cells. The rate of water vapor transmission (WVTR) through films/adhesives is being studied through the use of a film pouch (or "pillow pack"). Pouches were used for measuring WVTR before and after temperature cycling (-40 to +90°C) and after ultraviolet exposure for 500 and 1000 hours.

The pouches were prepared* by bonding three sides, inserting the desiccant (10 grams of Drierite), and sealing the fourth side. Temperature cycling and ultraviolet exposures of the test pouches were carried out prior to adding the desiccant and sealing the fourth side. Following preparation, the pouches were placed in a closed environment in which the relative humidity was 95% and the temperature 23°C. Periodically, the pouches were removed from the environment and weighed.

In all experiments to date, the weight increase has been a linear function of exposure time. Thus, the slope of the weight-time relationship is proportional to the water vapor transmission rate.

Photon Emission Measurements

Measurements of photon emissions from materials owing to oxidation reactions (chemiluminescence) have been made to determine if such measurements can be used as a diagnostic tool to evaluate degradation rates. Initial measurements have been made on "sandwich" specimens in which Mylar and FEP films were used as the sandwich material; RTV-118 and Scotch Weld 2216 B/A were the adhesives. Exposures have included ultraviolet radiation and temperature cycling of the type described previously. Actual measurements (photon counting) were made in an air enclosure at 26°C.

---

*Two square films, 8.9 cm (3.5 in.) on a side, are bonded together along the outside edges of the films. The bond area is 1.27 cm (0.50 in.) wide; the total bonded area is thus 38.7 $cm^2$ (6.0 $in.^2$). Water-permeation-rate calculations are based on the total film area containing the desiccant (0.08 $m^2$).

b. Glass Materials Studies

Study 1 identified three areas of primary importance in long-life performance of encapsulation systems incorporating glass covers: (1) the cover glass/solar-cell organic bond, (2) the "hermetic" sealing of the array, and (3) the corrosion of electrical conductors (metallization, interconnects. and leads) at the interfaces with either adhesives or sealants. Thus, the material properties of prime importance to long life are those bearing on the interactions and behavior at these interfaces. The methods evolved for life testing must therefore reflect changes in properties which are critical to interface degradation problems.

The organic adhesive layer between a cover glass and a silicon solar cell that is being investigated in this study, should serve several functions. First, it should provide optical coupling with maximum transmission over the wavelength range of 280 to 1100 nanometers. Second, it should maintain its mechanical integrity plus the bond integrities at both the glass-adhesive and cell-adhesive interfaces. Third, it should avoid thermal stress levels which would damage the cell, cell metallization, or interconnects. Finally, the adhesive should be noncorrosive.

Large thermal mismatches among organic adhesives, silicon cells. and soda-lime glass (which is preferred over borosilicate for its low cost) provide the potential for severe thermal stress over the specified temperature cycle between -40 and +90 C. The most promising solution to this thermal stress problem appears to be the use of low-modulus adhesives.

The experimental studies included two subject areas: (1) screening-type tests of cell-adhesive-glass interface samples and (2) adhesive-property measurements. Screening tests were performed on sandwich-type samples consisting of a single cell, adhesive, and glass. A portion of the samples contained leads to permit pre- and post-test electrical measurements on the cell. Sample sandwiches utilized either soda-lime float glass or 7740 borosilicate glass plates. Adhesives were selected on the basis of Study 1 information and discussions with adhesive manufacturers, and additional candidates are expected to be identified for screening evaluations.

4. Study 4: Analysis of Accelerated/Abbreviated Encapsulant Test Methods - Battelle

A literature search has revealed no data suitable for use in the validation of life prediction studies. This finding has been a serious blow to the development of a suitable methodology for designing statistical and experimental techniques. The inadequacies of the data include a lack of sufficient replication, insufficient precision and accuracy of measurements, and a lack of established relationships between degradation modes and measurement methods/techniques.

In previous reports on Study 4, several aspects relative to developing a methodology for aging tests have been treated; among these topics are aging mechanisms in polymers and in glasses, sensitivity analyses required to give detectable property changes with statistical validity, and discrimination among mathematical models of aging data during the acquisition of such data. During the past quarter, investigations were conducted on discrimination among the test methods used in acquiring aging data on the basis of precision and cost.

Considerable attention was given to abbreviated testing. In such testing, samples are exposed under "normal" terrestrial conditions for some period of time, $t_i$. Using data collected in this time interval, properties of the material or system are forecast for a future time, $t_f$. Guideline values for $t_i$ and $t_f$ in Study 4 are 2 and 20 years, respectively. For successful prediction over such a long period, the properties measured in the initial 2-year interval have to be measured with high precision. A means of discriminating among various test methods on the basis of precision as well as cost and other factors is therefore required.

Published information was reviewed to find information on precision, accuracy, repeatability, reproducibility, etc., as applied to polymer testing. In this effort the Engineering Index, Chemical Abstracts, and NTIS files were interrogated. Out of a total of 249 documents identified through this interrogation, only 21 appeared relevant to the problem of test comparison. Most of the 21 have been received and found to be of little value with regard to test discrimination.

Perhaps the largest repository of information on test accuracy and precision is the American Society for Testing and Materials published test methods. Accordingly, the 1975 Annual Book of ASTM Standards, Part 35 for General Test Methods for Plastics, was scrutinized for precision information. The methods for which the coefficient of variation was given, or was calculable from the information included, showed a wide range of precision, and underscored the need for a systematic methodology for test discrimination. Mandel recognized the problem and defined a relatively sensitive statistic for test discrimination. Mandel's sensitivity ratio, transformations of scale, sample size (number of specimens), and cost were explored using methods developed by Mandel.

## 5. Experimental Evaluation of Accelerated/Abbreviated Encapsulant Test Methods - Rockwell International

The objective of this study is to develop methodology for the accelerated/abbreviated testing of solar cell encapsulant systems and to predict encapsulant performance during 20 years' exposure. Steps in the program are as follows:

(1) Attempt to fit literature weathering data for plastics/encapsulants into statistical models. References were supplied by Dattelle (Study 1). Other statistical aspects

have been included, such as the number of replicates required for tests.

(2) Generate a test program plan including field tests to verify and refine the proposed statistical models. Abbreviated test methodology has been developed. Weather data from the selected outdoor sites were used to set the levels of primary weather variables (light intensity, temperature, humidity) in the accelerated tests. These weather data were supplied by Battelle (Study 2).

(3) Design and fabricate a Universal Test Specimen (UTS) for evaluating encapsulants in both outdoor and accelerated tests. The UTS design uses three selected encapsulant systems: Sylgard 184 transparent silicone rubber, Sylgard 184 surfaced with Tedlar polyvinyl fluoride film, and Sylgard 184 surfaced with unstabilized Lexan polycarbonate film. The UTS design employs electrically active solar cells.

(4) Carry out the test program plan. An artificial weathering chamber was constructed. This comprises 24 rectangular tubes, each with a different combination of light intensity, temperature, and humidity. UTSs and plastic film samples, exposed for different periods of time to outdoor and accelerated conditions, are being subjected to a variety of property measurements. Degradation rates will be calculated from these data.

Steps 1, 2, 3 and most of the accelerated exposure tests of Step 4 have been completed. Data must be correlated and interpreted to complete the first year's program.

Phoenix (Arizona) and Miami (Florida) were selected as suitable sites for outdoor weathering tests. Complete weather data and outdoor exposure services are available at both locations. The encapsulated test specimens (UTSs) were placed outdoors on racks and are being returned at predetermined time intervals. Upon receipt, they are being examined chemically, physically, and electrically to establish the degradation rate and suggest probable degradation mechanisms.

Similar test specimens are being exposed in a weathering chamber (xenon lamp) in the laboratory. The factors being studied are light intensity, temperature, and humidity in 24 combinations. Degradation rates are being measured and will be compared with those found for outdoor exposure.

The test specimens are holding up well under all exposure conditions with no catastrophic failures. Yellowing of the plastic film cover in encapsulant systems is the principal reaction noted to

date. This yellowing is 3 to 4 times faster on the EMMA* and EMMAQUA** sunlight-concentrators at Phoenix than under normal exposure at 45°C. Humidity appears to play little or no role in yellowing. The rate is rather faster in Phoenix than in Miami.

Film yellowing occurs over 300 times faster under a xenon lamp (indoor weathering) than under sunlight. This is due to the effects of short ultraviolet radiation in the range of 295-330 nanometers. The output of this damaging ultraviolet radiation decreases as the xenon lamp ages.

The electrical power output of the solar cells has not changed appreciably after 30 days' exposure of the UTSs outdoors or under the xenon lamp. Consequently, neither the film yellowing nor any other reaction has reduced solar cell performance appreciably.

Advanced analytical methods have been used successfully to identify the new chemical groups at or near the surface that are formed as a result of photochemical, oxidative, and perhaps hydrolytic reactions. These methods include ultraviolet spectral change, attenuated total reflectance (ATR), infrared analysis, electron surface chemical analysis, and Fourier transform ATR.

The experimental data fit the Weibull mathematical model. The constants in the Weibull equation are $\alpha$, $\beta$, and $\gamma$. These are being defined and understood. Seasonal weather factors play an important role in the rate of degradation as expressed by the magnitude of $\gamma$.

## 6. Electrostatically-Bonded Integral Glass Covers - Simulation Physics

The objective of this program is to develop integral glass encapsulation for solar cell arrays. Progress to date demonstrates that integral glass encapsulation by electrostatic bonding is unquestionably feasible. Integral glass encapsulation has promise for major improvements in module performance and stability at substantially lower cost than state-of-the-art organic material encapsulants.

Electrostatic bonding can be used to form a permanent adhesiveless seal between silicon solar cells and a sheet of glass. This program involves investigation of the requirements and limitations of this process for array encapsulation, development of utilization techniques, and evaluation of integral module test configurations. At this time it is evident that the electrostatic bonding process is fully compatible with the components of the solar cell array; techniques for its use have been established. All evaluation data now available suggest that

---

*Approximately 8 times sunlight concentration (Desert Sunshine Exposure Test, Inc.).

**Approximately 8 times sunlight concentration with intermittent water spray (Desert Sunshine Exposure Test, Inc.).

the electrostatic bond is extremely strong and apparently absolutely stable. A correctly designed and assembled integral glass solar array should be characterized by excellent functional lifetime.

Efforts of the past three months involved the following items:

(1) Assembly and testing of the controlled environment bonder.

(2) A partial assessment of the effects of various atmospheres, including nitrogen, forming gas, argon, and vacuum, on bond quality.

(3) Contact and interconnect metallization studies including evaluation of bonds formed with evaporated films of several refractory metals, e.g., bonding with silver, bonding with silk-screened metallization on glass.

(4) Glass surface evaluation including bonding to as-pressed 7070 glass, re-pressing of irregular glass surfaces, and the formation of cavities in glass by pressing.

(5) Preparation of samples for testing shear strength and hermeticity of electrostatic bonds.

(6) Module design specification and development.

With the controlled environment bonder it has been possible to bond a wide range of materials which would not bond in an oxidizing atmosphere. This bonder, capable of handling 6-inch-square samples, has already demonstrated the feasibility of large area bonds by simultaneously bonding five 2-1/4-inch-diameter electrically active solar cells to single pieces of glass. A mechanical vacuum pump brings the chamber pressure, for vacuum bonding, to the working level of 10 micrometers Hg within 5 minutes. A gas manifold allows the introduction of four separate gases when backfilling is desired. A diffusion pump may be added for lower pressure during vacuum bonding, but at present this appears unnecessary. Bonding temperature and voltage limitations are in excess of 620°C and 1500 volts, respectively.

With this bonder, it is now possible for the first time to evaluate the effect of atmospheric composition on the quality of electrostatic bonds. Furthermore, it is now possible to join materials that are not bondable in air. Bonding has been performed with a number of materials in atmospheres of nitrogen, forming gas, and argon as well as under vacuum. The use of argon has been limited by the rather low voltage breakdown strength of this gas. Bonds formed in atmospheres of nitrogen and forming gas are much cleaner than those formed in air but vacuum bonds are superior, at least in appearance. An additional advantage of vacuum bonding is that the possibility of trapping gas bubbles between bonded surfaces is greatly reduced. A full evaluation of the effects of atmospheric composition would require, at a minimum, measurements of bond strength as a function of bonding environment. In the case of metals used as solar cell contacts, a measurement of contact resistance to silicon will also be necessary. A number of samples

designed to test bond shear strength and hermeticity have been prepared. Preparation of such test samples will continue. For the present, solar cell bonds are being made primarily under vacuum.

7. Polymer Properties and Aging - Springborn Laboratories (formerly DeBell and Richardson)

The goal of this program is to develop and test encapsulation materials and processes that will be suitable for protecting solar cells during a service life of at least 20 years in a terrestrial environment. The work is being conducted at Springborn Laboratories facilities in Enfield, Connecticut, with cell performance being evaluated under subcontract by Solar Power Corporation.

The materials selected for this program have been chosen for three general properties: clarity, toughness, and weatherability. The testing program incorporates evaluation of initial properties and subsequent retesting after exposure to accelerated aging conditions. The aging environments consist of combinations of heat, humidity, and ultraviolet light, with sample testing at four time intervals. The testing program involves three basic areas:

(1) Mechanical - tensile strength, modulus, brittleness, impact strength.

(2) Optical - total integrated transmittance, haze, absorption versus wavelength, infrared attenuation.

(3) Miscellaneous - water vapor permeability, insulation resistance, fungus resistance, abrasion resistance.

In addition to the testing of aged materials, efforts are being made to develop predictive methods to aid in the correlation of artificial to natural weathering processes.

The overall program is also structured to include four other technical endeavors: cost analysis, selection of primers and enhancement of adhesion, upgrading of stability under exposure to ultraviolet, and processing repair studies. The final report will encompass an overall performance analysis and will include recommendations for several optimized designs for complete solar panels.

Twenty-four polymers were selected for testing and evaluation as potentially useful encapsulating compounds. These materials have been exposed to six accelerated aging conditions and subsequently tested for mechanical and optical properties.

After 120 days of exposure to accelerated aging conditions, 11 materials have been dropped from the testing program because of low mechanical strengths, low optical transmission, ultraviolet degradation, poor optical stability, and/or poor processability. The remaining 13 plastics will continue through to 240-day evaluations and, in addition, will be used for advanced tests. Advanced testing includes flammability

(UL 94), insulation resistance (ASTM D257), coefficient of thermal expansion (ASTM D 696), water vapor permeability (ASTM E 96), and temperature versus tensile property measurements. In the temperature/tensile tests dog bone specimens will be analyzed for stress/strain characteristics from -60 to +140°C in 20°C intervals. This will permit observation of some of the changes in material properties under conditions that might be encountered in both arctic and tropical regions. Room temperature (20°C) properties have already been obtained.

The most significant property to be measured in the testing program is the amount of usable solar energy that passes through the encapsulant material after exposure to the various aging conditions. A procedure combining the desired characteristics of both haze and luminous transmittance has been developed. A Beckman 505 spectrometer has been modified to provide rapid and accurate assessment of total integrated transmittance from 350 to 800 nanometers. This was achieved by relocating the sample compartment to a position in which an optically reflective integrating sphere could be used to measure both direct-beam and 60° angle scatter transmission simultaneously. Measurements are made every 50 nanometers, normalized to the solar spectrum, and integrated on a Monroe 1860 programmable calculator to give the final total integrated transmittance value. Ultraviolet values (280-350 nanometers) are calculated in a separate procedure.

In all cases the transmission values can be seen to decrease from the control measurement made on unaged material. The two most severe conditions are produced by the carbon arc Weather-Ometer and the RS-4 Sunlamp exposure at 100°C. In some cases the material did not survive to be tested. The greatest effects can generally be noticed in conditions incorporating ultraviolet light sources.

For all materials and all conditions, surface hardness is found to decrease with increasing exposure time except for two silicone rubbers. These materials show steady increases in surface hardness with time regardless of aging condition and are probably continuing the process of curing at a very slow rate. This is not supported by the tensile results, however, which show general trends towards decreased tensile strengths and increased elongations.

The candidate encapsulant materials were mounted on a rack (45° inclination due south) on the roof of Springborn Laboratories facility in Enfield, Connecticut for a period of six months for a soil accumulation study. The materials were routinely inspected for damage and accumulation of surface debris. All of the relatively hard plastic materials were found to have clean surfaces covered by a very thin layer of easily removable dust. The materials showing permanently adhering accumulation of dirt were all rubbers (silicones and fluorocarbons).

The materials were tested for fungus attack resistance using standard ASTM procedure G 21. Three specimens of each material were placed in petri dishes on inoculated agar and incubated for 21 days at 28-30°C. A mixed sport suspension of five fungi known to attack

synthetic materials was used to inoculate the medium. At the end of the incubation period the polymer discs were removed, washed, and examined for persistent growth.

Most materials supported light coverings of fungi but showed no great evidence of surface attack. Three materials, however, were very obviously damaged. Cellulose acetate-butyrate showed surface hazing and many large dark green splotches of adhering fungus. Two silicone rubbers were much less affected but still had a light covering of readily visible green dots. These materials may require fungus resistant coatings in field use.

A section of the present contract provides for the actual encapsulation of cell systems with the materials under study and subsequent exposure to both artificial and natural weathering conditions prior to testing. Because the cells and interconnects are not self-supporting, a rigid structural component is required. Three substrates were selected for this purpose from a list of previously identified potential substrate materials. Polyester/fiberglass, aluminum, and epoxy-glass (Nema G10) will be used in the construction of all miniature cell modules. These test modules are being prepared by Solar Power Corporation under subcontract and consist of two electrically active cells bonded to the substrate with one interconnect between them. Power leads are soldered to either side of the cell fixture and come out through the underside of the substrate to permit electrical testing.

Completed cell modules will be exposed to Weather-Ometer, oven, and RS-4 fluorescent sunlamp conditions for two time periods. Testing of electrical characteristics (I/V curve) will be performed before and after encapsulation, to determine if cell or interconnect damage has occurred, and again after the exposure times. It is hoped that the effects of moisture, delamination, corrosion, etc. will be observable in this study.

The most expedient methods of fabricating the encapsulant systems are still being developed. In the easiest cases, the primary encapsulant is merely poured into place as a liquid and cured in an oven. Compression molding is also a facile technique but cannot be used with any material other than cellulose acetate-butyrate. The reason for this is that all the other polymers of interest have "melting" points in excess of the solder and metallization melt temperature. Present experiments show that sintering is a feasible process, however. In this procedure the cell module is covered with a layer of powdered resin and heated to flow temperature in an oven. The molten solder on the cell surfaces does not appear to migrate as the resin fuses and solidifies intact during the cooling cycle. An alternative method that may be employed is solution coating. A disadvantage of this process is that multiple coats have to be built up, with a drying period allowed after each coat, in order to achieve the required thickness.

8. Consultant Services - Professor C. E. Rogers, Case Western Reserve University

Diffusion/permeability studies of various gases and encapsulation materials are in progress. Professor C. E. Rogers, principal investigator, is also available to consult on various diffusion/permeability problems and for reviewing literature articles, contractor reports, and miscellaneous documentation.

9. JPL In-House Activities

Fracture Mechanics of Interfaces

Basic studies of adhesive bonding from a fracture mechanics standpoint are being continued by Dr. W. Knauss of Caltech.

Test Module Development

Development of a test module for in-house fabrication, exposure, and test has been suspended owing to manpower problems. The object of this program is to establish design criteria for encapsulation systems and to apply current life prediction methodology. Program development is planned for the next quarter.

Failure Analyses of Block 1 and Block 2 Procurement Modules

This work was also suspended because of lack of manpower. Full support to the failure analysis effort will be resumed in the next quarter.

# SECTION VII

# SOLAR ARRAY AUTOMATED ASSEMBLY TASK

The overall objective of the Solar Array Automated Assembly Task is to develop the technology necessary to achieve high-volume, low-cost production of silicon solar array modules. The goal of this task is to develop the capability to fabricate solar array modules of 10% or better conversion efficiency at a selling price of $0.50/watt or less, at a rate of 500 megawatts per year, with a 20-year operating life. Many of the decisions that must be made during the task effort cannot be made independently and will result from trade-offs with other decisions that are made both within this task and in conjunction with other tasks of the Project.

## A. TECHNICAL BACKGROUND

The manufacture of solar cells and arrays is presently accomplished under the judgment and direct control of individual operators. Because of the limited quantities of solar cells and arrays produced, costs are high. Automated solar cell production, as proposed, will lead to significant reductions in manufacturing cost. In addition, automation will result in uniformity of cell processing with a reduction of waste due to rejected product.

## B. ORGANIZATION AND COORDINATION OF THE SOLAR ARRAY AUTOMATED ASSEMBLY TASK EFFORT

The Solar Array Automated Assembly Task is divided into five phases, occurring over a 10-year period of time (Figure 7-1). The phases are:

I. Technology assessment.
II. Process development.
III. Facility and equipment design.
IV. Experimental plant construction.
V. Conversion to mass production plant (by 1986).

Phase I was initiated in February 1976 and has been under way for 9 months. Phase I has these specific objectives:

(1) To identify the requirements for economical manufacturing processes and facilities.

(2) To assess the technology currently used in the manufacture and assembly processes that could be applied to solar arrays.

(3) To determine the level of technology readiness to achieve high-volume, low-cost production.

(4) To propose processes for development.

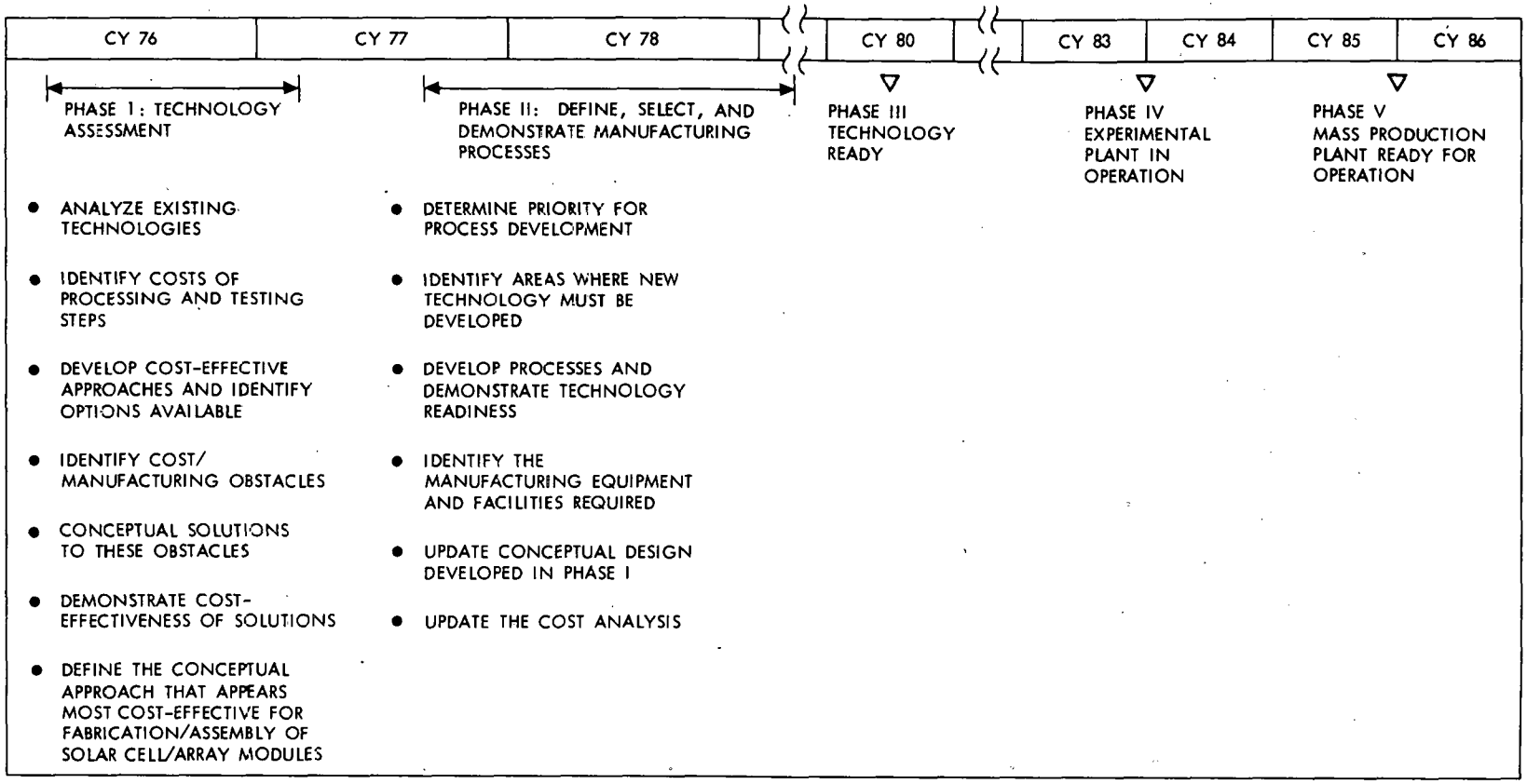


Figure 7-1. Solar Array Automated Assembly Task Schedule

It is anticipated that the Request for Proposal package for Phase II will be distributed to industry early in 1977.

## C. SOLAR ARRAY AUTOMATED ASSEMBLY TASK CONTRACTS

Under Phase I contracts, three contractors (Motorola, RCA, and Texas Instruments) are performing parallel efforts (Table 7-1). The three-contractor parallel-effort philosophy was selected to obtain the broadest possible view of recommendations and conclusions upon which to base the contractual efforts of Phase II (Figure 7-1). During Phase I, these contractors are defining the requirements for an automated solar cell manufacturing sequence by evaluating processes now used by the semiconductor industry and the ways in which these processes can be modified/selected for high-volume, low-cost production of solar cell modules. Cost analyses are being conducted to provide economic guidelines to maintain an overall view of LSSA Project objectives.

The Phase I contractors nearly completed the technology assessment activities during this quarter. Under the basic contract, these studies were planned to conclude in January; however, selected contracts are being extended approximately 6 months to pursue analysis of key process vatiables.

Table 7-1. Solar Array Automated Assembly Task Contractors

| Contractor | Type Contract | Technology Area |
|---|---|---|
| Motorola<br>Phoenix, Arizona<br>(JPL Contract No. 954363) | Phase I | Manufacturing processes assessment |
| RCA<br>Princeton, New Jersey<br>(JPL Contract No. 954352) | Phase I | Manufacturing processes assessment |
| Texas Instruments<br>Dallas, Texas<br>(JPL Contract No. 954405) | Phase I | Manufacturing processes assessment |
| Texas Instruments<br>Dallas, Texas<br>(JPL Contract No. 954475) | Support | Large area Czochralski silicon ingot growth and wafering improvements |

## D. SOLAR ARRAY AUTOMATED ASSEMBLY TASK TECHNICAL ACTIVITY

A number of different manufacturing sequences suitable for low-cost mass production have been put forth by contractors during this quarter. Proposed processes have been investigated and defined individually, and have in many cases been tested within complete sequences for synergistic interaction. This has led to recommended modifications of some process sequences, and in recommendations for more detailed development of others.

A process cost analysis chart has been prepared by task personnel based upon contractor-supplied data (Table 7-2), The chart presents detailed cost data in such a manner as to provide subtotal costs for any combination of process sequences currently being considered. The Motorola, RCA, and Texas Instruments contracts have been recommended for extension to allow the contractors to establish manufacturing process tolerances-vs.-cost ratios that will underlie ultimate process specifications.

Contractor investigation of polymer doping is continuing, as is an exploration of ohmic contact metallization for cost and performance optimization. A contractor stated during this period that ~6 cm appears to be the optimum ingot diameter. The introduction of different encapsulation designs by the three contractors is expected to enhance cost flexibility.

### 1. Manufacturing Processes Assessment - Motorola, RCA, and Texas Instruments

Motorola

Studies for this period have included further technical evaluations of processes and process sequences, solar cell fabrication and encapsulation, and analysis of processing costs.

Experiments were performed to measure light reflection from the back surface of silicon wafers having various front-surface and back-surface optical conditions. These studies have shown that light can be readily absorbed, not reflected, from silicon-metal interfaces, whereas reflection from silicon-dielectric interfaces is much greater. This suggests that patterned back metal could increase solar cell efficiency.

Three-inch-diameter solar cells were fabricated utilizing an ion-implanted planar P-N junction and a textured front surface. Evaluation of such cells has shown an AMO efficiency of 13.1% based on total junction area. These efficiency figures indicate that ion implantation is a viable process technique for high efficiency solar cells.

Plasma processing has been evaluated and has been recategorized in the processing matrix as a process having a high chance of future use.

RCA Laboratories

The RCA program is now including a more substantial activity in the experimental evaluation of the processes which appear to be the most cost effective. In addition, the theoretical evaluation of solar array module performance is being developed to provide a sound basis for the projection of performance at the conclusion of this phase.

Experiments with solar cells fabricated by ion implantation and vapor phase epitaxy suggest that both of these interesting technologies are worthy of pursuit.

RCA has developed an understanding of the impact of metallization costs upon cell size. There is an increase in metallization cost/watt as cell size increases. However, the cost/watt of other cell processes decreases with increasing cell size.

Analysis of the power-loss penalty in a hierarchy of metallizations on a large cell has been extended. The goal is to determine if the total power loss, when minimized, can optimize a maximum cell size that is practical.

The problems of optimizing the output power of a cell with several levels of current collectors has been found to be generally insoluble unless some arbitrary external conditions are imposed. It is desirable to minimize the number of arbitrary conditions and where possible to use existing physical properties as the basis for the additional choices. A very real related consideration is the restriction imposed by the metallization technology utilized.

These considerations are illustrated in Figure 7-2 by application to currently used 7.6-cm-diameter wafers with the requirement that screen-printed Ag metal be used for both fine grid and collector. The fine grid lines are 12 $\mu$m thick and 125 $\mu$m wide, and have a metal sheet resistance of $2.7 \times 10^{-3}$ $\Omega/\square$.

The collection strip is 500 $\mu$m thick and the minimum width is 1000 $\mu$m, and the metal sheet resistance is $6.4 \times 10^{-5}$ $\Omega/\square$. The grid length is chosen arbitrarily to fix a basic pattern size; a commonly used value has been L = 2 cm with a contact strip on one end, or 4 cm with double-sided contacts. Once the values of $J_m$ (current density at maximum power) and $V_m$ (voltage at maximum power) have been chosen, the general equation may be differentiated over a wide range of values of $\rho_c$ (the specific contact resistance), which is generally the least-known physical property of metallization systems. The curves of the figure were calculated in this manner and allowed direct observations of the effect of different values of $\rho_c$.

Table 7-2. Silicon Solar Module Manufacturing Cost-Breakdown in Dollars Per Watt

| SILICON FORM A. CZOCHRALSKI B. RIBBON C. SHEET SUBSTRATE | | | PROCESS STEPS (ITEMIZED) | MATERIALS | | | EXPENSE ITEMS | | | LABOR | | | OVERHEAD | | | INTEREST (9%) | | |
|---|---|---|---|---|---|---|---|---|---|---|---|---|---|---|---|---|---|---|
| RCA | TI | MOT. | SURFACE PREPARATION | RCA | TI | MOT. | RCA | TI | MOT. | RCA | TI | MOT. | RCA | TI | MOT. | RCA | TI | MOT. |
| A,B,C | | A,B,C | 1. BRUSHING | 0.0 | 0.0125 | 0.0 | 0.004 | | 0.0073 | 0.038 | 0.0088 | 0.0134 | 0.022 | 0.0088 | 0.0066 | 0.003 | | 0.0023 |
| A,B,C | | A,B,C | 2. PLASMA (CLEANING) | 0.0 | | 0.0 | 0.045 | | 0.0009 | 0.021 | | 0.0084 | 0.026 | | 0.0049 | 0.003 | | 0.0004 |
| | | A,B,C | 3. REVERSE SPUTTERING | | 0.0002 | 0.0 | | | 0.0032 | | 0.0023 | 0.0318 | | 0.0023 | | | | 0.0236 |
| A,B,C | | | 4. SC-1 CLEANING | 0.0 | | | 0.035 | | | 0.007 | | | 0.004 | | | 0.001 | | |
| A,B,C | | A,B,C | 5. ULTRASONIC CLEANING | 0.0 | 0.0002 | 0.0 | 0.008 | | | 0.020 | 0.0044 | | 0.014 | 0.0044 | | 0.002 | | |
| A,B,C | | A,B,C | 6. STANDARD SOLUTIONS | 0.0 | | 0.0 | 0.002 | | 0.0041 | 0.013 | | 0.0061 | 0.009 | | 0.0042 | 0.000 | | 0.0006 |
| | | A,B,C | 7. BLOW DRY | | | 0.0 | | | | | | | | | | | | |
| | | A,B,C | 8. CENTRIFUGE | | | 0.0 | | | 0.0014 | | | 0.0042 | | | 0.0035 | | | 0.0003 |
| A,B,C | | A,B,C | 9. ETCHING (TWO SIDES) | 0.0 | | 0.0 | 0.046 | | 0.0161 | 0.008 | | 0.0243 | 0.006 | | 0.0102 | 0.001 | | 0.0012 |
| A,B,C | | A,B,C | 10. ETCHING (ONE SIDE) | 0.0 | | 0.0 | 0.023 | | 0.0124 | 0.008 | | 0.0243 | 0.006 | | 0.0102 | 0.001 | | 0.0012 |
| A,B,C | | | 11. EDGE ETCH | 0.0 | | | 0.034 | | | 0.007 | | | 0.011 | | | 0.002 | | |
| A | | A | 12. EDGE GRINDING | 0.0 | | 0.0 | 0.021 | | 0.0209 | 0.002 | | 0.0269 | 0.001 | | 0.0113 | 0.000 | | 0.0046 |
| A,B,C | | | 13. TEXTURIZE (HYDRAZINE) | 0.0 | 0.0178 | | 0.020 | | | 0.027 | 0.0088 | | 0.030 | 0.0088 | | 0.001 | | |
| A,B,C | A | A,B,C | 14. TEXTURIZE (HYDROXIDE) | 0.0 | 0.0014 | 0.0 | 0.004 | | 0.0097 | 0.027 | 0.0088 | 0.0243 | 0.030 | 0.0088 | 0.0102 | 0.001 | | 0.0012 |
| A,B,C | | A,B,C | 15. PHOTO-RESIST (APPLY & DEVELOP) | 0.0 | 0.0205 | 0.0 | 0.071 | | 0.0107 | 0.004 | 0.0081 | 0.0403 | 0.003 | 0.0162 | 0.0159 | 0.002 | | 0.0073 |
| A,B,C | | A,B,C | 16. PHOTO-RESIST (REMOVE) | 0.0 | 0.0001 | 0.0 | 0.010 | | 0.0213 | 0.003 | 0.0044 | 0.0061 | 0.003 | 0.0044 | 0.0042 | 0.001 | | 0.0006 |
| | | A,B,C | 17. PLASMA (DIELECTRIC ETCH) | | | 0.0 | | | 0.0131 | | | 0.0084 | | | 0.0050 | | | 0.0064 |
| | | A,B,C | 18. ETCHING (DIELECTRIC) | | | 0.0 | | | 0.0044 | | | 0.0081 | | | 0.0047 | | | 0.0004 |
| | | A,B,C | 19. MASK (ETCH STOP) | | | 0.0 | | | 0.0091 | | | 0.0067 | | | 0.0044 | | | 0.0023 |
| | | | JUNCTION FORMATION | RCA | TI | MOT. | RCA | TI | MOT. | RCA | TI | MOT. | RCA | TI | MOT. | RCA | TI | MOT. |
| A,B,C | A | A | 1. SPIN-ON | 0.0 | 0.0012 | 0.0 | 0.006 | | 0.0154 | 0.016 | 0.0073 | 0.0067 | 0.013 | 0.0073 | 0.0044 | 0.001 | | 0.0023 |
| A,B,C | A,B | A,B,C | 2. SPRAY-ON | 0.0 | 0.0012 | 0.0 | 0.005 | | 0.0152 | 0.014 | 0.0073 | 0.0034 | 0.017 | 0.0073 | 0.0032 | 0.001 | | 0.0011 |
| A,B,C | A,B | A,B,C | 3. BAKE | 0.0 | 0.0 | | 0.000 | | | 0.011 | 0.0073 | | 0.008 | 0.0073 | | 0.000 | | |
| A,B,C | A,B | A,B,C | 4. DRIVE-IN (DIFFUSION) | 0.0 | 0.001 | 0.0 | 0.004 | | 0.0099 | 0.009 | 0.0073 | 0.0102 | 0.008 | 0.0073 | 0.0057 | 0.001 | | 0.0026 |
| A,B,C | | A,B,C | 5. SILICON SOURCE (SOLID) | 0.0 | 0.090 | 0.0 | 0.018 | | 0.0173 | 0.010 | 0.0073 | 0.0407 | 0.009 | 0.0073 | 0.0610 | 0.002 | | 0.0053 |
| | | | 6. ALLOY | | | | | | | | | | | | | | | |
| A,B,C | A,B | A,B,C | 7. GAS DEPOSITION AND DIFFUSION | 0.0 | 0.030 | 0.0 | 0.028 | | 0.0174 | 0.009 | 0.0073 | 0.0102 | 0.007 | 0.0073 | 0.0057 | 0.004 | | 0.0026 |
| A,B,C | | A,B,C | 8. DOPED OXIDE (CVD) | 0.0 | | 0.0 | 0.033 | | 0.0174 | 0.021 | | 0.0102 | 0.021 | | 0.0057 | 0.008 | | 0.0026 |
| A,B,C | | A,B,C | 9. EPITAXY | 0.0 | H | | 1.448 | | | 0.100 | H | | 0.360 | H | | 0.150 | | |
| A,B,C | | | 10. EPITAXY (CLOSED SPACE) | 0.0 | H | | 0.248 | | | 0.041 | H | | 0.028 | H | | 0.039 | | |
| A,B,C | A,B | A,B,C | 11. ION IMPLANT (ONE SIDE) | 0.0 | 0.010 | 0.0 | 0.012 | | 0.0097 | 0.026 | 0.0182 | 0.0746 | 0.030 | 0.0182 | 0.0357 | 0.039 | | 0.1406 |
| A,B,C | A,B | A,B,C | 12. ION IMPLANT (ADVANCED) (ONE SIDE) | 0.0 | 0.010 | 0.0 | 0.004 | | 0.0014 | 0.005 | 0.0088 | 0.0022 | 0.017 | 0.0088 | 0.0030 | 0.008 | | 0.0067 |
| | | | METALLIZATION | RCA | TI | MOT. | RCA | TI | MOT. | RCA | TI | MOT. | RCA | TI | MOT. | RCA | TI | MOT. |
| A | A,B | A,B,C | 1. VACUUM METALLIZATION (Cu, Al) | 0.0 | 0.035 | 0.0024 | 0.017 | | 0.0490 | 0.088 | 0.0194 | 0.0318 | 0.077 | 0.0194 | 0.0146 | 0.026 | | 0.0236 |
| A | A,B | A,B,C | 2. VACUUM, Ti/Ag FRONT | 0.019 | 0.060 | | 0.017 | | | 0.088 | 0.0194 | | 0.077 | 0.0194 | | 0.030 | | |
| A | A,B | A,B,C | 3. VACUUM, Ti/Ag BACK | 0.022 | 0.060 | | 0.017 | | | 0.088 | 0.0194 | | 0.077 | 0.0194 | | 0.030 | | |
| A | | A,B,C | 4. SPUTTERING | 0.006 | | | 0.013 | | | 0.020 | | | 0.016 | | | 0.026 | | |
| A | | A,B,C | 5. SPUTTERING, Ti/Ag FRONT | 0.019 | | | 0.009 | | | 0.020 | | | 0.022 | | | 0.023 | | |
| A | | A,B,C | 6. SPUTTERING, Ti/Ag BACK | 0.022 | | | 0.012 | | | 0.020 | | | 0.016 | | | 0.023 | | |
| A | A,B | A,B,C | 7. THICK FILM (BASE METAL-FRONT) | 0.0 | 0.0015 | | 0.008 | | | 0.002 | | | 0.008 | | | 0.002 | | |
| A | A,B | A,B,C | 8. THICK FILM, Ag FRONT | 0.004 | 0.0024 | 0.0457 | 0.008 | | 0.0040 | 0.002 | 0.0036 | 0.0060 | 0.008 | 0.0036 | 0.0040 | 0.002 | | 0.0011 |
| A | A,B | A,B,C | 9. THICK FILM, Ag BACK | 0.029 | 0.024 | 0.1988 | 0.008 | | 0.0040 | 0.002 | 0.0036 | 0.0060 | 0.008 | 0.0036 | 0.0040 | 0.002 | | 0.0011 |
| A | | A,B,C | 10. THICK FILM, Al, Ag, BACK | 0.005 | | | 0.016 | | | 0.003 | | | 0.016 | | | 0.004 | | |
| A | A,B | A,B,C | 11. THICK FILM, (BASE METAL-BACK) | 0.003 | 0.0150 | | 0.008 | | | 0.002 | 0.0036 | | 0.008 | 0.0036 | | 0.002 | | |
| | | A,B,C | 12. ELECTROLESS PLATING | | | 0.0305 | | | 0.0256 | | | 0.0145 | | | 0.0089 | | | 0.0011 |
| | | A,B,C | 13. ELECTROLYTIC PLATING | | | 0.0305 | | | 0.0256 | | | 0.0145 | | | 0.0089 | | | 0.0011 |
| | | | 14. | | | | | | | | | | | | | | | |
| | | A,B,C | 15. SOLDER COATING | | | 0.0223 | | | 0.0002 | | | 0.0014 | | | 0.0025 | | | 0.0002 |
| | A,B | A,B,C | 16. PIMDEP (PHOTO-IMPEDED MTL DEP) | | 0.0352 | | | | | | 0.1076 | | | 0.0538 | | | | |

* LEGEND L = LOW M = MEDIUM H = HIGH U = UNKNOWN

| | DEPRECIATION | | | TOTALS | | | AUTOMATION PROBABILITY | | | PROCESS YIELD (%) | | | LIMITING MAX CELL EFF. (%) | | | INVESTMENT | | | | | |
|---|---|---|---|---|---|---|---|---|---|---|---|---|---|---|---|---|---|---|---|---|---|
| | | | | | | | | | | | | | | | | CAPITAL EQUIP. | | | FACILITIES | | |
| | RCA | TI | MOT. | RCA | TI | MOT. | RCA | TI | MOT. | RCA | TI | MOT. | RCA | TI | MOT. | RCA | TI | MOT. | RCA | TI | MOT. |
| 1. | 0.004 | 0.0033 | 0.0031 | 0.071 | 0.0210 | 0.0327 | H | H | 80 | 99.5 | 98 | 99.5 | 20 | | > 20 | 0.031 | 0.0167 | 0.0205 | | | 0.0053 |
| 2. | 0.006 | | 0.0003 | 0.100 | | 0.0149 | H | | 80 | 99.0 | | 99.9 | 20 | | > 20 | 0.039 | | 0.0034 | | | 0.0032 |
| 3. | | 0.0054 | 0.0326 | | 0.0102 | | | H | 10 | | 99 | | | | | | 0.0271 | 0.2211 | | | 0.0413 |
| 4. | 0.001 | | | 0.048 | | | H | | | 99.5 | | | 20 | | | 0.010 | | | | | |
| 5. | 0.002 | 0.0030 | | 0.045 | 0.0118 | | H | H | 10 | 99.0 | 99 | 90.0 | 20 | | ? | 0.017 | 0.0149 | | | | |
| 6. | 0.001 | | 0.0005 | 0.024 | | 0.0155 | H | | 70 | 99.0 | | 99.8 | | | > 20 | 0.005 | | 0.0031 | | | 0.0032 |
| 7. | | | | | | | | | | | | 97.0 | | | > 20 | | | | | | |
| 8. | | | 0.0002 | | | 0.0096 | | | 90 | | | 99.8 | | | > 20 | | | 0.0013 | | | 0.0015 |
| 9. | 0.001 | | 0.0012 | 0.061 | | 0.0530 | H | | 10 | | | 99.5 | | | > 20 | | | 0.0076 | | | 0.0063 |
| 10. | 0.001 | | 0.0012 | 0.038 | | 0.0493 | H | | 10 | 99.5 | | 99.5 | 20 | | > 20 | 0.008 | | 0.0076 | | | 0.0063 |
| 11. | 0.004 | | | 0.057 | | | H | | | 95.0 | | 95.0 | 20 | | | 0.028 | | | | | |
| 12. | 0.001 | | 0.0061 | 0.025 | | 0.0698 | H | | 50 | 95.0 | | | 19 | | | 0.005 | | 0.0407 | | | 0.0106 |
| 13. | 0.002 | 0.0044 | | 0.080 | 0.0398 | | H | H | | 95.0 | 98 | | ? | | | 0.013 | 0.0223 | | | | |
| 14. | 0.002 | 0.0030 | 0.0011 | 0.064 | 0.022 | 0.0465 | H | H | 90 | 95.0 | 98 | 99.6 | ? | 13.5 | > 20 | 0.013 | 0.0149 | 0.0068 | | | 0.0063 |
| 15. | 0.004 | 0.0112 | 0.0097 | 0.084 | 0.0460 | 0.0839 | H | H | 80 | 99.0 | 99 | 99.4 | 20 | 13.5 | > 20 | 0.027 | 0.0550 | 0.0648 | | | 0.0160 |
| 16. | 0.002 | 0.0015 | 0.0006 | 0.018 | 0.0104 | 0.0328 | H | H | 80 | 99.5 | 99 | 99.7 | 20 | 13.5 | > 20 | 0.011 | 0.0074 | 0.0663 | | | 0.0053 |
| 17. | | | 0.0096 | | | 0.0425 | | | 80 | | | 99.8 | | | > 20 | | | 0.0016 | | | 0.0026 |
| 18. | | | 0.0004 | | | 0.0180 | | | 70 | | | 99.6 | | | > 20 | | | 0.0407 | | | 0.0106 |
| 19. | | | 0.0031 | | | 0.0256 | | | 80 | | | 99.8 | | | > 20 | | | 0.0211 | | | 0.0047 |
| | | | | | | | | | | | | | | | | | | | | | |
| | RCA | TI | MOT. | RCA | TI | MOT. | RCA | TI | MOT. | RCA | TI | MOT. | RCA | TI | MOT. | RCA | TI | MOT. | RCA | TI | MOT. |
| 1. | 0.002 | 0.0030 | 0.0031 | 0.038 | 0.0188 | 0.0319 | H | H | 50 | 95.0 | 99.5 | — | 15 | 13.5 | 12 | 0.012 | 0.0297 | 0.0211 | | | 0.0047 |
| 2. | 0.002 | 0.0030 | 0.0014 | 0.039 | 0.0188 | 0.0243 | H | H | 50 | 99.0 | 99.5 | — | 15 | 13.5 | 12 | 0.012 | 0.0297 | 0.0095 | | | 0.0023 |
| 3. | 0.000 | 0.0015 | | 0.019 | 0.0161 | | H | H | | 99.0 | 99 | | 20 | 13.5 | | 0.001 | 0.0074 | | | | |
| 4. | 0.002 | 0.0017 | 0.0032 | 0.024 | 0.0173 | 0.0316 | H | M | 90 | 98.0 | 99 | 99.5 | 20 | 13.5 | > 20 | 0.012 | 0.0087 | 0.0212 | | | 0.0081 |
| 5. | 0.003 | 0.0017 | 0.0065 | 0.041 | 0.1063 | 0.0859 | H | M | 40 | 98.0 | 99 | 98.0 | 20 | | ? | 0.018 | 0.0087 | 0.0423 | | | 0.0162 |
| 6. | | | | | | | | | | | | 50 | 11 | | | | | | | | |
| 7. | 0.006 | 0.0022 | 0.0032 | 0.055 | 0.0468 | 0.0391 | H | M | 70 | 99.0 | 99 | 99 | 18 | 13.5 | > 20 | 0.044 | 0.0111 | 0.0212 | | | 0.0081 |
| 8. | 0.013 | | 0.0032 | 0.096 | | 0.0391 | H | | 70 | 99.0 | | 99 | 20 | | > 20 | 0.092 | | 0.0212 | | | 0.0081 |
| 9. | 0.238 | H | | 2.297 | H | | H | M | 10 | 75.0 | 80 | 75 | 20 | | | 1.666 | | | | | |
| 10. | 0.062 | H | | 0.418 | H | | H | L | | 85.0 | 80 | — | 20 | | | 0.435 | | | | | |
| 11. | 0.061 | 0.0185 | 0.2029 | 0.168 | 0.0649 | 0.4635 | H | H | -0- | 99.0 | 99 | 98 | 20 | 13.5 | > 20 | 0.430 | 0.0930 | 1.390 | | | 0.1723 |
| 12. | 0.013 | 0.0178 | 0.0101 | 0.047 | 0.0454 | 0.0234 | H | H | 90 | 99.0 | 99 | 99.5 | 20 | 13.5 | > 20 | 0. 88 | 0.0890 | 0.0695 | | | 0.0052 |
| | | | | | | | | | | | | | | | | | | | | | |
| | | | | | | | | | | | | | | | | | | | | | |
| | | | | | | | | | | | | | | | | | | | | | |
| | RCA | TI | MOT. | RCA | TI | MOT. | RCA | TI | MOT. | RCA | TI | MOT. | RCA | TI | MOT. | RCA | TI | MOT. | RCA | TI | MOT. |
| 1. | 0.041 | 0.0515 | 0.0326 | 0.250 | 0.1251 | 0.1540 | H | M | 40 | 98.0 | 98 | 99 | 20 | 13.5 | > 20 | 0.289 | 0.2650 | 0.2211 | | | 0.0413 |
| 2. | 0.048 | 0.0515 | | 0.280 | 0.1501 | | H | M | | 98.0 | 98 | | 20 | 13.5 | > 20 | 0.338 | 0.2650 | | | | |
| 3. | 0.048 | 0.0515 | | 0.282 | 0.1501 | | H | M | | 98.0 | 98 | | 20 | 13.5 | > 20 | 0.338 | 0.2650 | | | | |
| 4. | 0.041 | | | 0.122 | | | H | M | | 98.0 | 98 | | 20 | | > 20 | 0.288 | | | | | |
| 5. | 0.037 | | | 0.131 | | | H | M | | 98.0 | 98 | | 20 | | > 20 | 0.259 | | | | | |
| 6. | 0.037 | | | 0.131 | | | H | M | | 98.0 | 98 | | 20 | | > 20 | 0.259 | | | | | |
| 7. | 0.004 | 0.0012 | | 0.024 | 0.0099 | | H | H | | 98.0 | 98 | | 20 | 13.5 | > 20 | 0.028 | 0.0062 | | | | |
| 8. | 0.004 | 0.0012 | 0.0016 | 0.028 | 0.0108 | 0.0624 | H | H | 70 | 98.0 | 98 | 99.8 | 20 | 13.5 | > 20 | 0.028 | 0.0062 | 0.0107 | | | 0.0018 |
| 9. | 0.004 | 0.0012 | 0.0016 | 0.053 | 0.0324 | 0.2155 | H | H | 70 | 98.0 | 98 | 99.8 | 20 | 13.5 | > 20 | 0.028 | 0.0062 | 0.0107 | | | 0.0018 |
| 10. | 0.007 | | | 0.050 | | | H | | | 98.0 | | | 20 | | > 20 | 0.046 | | | | | |
| 11. | 0.004 | 0.0012 | | 0.027 | 0.0234 | | H | H | | 98.0 | 98 | | 20 | 13.5 | > 20 | 0.028 | 0.0062 | | | | |
| 12. | | | 0.0012 | | | 0.0818 | | M | 80 | | 98 | 99.6 | | | > 20 | | | 0.0073 | | | 0.0049 |
| 13. | | | 0.0012 | | | 0.0818 | | M | 80 | | 98 | 99.6 | | | > 20 | | | 0.0073 | | | 0.0049 |
| 14. | | | | | | | | | | | | | | | | | | | | | |
| 15. | | | 0.0003 | | | 0.0269 | | | 90 | | | 99.8 | | | > 20 | | | 0.0021 | | | 0.0005 |
| 16. | | 0.1568 | | | 0.3534 | | | H | | | 98 | | | 13.5 | | | | | | | |

Table 7-2 (Contd)

| SILICON FORM A. CZOCHRALSKI B. RIBBON C. SHEET SUBSTRATE | | | PROCESS STEPS (ITEMIZED) | MATERIALS | | | EXPENSE ITEMS | | | LABOR | | | OVERHEAD | | | INTEREST (9%) | | |
|---|---|---|---|---|---|---|---|---|---|---|---|---|---|---|---|---|---|---|
| RCA | TI | MOT. | AR COATING | RCA | TI | MOT. | RCA | TI | MOT. | RCA | TI | MOT. | RCA | TI | MOT. | RCA | TI | MOT. |
| A,B,C | | A,B,C | 1. SILICON NITRIDE (CVD) | 0.0 | | 0.0 | 0.007 | | 0.0098 | 0.032 | | 0.0102 | 0.029 | | 0.0057 | 0.012 | | 0.0026 |
| | A | A,B,C | 2. OXIDE GROWTH | | 0.0005 | 0.0 | | | 0.0049 | | 0.0073 | 0.0051 | | 0.0073 | 0.0039 | | | 0.0013 |
| A,B,C | A | A | 3. SPIN-ON | 0.0 | 0.0012 | 0.0 | 0.019 | | 0.0079 | 0.029 | 0.0073 | 0.0067 | 0.027 | 0.0073 | 0.0044 | 0.001 | | 0.0023 |
| A,B,C | A,B | A,B,C | 4. EVAPORATE | 0.0 | 0.004 | | 0.028 | | | 0.087 | 0.0109 | | 0.093 | 0.0109 | | 0.025 | | 0.0236 |
| | A,B | | 5. SPUTTERING | | 0.004 | | | | | | 0.0109 | | | 0.0109 | | | | |
| | | A,B,C | 6. SPRAY-ON | | | | | | | | | 0.0034 | | | | | | 0.0011 |
| | | | INTERCONNECTION | RCA | TI | MOT. | RCA | TI | MOT. | RCA | TI | MOT. | RCA | TI | MOT. | RCA | TI | MOT. |
| | | A,B,C | 1. ADD SOLDER | | | 0.0014 | | | 0.0001 | | | 0.0007 | | | 0.0022 | | | 0.0001 |
| A,B,C | | A,B,C | 2. REFLOW SOLDER | 0.003 | L | 0.0 | 0.005 | | 0.0001 | 0.001 | L | 0.0170 | 0.001 | L | 0.0032 | 0.003 | | 0.0008 |
| A,B,C | | | 3. ULTRASONIC BONDING | 0.006 | L | | 0.005 | | | 0.001 | M | | 0.001 | M | | 0.003 | | |
| | | | 4. THERMAL COMPRESSION BONDING | | L | | | | | | M | | | M | | | | |
| | | A,B,C | 5. CONDUCTIVE ADHESIVES | | H | 0.0045 | | | 0.0002 | | M | 0.0060 | | M | 0.0040 | | | 0.0011 |
| A,B,C | | | 6. WELDING | 0.003 | L | | 0.008 | | | 0.001 | M | | 0.001 | M | | 0.003 | | |
| | | | ENCAPSULATION | RCA | TI | MOT. | RCA | TI | MOT. | RCA | TI | MOT. | RCA | TI | MOT. | RCA | TI | MOT. |
| A,B,C | A,B | A,B,C | 1. GLASS SUPERSTRATE | 0.153 | 0.066 | 0.1817 | 0.000 | | 0.0004 | 0.017 | 0.0219 | 0.0006 | 0.012 | 0.0219 | 0.0027 | 0.003 | | 0.0012 |
| | A,B | A,B,C | 2. GLASS WITH SUBSTRATE | | 0.069 | 0.3448 | | | 0.0004 | | 0.0219 | 0.0006 | | 0.0219 | 0.0027 | | | 0.0013 |
| A,B,C | | | 3. CELLS IN TUBES | 0.198 | | | 0.000 | | | 0.017 | | | 0.012 | | | 0.003 | | |
| | A,B | | 4. SUBSTRATE WITH CONFORMAL COATING | | 0.045 | | | | | | 0.0219 | | | 0.0219 | | | | |
| | A,B | | 5. HERMETIC | | 0.247 | | | | | | | | | | | | | |
| A,B,C | | | 6. DOUBLE GLASS | 0.110 | | | 0.001 | | | 0.017 | | | 0.012 | | | 0.003 | | |
| | | | TEST | RCA | TI | MOT. | RCA | TI | MOT. | RCA | TI | MOT. | RCA | TI | MOT. | RCA | TI | MOT. |
| A,B,C | A | A,B,C | 1. ELECTRICAL TEST (CELLS) | 0.0 | 0.0 | 0.0 | 0.000 | | 0.0001 | 0.012 | 0.0044 | 0.0085 | 0.013 | 0.0044 | 0.0048 | 0.005 | | 0.0008 |
| A,B,C | A,B | A,B,C | 2. ELECTRICAL TEST (MODULES) | 0.0 | 0.0 | 0.0 | 0.0 | | 0.0 | 0.002 | 0.0003 | 0.0003 | 0.001 | 0.0003 | 0.0021 | 0.00 | | 0.0001 |

* LEGEND L = LOW M = MEDIUM H = HIGH U = UNKNOWN

| | DEPRECIATION | | | TOTALS | | | AUTOMATION PROBABILITY | | | PROCESS YIELD (%) | | | LIMITING MAX CELL EFF. (%) | | | INVESTMENT | | | | | |
|---|---|---|---|---|---|---|---|---|---|---|---|---|---|---|---|---|---|---|---|---|---|
| | | | | | | | | | | | | | | | | CAPITAL EQUIP. | | | FACILITIES | | |
| | RCA | TI | MOT. | RCA | TI | MOT. | RCA | TI | MOT. | RCA | TI | MOT. | RCA | TI | MOT. | RCA | TI | MOT. | RCA | TI | MOT. |
| 1. | 0.020 | | 0.0032 | 0.100 | | 0.0315 | H | | 90 | 99.0 | | 99.8 | 16 | | >20 | 0.138 | | 0.0212 | | | 0.0081 |
| 2. | | 0.0017 | 0.0016 | | 0.0168 | 0.0168 | | M | 20 | | 99 | 99.8 | 15 | 12 | >20 | | 0.0087 | 0.0106 | | | 0.0040 |
| 3. | 0.002 | 0.0030 | 0.0031 | 0.078 | 0.0188 | 0.0244 | H | H | 50 | 95.0 | 99 | 97.0 | 18 | 13.5 | >20 | 0.012 | 0.0148 | 0.0211 | | | 0.0047 |
| 4. | 0.040 | 0.0145 | 0.0326 | 0.274 | 0.0403 | | H | H | 60 | 99.0 | 99 | | 18 | 13.5 | >20 | 0.281 | 0.0744 | | | | |
| 5. | | 0.0145 | | | 0.0403 | | | H | | | 99 | | | 13.5 | | | 0.0744 | | | | |
| 6. | | | 0.0014 | | | | | | 20 | | | 95.0 | | | >20 | | | 0.0095 | | | 0.0023 |
| | | | | | | | | | | | | | | | | | | | | | |
| | | | | | | | | | | | | | | | | | | | | | |
| | RCA | TI | MOT. | RCA | TI | MOT. | RCA | TI | MOT. | RCA | TI | MOT. | RCA | TI | MOT. | RCA | TI | MOT. | RCA | TI | MOT. |
| 1. | | | 0.0001 | | | 0.0046 | | | 90 | | | 99.8 | | | | | | 0.0008 | | | 0.0002 |
| 2. | 0.005 | L | 0.0011 | 0.019 | | 0.0222 | H | | 90 | | | 99.8 | | | | 0.034 | | 0.0074 | | | 0.0015 |
| 3. | 0.005 | L | | 0.022 | | | H | | | | | | | | | 0.034 | | | | | |
| 4. | | L | | | | | | | | | | | | | | | | | | | |
| 5. | | L | 0.0016 | | | 0.0174 | | | 50 | | | 99.5 | | | | | | 0.0107 | | | 0.0018 |
| 6. | 0.005 | L | | 0.022 | | | H | | | | | 98 | | | | 0.034 | | | | | |
| | | | | | | | | | | | | | | | | | | | | | |
| | | | | | | | | | | | | | | | | | | | | | |
| | | | | | | | | | | | | | | | | | | | | | |
| | RCA | TI | MOT. | RCA | TI | MOT. | RCA | TI | MOT. | RCA | TI | MOT. | RCA | TI | MOT. | RCA | TI | MOT. | RCA | TI | MOT. |
| 1. | 0.005 | 0.0241 | 0.0010 | 0.189 | 0.1339 | 0.1876 | H | H | 80 | | 96 | 99.4 | | | | 0.032 | 0.1213 | 0.0057 | | | 0.0074 |
| 2. | | 0.0226 | 0.0011 | | 0.1354 | 0.3509 | | H | 80 | | 96 | 99 | | | | | 0.1138 | 0.0063 | | | 0.0081 |
| 3. | 0.005 | | | 0.234 | | | H | | | | | | | | | 0.032 | | | | | |
| 4. | | 0.0226 | | | 0.1114 | | | H | | | 96 | | | | | | 0.1138 | | | | |
| 5. | | | | | | | | H | | | 96 | | | | | | | | | | |
| 6. | 0.005 | | | 0.148 | | | H | | | | | | | | | 0.032 | | | | | |
| | | | | | | | | | | | | | | | | | | | | | |
| | RCA | TI | MOT. | RCA | TI | MOT. | RCA | TI | MOT. | RCA | TI | MOT. | RCA | TI | MOT. | RCA | TI | MOT. | RCA | TI | MOT. |
| 1. | 0.007 | 0.0030 | 0.0012 | 0.037 | 0.0188 | 0.0154 | H | H | 100 | 80.0 | 85 | | | | | 0.051 | | 0.0079 | | | 0.0011 |
| 2. | 0.001 | 0.0006 | 0.0001 | 0.004 | 0.0012 | 0.0026 | H | H | 100 | | 98 | | | | | 0.005 | | 0.0010 | | | 0.0002 |
| | | | | | | | | | | | | | | | | | | | | | |
| | | | | | | | | | | | | | | | | | | | | | |

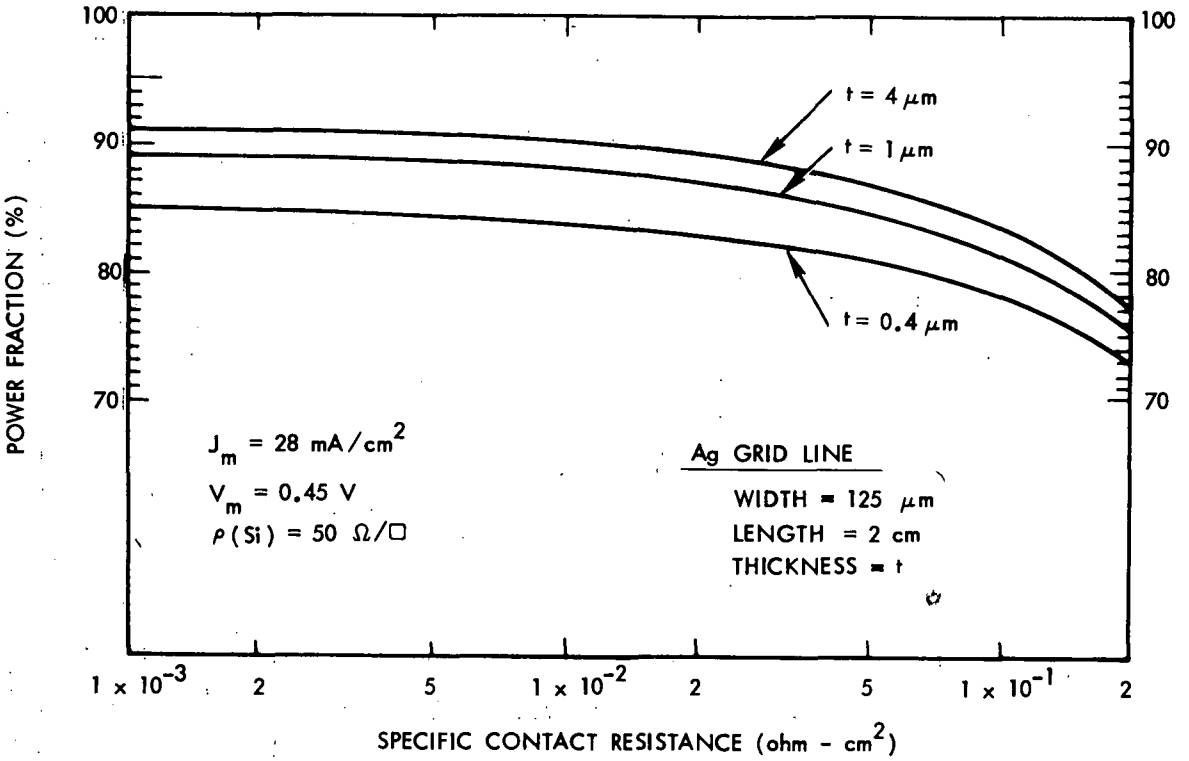


Figure 7-2. Output Power as a Fraction of That Generated by a Lossless Cell vs. $\rho_c$

Texas Instruments

Work during this quarter consisted of a computer-aided design analysis of metal pattern designs for solar cells, cost analyses for a large variety of potential solar cell process steps, feasibility of $N^+$ and $P^+$ layers from polymer dopant solutions, experimental evaluation of screen-printed base metal contacts, identification of a low cost module substrate material, evaluation of a test module, and development of module design recommendations. Solar cell process costing will continue in January 1977.

A computer program has been developed to optimize metallization pattern designs on hexagonal and rectangular solar cells. The program minimizes the fractional power losses due to shadowing, resistive loss due to current through the diffused region, and resistive loss due to current through the metal fingers as a function of metal line width. The computer calculates metal finger spacing and calculates the fractional loss components for shadowing and series resistance. A concentric metal finger pattern has been shown to be more efficient than the conventional fishbone pattern (Figure 7-3). Similar analysis of rectangular solar cells using a comb pattern shows that optimal metal finger losses and spacing are a function of cell width and optimal metal trunk line losses are a function of cell length (Figure 7-4).

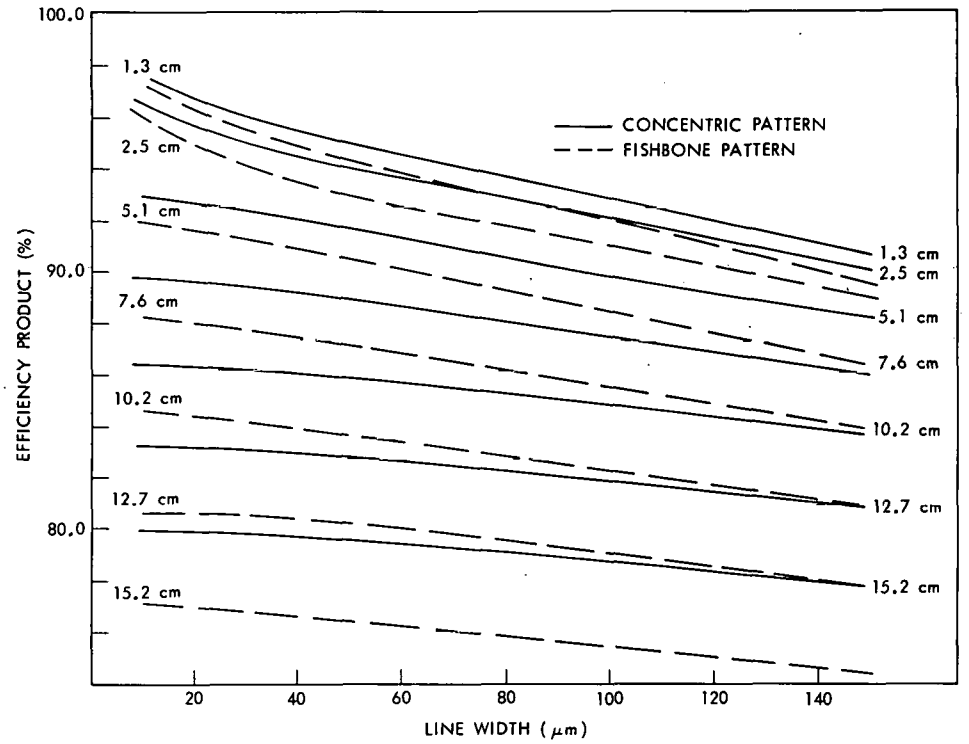


Figure 7-3. Efficiency Product for Metal Coverage and Series Resistance vs. Metal Finger Width as a Function of Cell Diagonal for Hexagonal Cells

These conclusions are significant to optimum performance for solar cell designs.

Process cost calculations were made for a large number of potential solar cell process steps. Metallization remains a significant cost item in the process. In module fabrication, the module encapsulation operation is the most significant cost factor.

Experimental feasibility has been demonstrated for simultaneous $N^+$ - $P^+$ diffusion from polymer dopant sources. Good solar cells have been fabricated using this low cost process.

Experimental evaluation of screen-printed base metal contacts has shown that Cu alloying through the shallow $N^+$ layer is a problem on the front side. Screen-printed contacts show some promise.

Porcelainized steel has been identified as an attractive low cost substrate for module fabrication. A four-cell minimodule was fabricated on porcelainized steel as a feasibility demonstration. A potential long-life module design has been developed but cost is still a problem.

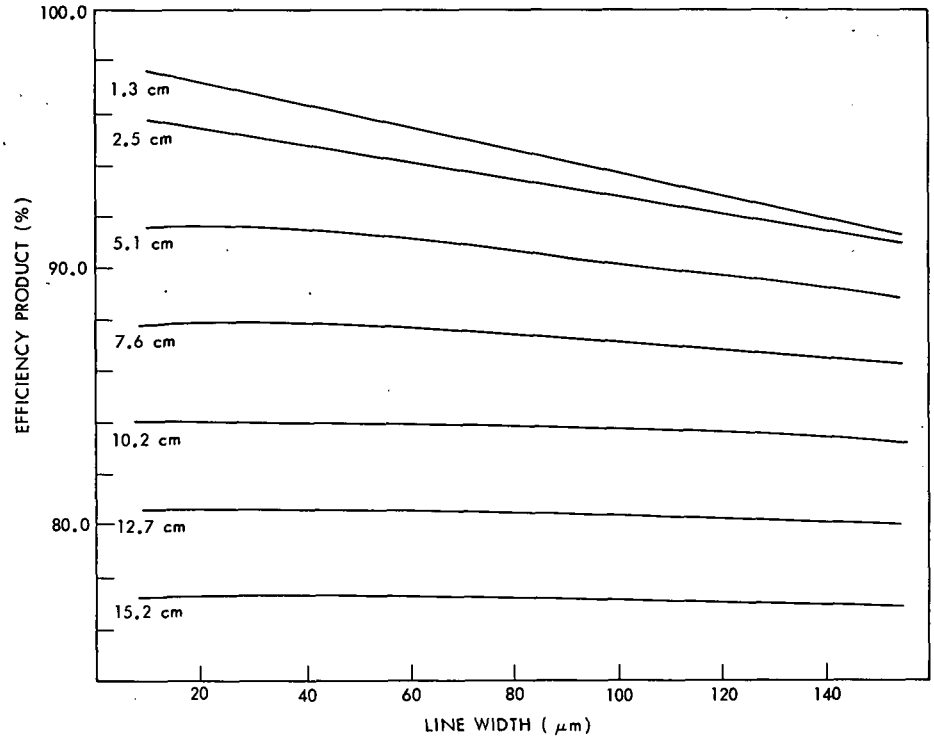


Figure 7-4. Efficiency Product for Metal Coverage and Series Resistance vs. Metal Finger Width as a Function of Cell Width for Rectangular Cells, Excluding Trunk Losses

2. Large-Area Czochralski Silicon Ingot Growth and Wafering Improvements - Texas Instruments

The purpose of work under this contract is to optimize current proven semiconductor techniques so as to produce silicon wafers in the most cost-effective manner. Accordingly, technical activity has primarily centered on establishing acceptable silicon crystal pulling and slicing rates.

Crystal Pulling

The Varian 12-kg puller was made fully operational during the quarter. Several trial 12-cm crystals have been pulled both from recycled silicon and new polysilicon. Average pull rates of 8-10 cm/h were achieved versus the program goal of 12 cm/h. Two attempts were made to hot-charge into an 8-kg crucible using chunk polycrystalline silicon. Although these attempts were unsuccessful because of excessive melt oxidation, the concept of using chunk polysilicon appears sound provided an airtight feed mechanism is used. An airtight nugget polysilicon feeder for use on multicharge runs was designed and is being fabricated.

Crystal Slicing

Multiblade slicing work continued with the optimal slurry flow experiment being repeated using 400-grit boron carbide abrasive in the usual 240 grams/liter slurry mixture. Results confirmed the previous obvservation that a slurry flow rate in the 5-10 ml/s range is optimal.

Several sawing experiments were performed with crystal spinning employed to enhance cutting rates. Results indicate a 4 to 5 times increase in cutting rate can be achieved on the multiblade saw with crystal spin. However, the practical application of crystal spinning offers a difficult technical challenge to reduce slice breakage, kerf, and blade wear. Experimental slurry sawing rates are shown in Figure 7-5.

Experiments with diamond-plated blades in the multiblade saw were started using a diamond matrix similar to that employed on conventional ID saw blades. Cutting rates for stationary crystal were equal to those observed with boron carbide abrasive slurry. With spinning crystal, however, diamond cutting rates were the best achieved to date. A 76-mm crystal was sawed down to a 19-mm core in 2.5 h for an average cutting rate of 23 mm/h. Saw yield was 90% on the spinning run. Additional experiments will be performed with blades having a coarser diamond matrix.

The economics of the Czochralski process were reexamined in view of current and projected information regarding crystal growth and wafering. Sheet cost in the $\$30\text{-}37/m^2$ range looks achievable for the longer term. A breakdown of the costs is shown in Figure 7-6.

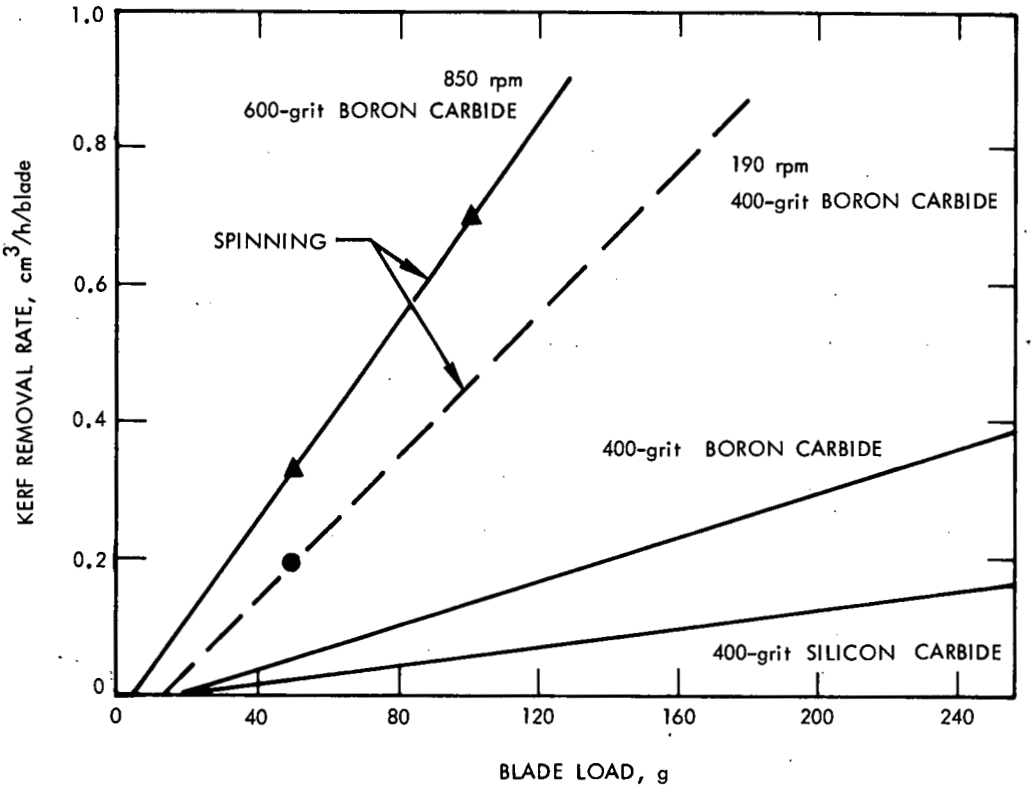


Figure 7-5. Experimental Slurry Sawing Results

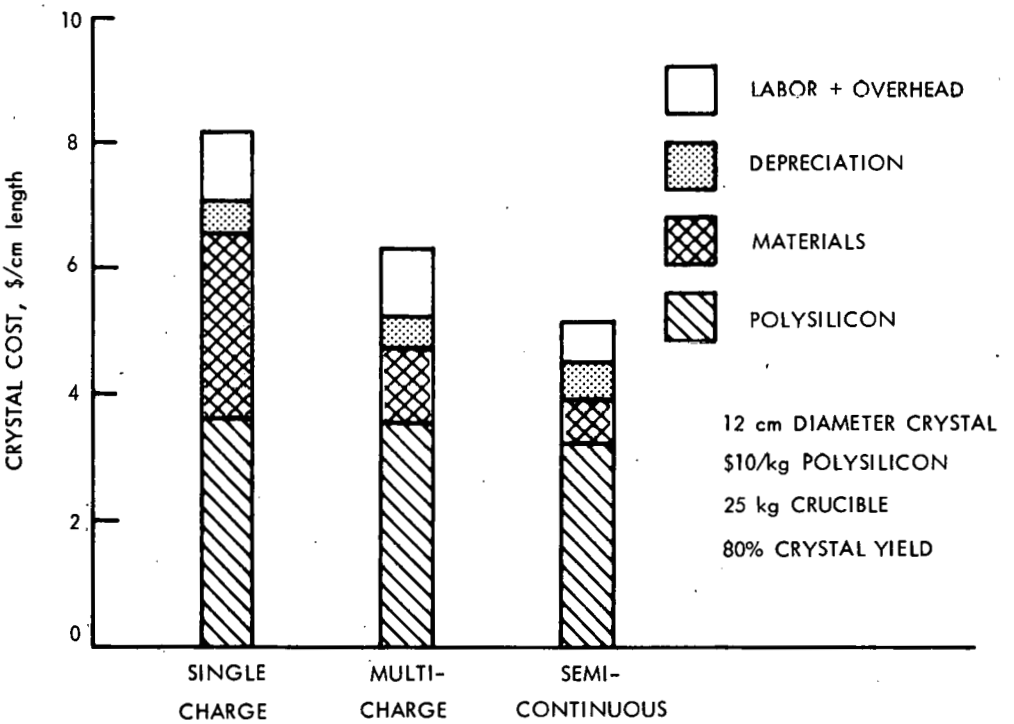


Figure 7-6. Czochralski Silicon Costs

# SECTION VIII

# ENGINEERING TASK

Engineering Task work during the quarter centered on six areas (reported on below) associated with the integration and development of solar cell module requirements. Emphasis was placed on generating module requirements for future large-scale module procurements and on closely following and iterating requirements for the Block 2 (130 kW) Procurement to meet the dynamic needs of the program. Based on early experience during the Block 1 (46 kW) Procurement, an improved method of defining module power output was devised, and a new specification issued. The studies made in generating future design factors and/or requirements included cell packing efficiency and series/parallel cell arrangements.

A major effort was concluded that will provide greatly increased correlation between measured performance and field performance of solar modules. This development of a nominal terrestrial environment (NTE) and a nominal operating cell temperature (NOCT) will also permit more accurate comparisons of alternative module designs, and form a foundation for standardization of module performance parameters.

## A. BLOCK 2 (130 kW) PROCUREMENT REQUIREMENTS

During the startup of the Block 2 (130 kW) Procurement it was found necessary to expand and clarify module specification #5-342-1 Rev. A to provide an improved definition of module power output, and a standard procedure for power output determination. The result of this effort was the revised specification #5-342-1, Rev. B.

In the Revision-A version of the specification, the maximum power output of each module was required to exceed 60/N watts at 100 $mW/cm^2$, AM1 insolation and 60°C cell temperature, where N is the number of modules which nest into a 4 by 4 foot subarray. In addition, the maximum-power voltage of each module was required to exceed 15.8 volts under the same test conditions. Compliance with this requirement was to be determined by testing at a standard test condition of 100 $mW/cm^2$, AM1, 60°C using a procedure to be developed by the vendor and approved by JPL.

Difficulties with this approach arose in four areas:

(1) Requiring that all maximum-power voltages be greater than 15.8 volts forced the maximum-power voltage of the average module to be higher than desired (see Figure 8-1), and required changes in the number of series cells per module from that initially proposed by some manufacturers.

(2) Because some manufacturers proposed modules with powers as much as 50% above the 60/N minimum, there was no effective criteria for rejecting unacceptable modules with powers well below average, and no incentive for

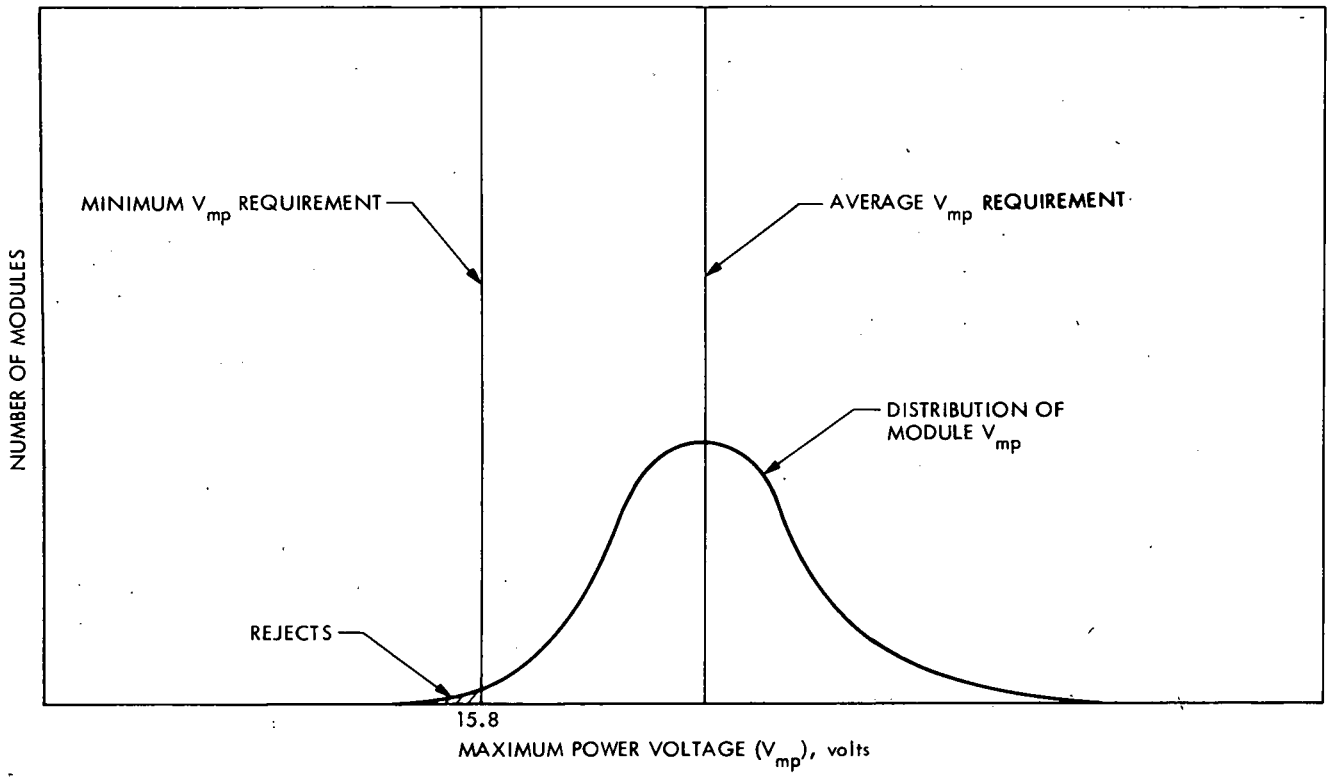


Figure 8-1. Effect of Maximum-Power-Voltage Specification on Maximum-Power Voltage of Average Module

manufacturers to reduce module-to-module variation which could result in substantial array mismatch losses.

(3) Many manufacturers preferred a temperature other than 28°C for making module performance measurements, depending on their type of measurement facility and method.

(4) There was poor agreement as to how to extrapolate from the measurement temperature to the reference temperature of 60°C.

To resolve these difficulties, the Revision-B specification requires that the average module power output ($P_{ave}$) at 100 mW/cm$^2$, 60°C and 15.8 volts be greater than 60/N, as determined by an agreed-upon sampling of modules. Specifying average power output at the reference voltage provides a better measure of module performance in battery-charging systems, where current level is of key importance. In addition, it allows the maximum-power point of the average module to be located at the reference voltage (15.8 volts) and not above it as previously required (Figure 8-1).

To provide a poor-module rejection criterion, the Revision-B specification further requires that the power of each module exceed 0.86 $P_{ave}$. This minimum level of performance guarantees that array-mismatch losses will be acceptable, yet is consistent with high module yields as determined from studies of the power variations of modules delivered as part of the Block 1 (46 kW) Procurement.

To resolve the module evaluation difficulties, the Revision-B specification also provides for measurements to be made at any temperature, referred to as an Optional Test Condition (OTC), and then extrapolated to 60°C using a specific procedure developed by JPL. The procedure is described in detail in 5-342-1, Rev. B and is based on required measurements of the temperature dependence of the module I-V curve near the maximum power point. Tests have shown that the procedure is repeatable, and accurate to better than 1%.

## B. MODULE CONFIGURATION STUDIES

During the past quarter a number of module configuration studies have been conducted in support of the development of requirements for future module buys. One study of particular interest focused on module efficiency considerations.

Present terrestrial silicon solar cell modules being procured by the LSSA project as part of the Block 1 Procurement have overall efficiencies at 28°C of around 11.5%, based on the total cell area. This includes losses due to encapsulation and cell mismatch. Unfortunately, when based on the module overall area, the typical efficiency drops to around 6.5% because of the 55 to 60% cell packing factor presently used. Though increased cell efficiency is one means of increasing future solar array efficiency, a second approach is clearly to attempt to increase the percent of the solar array which is active cell area.

Solar array active cell area is largely affected by three variables: (1) solar cell shape, which influences solar cell packing efficiency, (2) module size and shape, which influences the ratio of module border to enclosed module area, and (3) solar cell spacing as required to accommodate the electrical interconnection of the cells. Figure 8-2 describes the effect of solar cell shape and module size on cell nesting efficiency within a square module with cells in direct contact with one another*. it can be seen that solar cell nesting efficiency increases dramatically with increasing module size, though a point of diminishing returns is reached when the number of rows of cells exceeds approximately 15 or, in other words, the number of cells per module exceeds 200 or so. With 3 to 4 inch circular cells, this point of diminishing returns is reached with modules about 4 foot square, as contrasted with present modules which are 1 to 2 foot square.

---

*Rectangular modules have similar relationships, which depend on which way the cells are laid out with respect to the length and width.

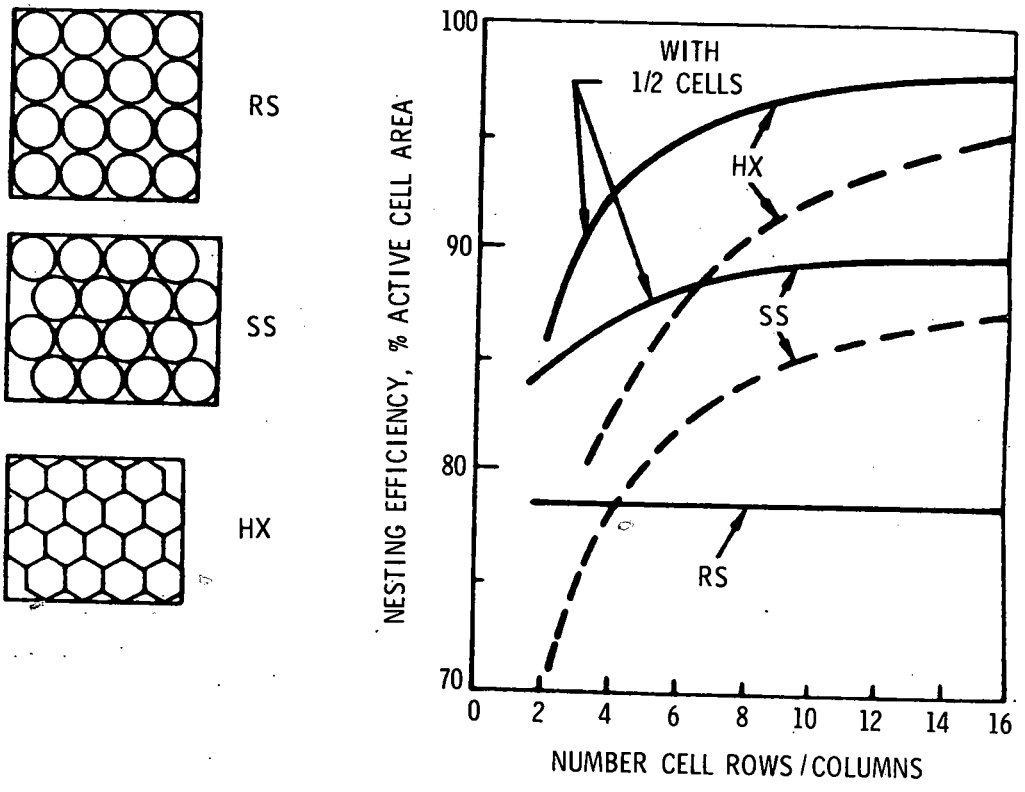


Figure 8-2. Solar Cell Nesting Efficiency for Square Modules

Another consideration addressed in Figure 8-2 is the use of half-cells to fill out the end spaces that are left when a staggered pack is used. With larger modules a gain of approximately 3% in nesting efficiency can be realized by utilizing half-cells. This can be accomplished with little impact on the cell interconnect system as long as a series/parallel arrangement is used with a half-cell in each group of parallel cells.

Table 8-1 summarizes typical overall packing effifiency values for a 4 foot square module of closely packed 3 to 4 inch diameter cells. The border, buss, and interconnect efficiencies correspond to the additional area lost due to the usual 0.75 inch exterior border required for module mounting, the lost space within the border for electrical busses, etc., and the approximately 0.1 inch between cells required for cell electrical interconnection. With these values it can be seen that overall packing efficiencies of 75 to 85 percent are easily achievable.

In addition to improving module efficiency, increased module size has a number of additional advantages as shown in Table 8-2. From Figure 8-2 it is clear that the primary reason for the increased efficiency of larger modules is the reduced ratio of border length to enclosed module area. A second advantage to the reduced border length is reduced cost for special border treatment or framing, and improved reliability. Because the module edge is

Table 8-1. Packing Efficiency for a 4 by 4 Foot Module

| Efficiency Component | Efficiency, % | |
|---|---|---|
| | Round Cells | Hex. Cells |
| Border Efficiency | 93 | 93 |
| Buss Efficiency | 97 | 97 |
| Interconnect Efficiency | 96 | 96 |
| Nesting Efficiency (from Figure 8-2; no half-cells) | 88 | 96 |
| Overall Packing Efficiency | 76 | 83 |

very susceptible to damage and degradation, the reduced border length effectively increases module reliability. Array reliability is also enhanced by the reduction in number of modules per kilowatt and thus the reduction in mechanical and electrical attachments for a given size system.

Table 8-2. Effect of Module Size/ Efficiency

| Module Type (ftxft) | Module* Efficiency | Cells/ Module | Modules/ kW | Border Length / Enclosed Area ($ft/ft^2$) | Module Prices** |
|---|---|---|---|---|---|
| 1x2 | 6 | 20 | 84 | 3 | $120 |
| 2x2 | 6 | 40 | 42 | 2 | 240 |
| 2x4 | 7 | 75-250 | 18 | 1.5 | 550 |
| 4x4 | 8 | 150-500 | 8 | 1.0 | 1250 |

*Cell efficiency = 11.5% (including transmission and mismatch losses).

**At $10/watt.

In contrast to the reduction in border and attachment fasteners, increased module size generally leads to increased numbers of cells per module and thus to decreased module reliability unless appropriate steps are taken. The effect on array reliability varies depending on the extent that fewer larger modules reflect into poorer series/parallel redundancy at the array level.

## C. MODULE RELIABILITY STUDIES

Additional studies during the past quarter examined the effect of solar cell series/paralleling on module reliability. When series/paralleling is incorporated into a module, the loss or shadowing of a single cell results in only a partial loss in module output, though it will be accompanied by "hot spot" cell heating effects as described by Blake and Hanson*. An important design consideration in the selection of which series/parallel configuration to use is the limiting of the "hot spot" cell heating to acceptable levels in the case where a module has a single cell failure.

To help visualize the "hot spot" cell heating phenomenon, consider the series/parallel module configuration shown in the left-hand side of Figure 8-3. The right-hand side of the figure indicates the effect of the loss of a single cell on the current-voltage (I-V) characteristics of each section of the module and on the resultant module output. In the case shown, the two remaining cell strings in section B dissipate nearly the entire maximum power output of section A under short-circuit-current conditions. Because the ratio of cells in section A to the functional cells in section B is 18/6 = 3, the section B cells are each called upon to dissipate approximately 3 times their normal maximum power output.

The degree to which this level of heating is of concern depends upon the expected temperature rise of the heated cells and on the temperature sensitivity of the cell/module construction. One means of estimating the expected "hot spot" cell temperature is to convert the heating to an equivalent solar insolation as described by Ross**. The chief difficulty is in determining the power dissipated in the "hot spot" cells under the worst-case operating conditions for the failed array system. If we are only interested in the relative performance of various series/parallel configurations, this and other difficulties can be circumvented by bounding the problem and examining the "hot spot" cell heating under module short-circuit conditions. This condition is the worst-case for a single module or group of parallel modules, and is the worst-case for series modules where bypass diodes are incorporated to prevent reverse module voltages.

---

*Blake, F. A., and Hanson, L. L., "The 'Hot Spot' Failure Mode for Solar Arrays," Paper #699070 in the Proceedings of the 1969 IECEC Conference, September 1969, pp. 575-581.

**Ross, R.G., Jr., "Interface Design Considerations for Terrestrial Solar Cell Modules", Proceedings of the 12th IEEE Photovoltaic Specialists Conference - 1976, Baton Rouge, Louisiana, pp. 801-806.

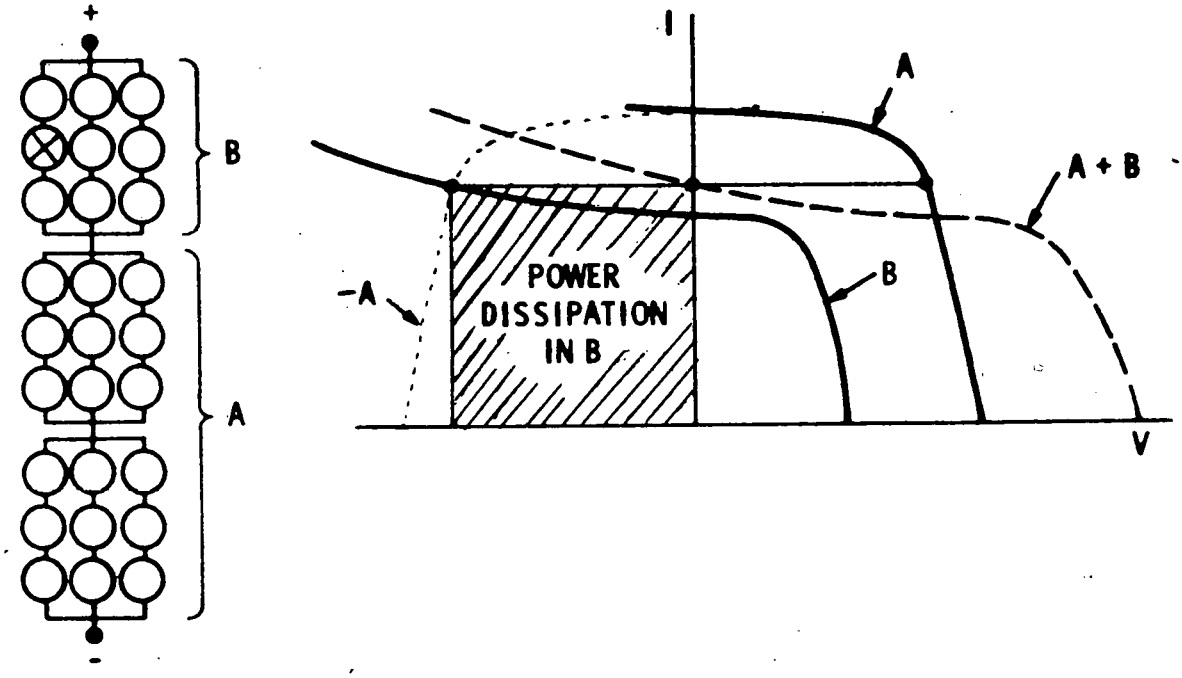


Figure 8-3. Visualization of "Hot-Spot" Cell Heating

As shown in Figure 8-3, the operation of a failed module under short-circuit conditions is characterized by the reverse voltage in the affected series block (section B) being equal to the forward voltage in the remaining sections of the module (section A). This operating condition is defined by the intersection of the I-V curve for the functional portion of section B with the I-V curve for section A, reflected about the ordinate into the negative voltage quadrant, i.e., the intersection of the B and -A curves in Figure 8-3.

To find the operating point for other series/parallel configurations requires constructing the B and -A I-V curves associated with these configurations. Figure 8-4 combines these curves in a single graph which provides a ready means for evaluating the "hot spot" heating associated with a single cell failure within a module with any series/parallel configuration. It is equally applicable to estimating the characteristics of series/parallel module configurations within an overall array system.

To use the figure, one locates the intersection of the parallel-cell and series-cell-block lines corresponding to the configuration of interest. The horizontal position of the intersection point establishes the "hot spot" cell heating under module short-circuit conditions as indicated on the lower scale. The vertical position of the intersection point establishes an estimate of the percent module

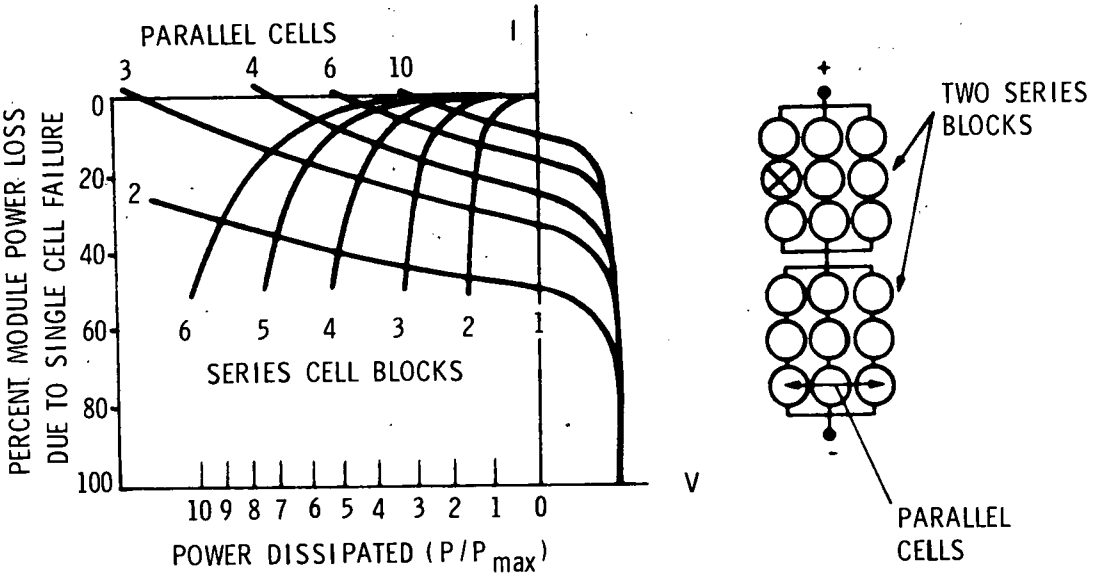


Figure 8-4. Effect of Series/Paralleling on "Hot Spot" Cell Heating

power loss due to a single cell failure, and is thus a measure of the improved reliability achieved by the series/paralleling. From Figure 8-4 it is clear that increased numbers of parallel cells and increased numbers of series blocks both decrease the percent module power loss due to a single cell failure. However, one must be careful about using large numbers of series blocks with low numbers of parallel cells because of the large "hot spot" cell heating which occurs under these conditions.

When large numbers of modules are in series together, the effect is to increase the number of series blocks. Under worst-case conditions a module with a failed cell can be driven to a current level equal to the module's original short-circuit current. The "hot spot" cell heating under this condition is given in Figure 8-4 by the intersection of the parallel-cells line for the module of interest and the 0%-module-power-loss line. For four cells in parallel it can be seen that the maximum "hot spot" cell heating is equal to about 7.5 times the cell maximum power. In cases where the "hot spot" cell heating is unacceptable at current levels above the module short-circuit current, a bypass diode can be used to limit the current at the short-circuit value.

## D. ELECTRICAL PERFORMANCE SPECIFICATION STUDIES

During the past quarter, work has also been directed toward improved electrical-performance specifications which are referenced to typical operating cell temperatures instead of a fixed 60°C. This approach has the advantage of providing greatly improved correlation between measured performance at rated conditions and expected performance in the field, provides for more accurate comparison of alternative module designs with different thermal properties and I-V-temperature characteristics, should cause module-cell performance optimization to be more closely aligned with actual field operating conditions, and is a necessary step toward eventual standardization of module electrical performance parameters and inter-manufacturer interchangeability.

The proposed approach to performance specification is based on first defining a nominal terrestrial environment (NTE) which is representative of the average environmental conditions in the United States during times when solar arrays are producing power. The cell temperature for a module under NTE conditions is referred to as the nominal operating cell temperature (NOCT) and is determined according to an easily implemented test procedure described in the next section of this report. The improved electrical-performance specifications simply make reference to the NOCT temperature instead of 60°C.

To determine an appropriate definition for the nominal terrestrial environment, a study was conducted using computer analysis of weather tapes which describe the measured hour-by-hour variation in ambient temperature and insolation in nine representative geographic locations in the continental United States. For each 3-hour interval, the following parameters were calculated.

(1) Insolation incident on a solar panel tilted to the local latitude and facing south.

(2) Solar cell temperature based on (1), the local air temperature, and the thermal properties of a typical solar cell module.

(3) Maximum power output of a solar cell module with typical I-V and temperature/intensity dependence characteristics.

Based on 10 years of weather at each site, the above parameters were organized to provide the average annual energy produced by a module at each combination of cell temperature and insolation level (on the tilted module). Figure 8-5 and 8-6 summarize these results and indicate that 50% of the energy from the assumed module is produced at insolation levels above and below about 80 $mW/cm^2$, and at cell temperatures above and below about 44°C. Using these values together with the assumed module thermal properties allows the properties of a sort of median environment to be calculated as:

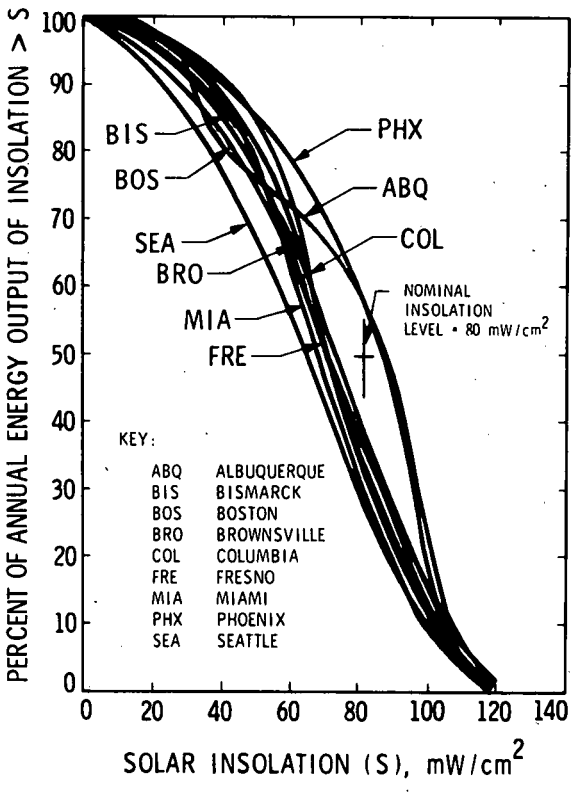


Figure 8-5. Module Annual Energy Output Versus Isolation Level on Tilted Array

Insolation = 80 mW/cm$^2$

Air temperature = 20°C

With this definition, 50% of the array energy output is produced at environmental conditions on either side of (less or more severe than) this median environment. This environment represents a logical point of specifying module electrical performance and hence has been adopted as the definition of the nominal terrestrial environment (NTE).

The nominal operating cell temperature (NOCT) used for performance specification is the measured cell temperature under the NTE conditions, and will generally be different for each module type. For the typical module used in the calculation procedure, the NOCT is 44°C.

A second analysis conducted during the past quarter utilized and expanded the above analysis to determine the optimum module voltage for charging typical float-service 12-volt lead-acid batteries. Work with present array manufacturers has suggested that this voltage is the logical voltage to specify for future module procurements.

The study was conducted in a manner similar to the above analysis except that the average annual energy delivered into a constant voltage

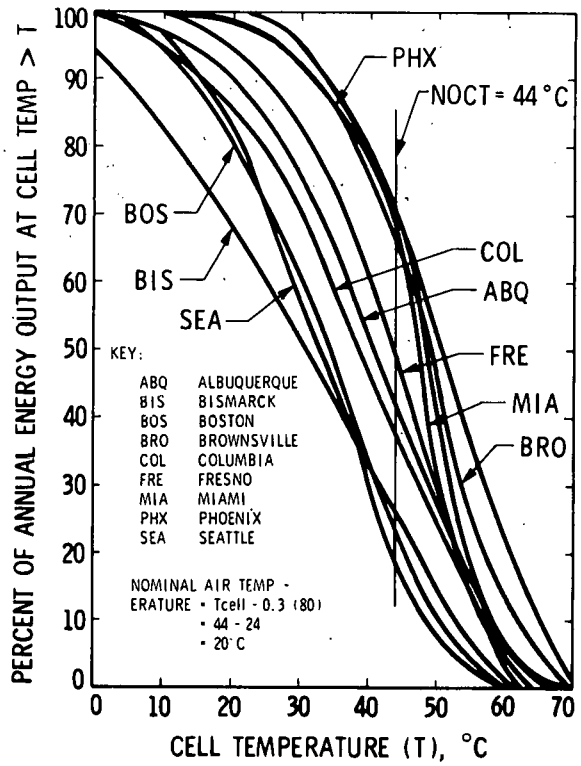


Figure 8-6. Module Annual Energy Output Versus Cell Temperature for a Typical Module With $T_{cell} - T_{air} = 0.3 \times$ Insolation (Ref. Figure 8-8)

load was calculated for each of a set of equal power modules with different maximum-power voltages, but otherwise identical I-V-temperature-intensity characteristics. Figure 8-7 presents these data as a function of the ratio of the module maximum-power voltage (at 100 mW/cm$^2$, NOCT) to the load voltage. Based on the typical charge voltage range of a 12-volt lead-acid battery, the optimum module is seen to have a maximum power voltage (at 100 mW/cm$^2$, NOCT) of approximately 15 volts.

## E. NOCT THERMAL TEST PROCEDURE DEVELOPMENT

Thermal testing and supporting analysis continued during the past quarter with the main thrust being to develop a test procedure for determining the nominal operating cell temperature (NOCT). A preliminary draft of these procedures has been issued for review and comments.

As described in the preceding section, the NOCT of the module is the module cell temperature under operating conditions in the nominal terrestrial environment which is defined more fully here as:

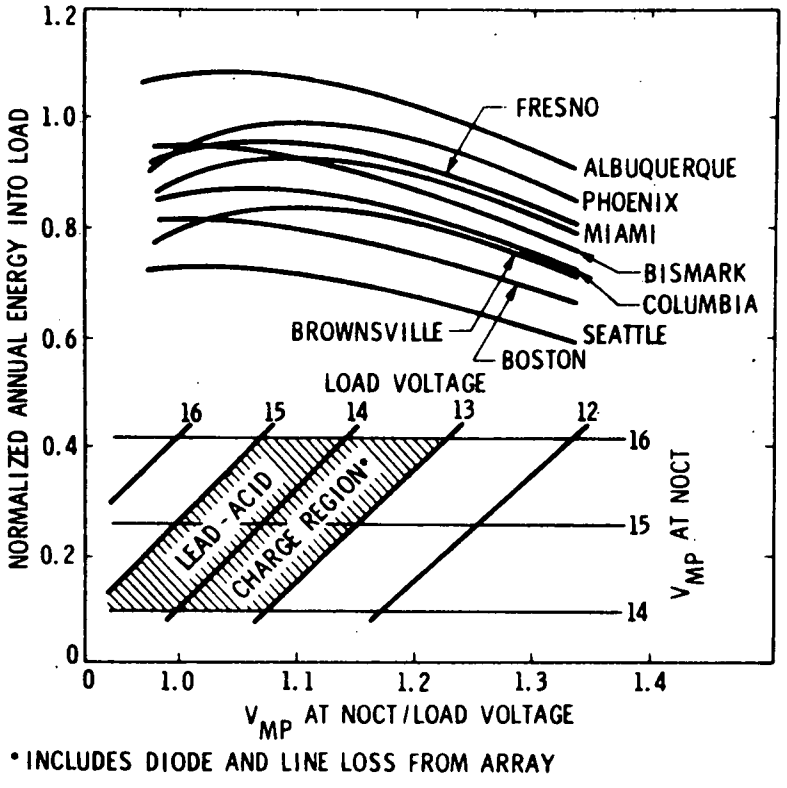


Figure 8-7. Annual Energy Versus Module Voltage for Constant Voltage Load

Insolation = 80 mW/cm$^2$

Air temperature = 20$^o$C

Wind average velocity = 1 m/s

Mounting = tilted, open back, open circuit

The objective of the NOCT test procedure is to provide a reliable, repeatable, low-cost and easily implemented approach for determining NOCT for a module of interest. The procedure is based on gathering actual measured cell temperature data via thermocouples attached directly to the cells of interest, for a range of environmental conditions similar to the NTE. The data are then presented in a way that allows accurate and repeatable interpolation of the NOCT temperature.

A key element of the approach is the fact that the temperature difference ($T_{cell}$-$T_{air}$) is largely independent of air temperature and is essentially linearly proportional to the insolation level. Figure 8-8 indicates that the linear assumption is quite good for insolation levels greater than about 40 mW/cm$^2$. The procedure calls for plotting ($T_{cell}$-$T_{air}$) against the insolation level as shown in Figure 8-9 for

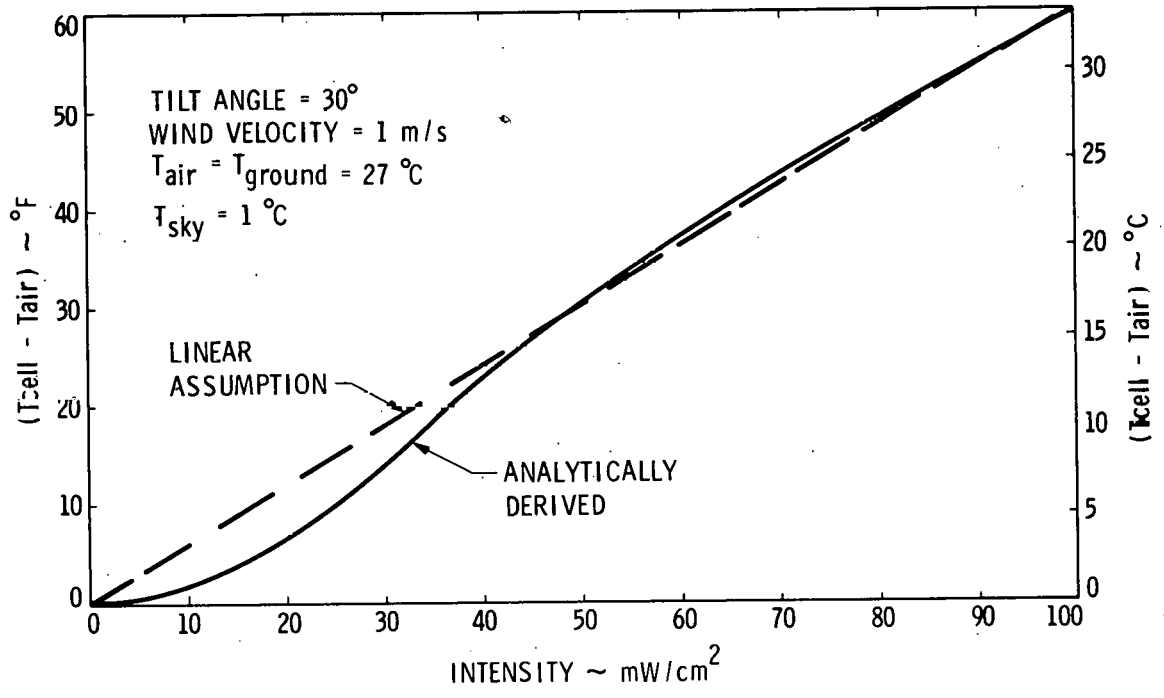


Figure 8-8. Variation of ($T_{cell}$-$T_{air}$) Versus Insolation Level for a Typical Solar Cell Module

a one or two day period when wind conditions are favorable. The NOCT value is then determined by adding $T_{air}$ = 20°C to the value of ($T_{cell}$-$T_{air}$) interpolated for the NTE insolation level of 80 mW/cm$^2$. Fine adjustments are then made to account for off-wind conditions and extreme air temperatures using the correction factors presented in Figure 8-10. These particular correction factors are calculated for modules without cooling fins, with backside open to the air, and with good solar and infrared optical properties, as is typical of the current LSSA modules.

Table 8-3 summarizes the tests used to substantiate the validity of the test procedure. It is estimated that NOCT can be determined to within ±1.5°C. With improvements in measuring $\overline{V}$, which are currently being pursued, a ±1°C accuracy is expected.

## F. ENVIRONMENTAL REQUIREMENTS DEVELOPMENT

During the past quarter, work has been initiated in several areas of environmental requirement development. In an attempt to improve current environmental test procedures, discussions were held with various experts in the field of environmental qualification including military test experts at Frankford Arsenal in Philadelphia and semiconductor

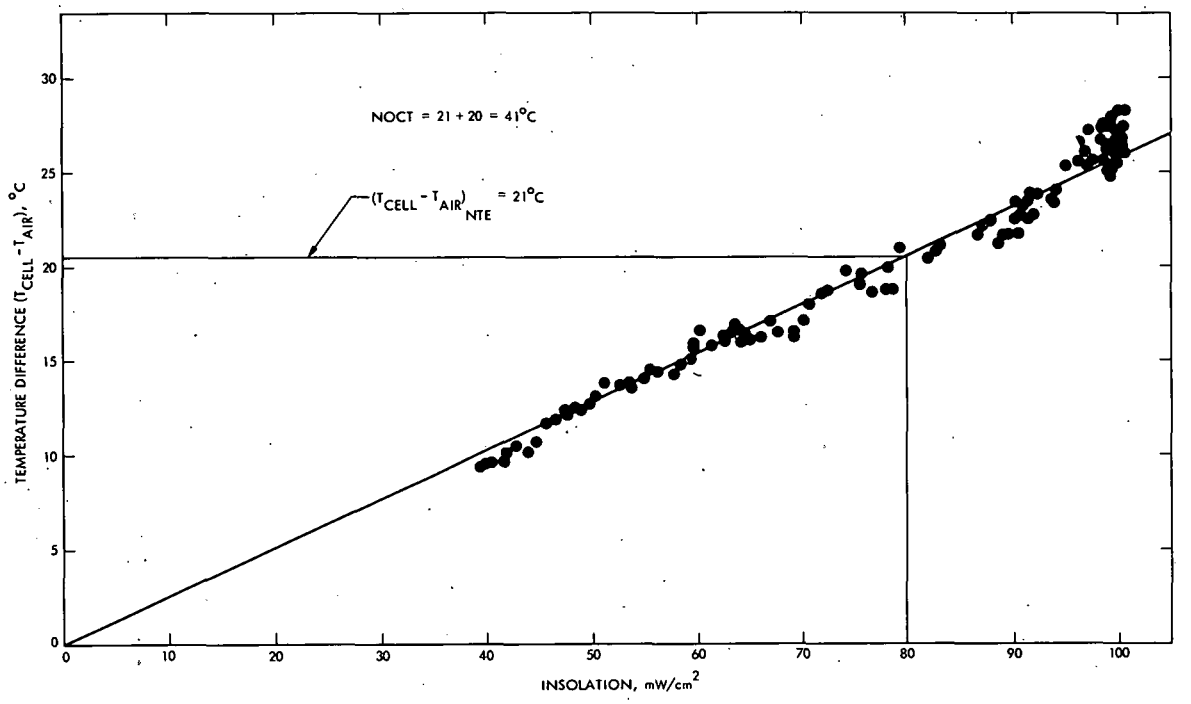


Figure 8-9. Determination of NOCT from Experimental Data

test experts at Motorola's Semiconductor Division in Phoenix. Based on these discussions, work has been initiated in the following areas:

(1) Development of bias-humidity test procedure which imposes an electrical stress on the module during a high-humidity/high-temperature soak. This type of test has been found to be one of the best indicators of field reliability by the semiconductor industry. It is felt to be especially effective at uncovering ion-migration problems, galvanic corrosion problems, and degradation of insulation resistance.

(2) Development of a hail or impact loading test. The survey indicated a lack of suitable test procedures for photovoltaic modules; therefore, a test development program has been initiated using a hail-gun previously developed at JPL for testing terrestrial deep space antennas.

(3) Computer analyses of terrestrial environmental data have been initiated to develop an improved understanding of the actual fatigue loading environment associated with cyclic thermal and wind loading. Design and fabrication of a wind-cyclic-loading spectrometer is under way to provide a means of accurately assessing the number and type of

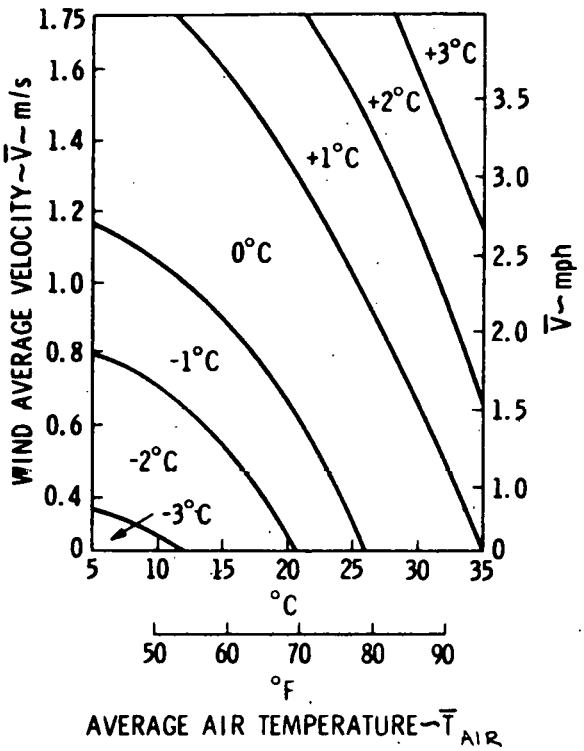


Figure 8-10. NOCT Correction Factors

wind loading cycles experienced in the field. When complete, the initial prototype instrument will be installed in the JPL Pasadena solar array test site for evaluation.

## Table 8-3. Thermal Performance Test Summary

| TEST NUMBER | DATE | TILT ANGLE (°) | MORNING AFTERNOON (M OR A) | $\bar{T}$air (°F) | $\bar{V}$ (mph) | SOLAREX 46 K | | | SPECTROLAB 130 K | | |
|---|---|---|---|---|---|---|---|---|---|---|---|
| | | | | | | Tcell-Tair (°C) | CORR FACTOR (°C) | NOCT (°C) | Tcell-Tair (°C) | CORR FACTOR (°C) | NOCT (°C) |
| 1 | 11-01-'76 | 45 | M | 90 | 2 TO 3 | 25.5 | +2 | 47.5 | N/A | N/A | N/A |
| 2 | 11-18-'76 | 55 | M | 77 | 1 TO 2 | 27.8 | 0 | 47.8 | 21.9 | 0 | 41.9 |
| 3 | 11-18-'76 | 55 | A | 80 | 1 TO 2 | 26.1 | 0 | 46.1 | 20.2 | 0 | 40.2 |
| 4 | 01-11-'77 | 55 | M | 63 | 2 TO 3 | 28.8 | 0 | 48.8 | 22.0 | 0 | 42.0 |
| 5 | 01-13-'77 | 55 | M | 56 | 3 TO 4 | 28.8 | 0 | 48.8 | 22.1 | 0 | 42.1 |
| 6 | 01-13-'77 | 55 | A | 64 | 3 TO 4 | 26.4 | +1 | 47.4 | 20.3 | +1 | 41.3 |
| 7 | 01-14-'77 | 55 | M | 60 | 1 1/2 TO 2 1/2 | 28.5 | -1 | 47.5 | 21.3 | -1 | 40.3 |
| 8 | 01-14-'77 | 55 | A | 65 | 1 1/2 TO 2 1/2 | 26.5 | 0 | 46.5 | 20.5 | 0 | 40.5 |
| 9 | 01-17-'77 | 55 | M | 70 | 1 TO 2 | 27.9 | 0 | 47.9 | 21.2 | 0 | 41.2 |
| 10 | 01-17-'77 | 55 | A | 80 | 1 TO 2 | 26.5 | 0 | 46.5 | 20.3 | 0 | 40.3 |
| | | | | | AVERAGE NOCT | | | 47.5 | | | 41.1 |

# SECTION IX

# OPERATIONS TASK

The purpose of the Operations Task is to identify and understand design defects so that module performance can be improved. The Operations Manager is responsible for the coordination and control of module testing, performance analysis, and the delivery of modules to users. Specific task activities include the following items:

(1) Liaison between JPL and module users on matters regarding delivery, interface compatibility, and field performance of modules.

(2) Implementation of acceptance and life testing at JPL for representative samplings of modules.

(3) Acquisition, interpretation, and reporting of module performance data from environmental testing and field service.

(4) Module failure analysis and implementation of a problem/failure reporting system.

(5) Management of traceability and configuration control systems for modules.

## A. ENVIRONMENTAL TESTING

### Block 1 Procurement*

Qualification testing of the late-production (Phase 2) Block 1 Procurement modules was completed during this quarter, and a number of prototype modules obtained from a manufacturer not previously involved in this program were tested. Environmental testing of the modules "added on" to the Block 1 Procurement was initiated.

Humidity/freezing exploratory tests were completed for all but one of the Block 1 Procurement module types during the quarter. This test cycle includes exposure to 65°C, 95% relative humidity, followed by freezing at -10°C.

Table 9-1 summarizes test results for the Phase 2 modules of the Block 2 Procurement. Figure 9-1 shows the results of qualification tests to which the Phase 2 modules were subjected. In the qualification test sequence, four of each manufacturer's modules were:

*Formerly called the 46 kilowatt procurement.

Table 9-1. Results of Environmental Testing of Late Production (Phase 2) Modules of the Block 1 Procurement - All Manufacturers

| Manufacturer | Fraction That Degraded > 5% in Electrical Output or Showed Open Circuit | | | | | | Other Observations |
|---|---|---|---|---|---|---|---|
| | Temp. Cycling | | Humidity | | Humidity/ Freezing | | |
| | Deg. | Open | Deg. | Open | Deg. | Open | |
| BLOCK 1 PROCUREMENT MODULES | | | | | | | |
| A | 0 | 0 | 0.75 | 0 | 0 | 0 | All samples showed some delamination. Humidity/ freezing caused cracked terminals and stains. |
| B | 0.12 | 0 | 0 | 0 | 0 | 0 | Poor junction box cover bonding. Encapsulant delamination. Cell cracking. |
| C | 0 | 0 | 0 | 0 | 0 | 0 | Cell discoloration. Some delamination. |
| D | 0 | 0 | 0 | 0 | 0 | 0 | Minor red-yellow spots after humidity/freezing. |
| E | 0.5 | 0.25 | - | - | - | - | Severe electrical degradation. Cracked cells. Tests discontinued. |
| ADD-ON MODULES (15 kW) | | | | | | | |
| | 0.5 | 0 | - | - | - | - | Some delamination. |
| SPECIALLY PROCURED PROTOTYPE MODULES | | | | | | | |
| | 0.2 | 0.2 | 0.2 | 0 | 0 | 0 | Some discoloration and delamination. Low electrical isolation for 50% of samples. Delamination and water entry for all modules after humidity/freezing. |

Note: Sample modules from Manufacturers B and D were exposed to 48 hours of salt fog, with little apparent effect.

(1) Exposed to 25 temperature cycles (+90 to -40°C).

(2) Examined.

(3) Exposed to 25 more temperature cycles (+90 to -40°C).

(4) Examined.

(5) Exposed to 168 hours of 90% relative humidity at 70°C.

(6) Examined.

In addition, a new set (i.e., not previously tested) of four modules of each type was exposed to 10 cycles of humidity/freezing.

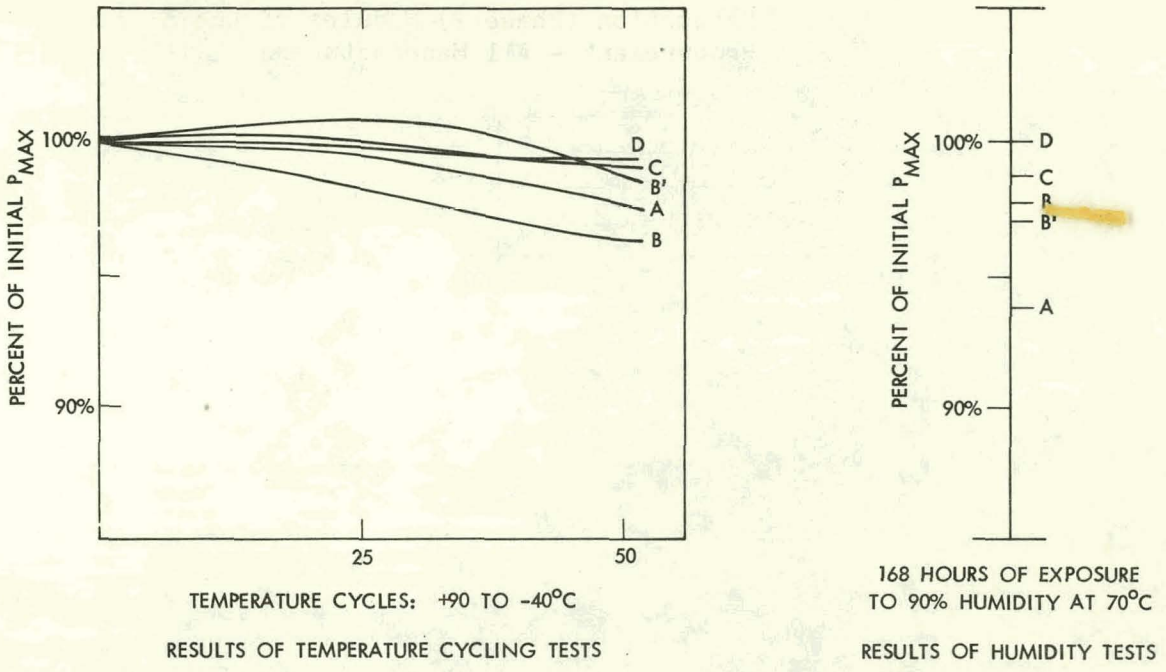


Figure 9-1. Block 1 Procurement Modules - Effect of Environmental Tests on Maximum Power Output

The results indicate that the late-production (Phase 2) modules were generally able to pass qualification testing without significant (greater than 5%) power degradation, but minor physical deterioration was common. One manufacturer's modules were sensitive to humidity, averaging a 6.3% decrease in power output after humidity exposure. The degradation (6-16%) in power of two of four "add-on" modules during the temperature cycling portion of the qualification tests was unexpected; problem/failure analysis is under way.

Block 2 Procurement*

During this quarter, Block 2 Procurement modules were received from two manufacturers. Qualification tests of the modules from one manufacturer (Manufacturer A) were completed, including tests in a wind load simulation apparatus (Figure 9-2). (As of the quarter's end, the second manufacturer's modules had completed only the initial electrical test and inspection.) The tests were carried out with the modules mounted in a stiff frame approximately 4 x 4 feet (Figure 9-3). Tests were performed in the following sequence: temperature cycling, humidity cycling, mechanical integrity (simulated wind load cycling). After each exposure the modules were inspected and electrical tests were made. Other tests include thermal coefficient testing in a heated box with a window (Figure 9-4), measurement of electrical isolation from the metal frame, and module flexing. The module flexing test is performed in a fixture that provides

*Formerly called the 130 kilowatt procurement.

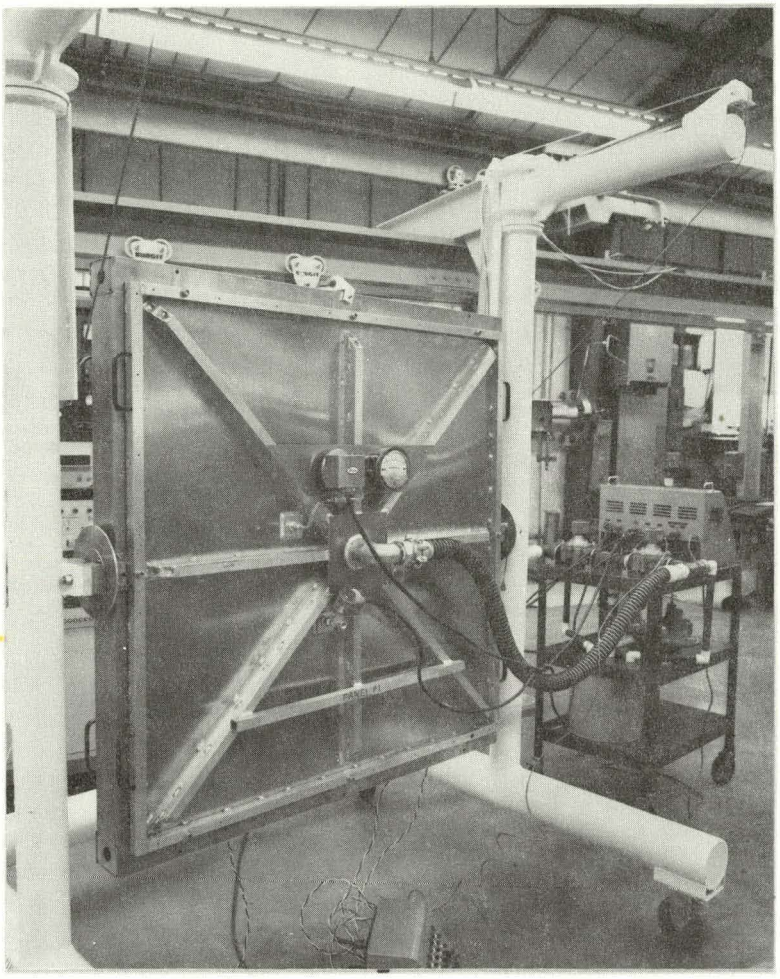

Figure 9-2. Wind Load Simulation Apparatus (Fabricated During This Quarter)

a ratio of 1-in-48 nonalignment of a mounting frame. Procedures for these tests are given in JPL Documents 5-342-1A and OTP-02, -03, -04, and -05.

The qualification test results for the first of the Block 2 Procurement prototype test modules are given in Table 9-2. The only potential problems of note revealed by this test series were (1) a tendency of some modules to show a temporary decrease in electrical isolation after exposure to moisture and (2) somewhat erratic power output behavior by one module during the test sequence. These phenomena are under investigation.

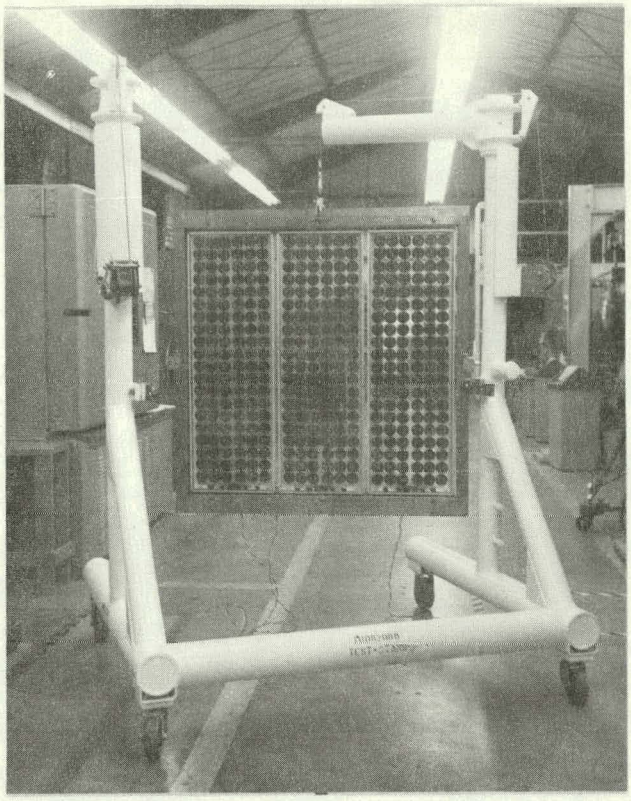

Figure 9-3. Test Stand for Wind Load Simulation Apparatus

B. FIELD TESTING

During this quarter, 30 modules were placed in the field at each of the secondary sites (Goldstone and Table Mountain). Figure 9-5 shows the Goldstone installation; the Table Mountain installation is similar. At the end of the quarter there were 121 modules in the field, distributed as follows:

| Manufacturer | JPL | Table Mtn. | Goldstone |
|---|---|---|---|
| Solar Power | 6 | 6 | 6 |
| Spectrolab | 9 | 9 | 9 |
| Solarex | 32 | 8 | 8 |
| Sensor Tech | 14 | 7 | 7 |

Table 9-2. Results of Testing Prototype Modules of the Block 2 Procurement from Manufacturer A

| Environment* | Results |
|---|---|
| Temperature (50 cycles) | One of three modules showed an anomalous increase in electrical output of 12% after temperature cycling. |
| Humidity (5 cycles) | One module showed temporary low electrical resistance to the frame (63 megohms between cell strings and frame). |
| Mechanical integrity (100 simulated wind Loading cycles) | One weld crack in aluminum support frame. One module showed marginal (approx. 5%) electrical degradation. |
| Salt fog (48-hour exposure; 3 different modules) | All three temporarily failed electrical isolation test (10-40 megohms between cell string and frame). After several days of drying out, all passed the test. |

*See also Table 10-2.

It is anticipated that JPL will receive additional modules from LeRC in the next quarter, permitting completion of the planned deployment of modules from the Block 1 Procurement. In the meantime, a 4 x 4 foot subarray containing three prototype Spectrolab modules from the Block 2 Procurement was put in the field at the JPL site; similar units will be installed at Table Mountain and Goldstone in the next quarter.

At the JPL site, LAPSS I-V data were obtained on each module every two weeks. Except for the complete failure of one module, the data show little apparent degradation. At Table Mountain, two modules failed during the first night after the installation, although the low temperature that night was only a moderate 40°F. A subsequent inspection (pressing the interconnect points) indicated that one of the interconnects failed on each of the modules. Further diagnostic checks on these two modules are pending.

A contract for the automated data system for the Pasadena site has been awarded to Instrument Technology Corporation. The system will have as its central processing unit a PDP 11/34 minicomputer which will control

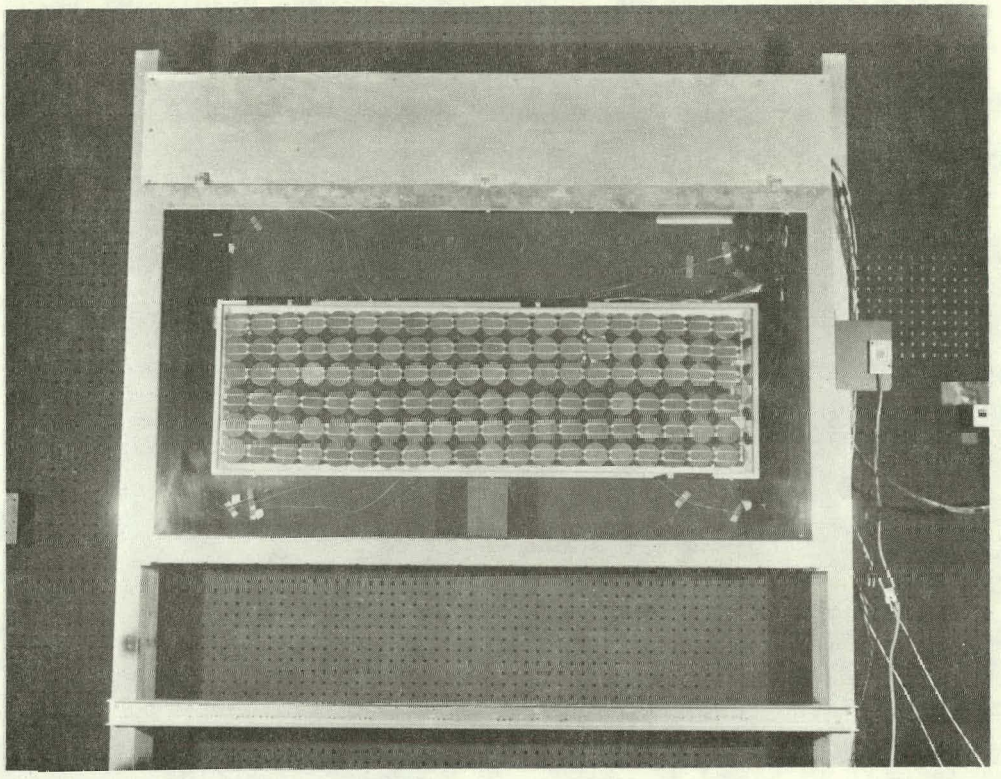

Figure 9-4. Heated Box

the acquisition of real-time data and analyze, summarize, and condense the data. It is expected that the system will be operational in the spring.

Thirty-two additional test stands have been ordered, a sufficient quantity to provide four more at each of the secondary sites and fill the Pasadena site. These stands will arrive in January. Seven will be installed immediately at the Pasadena site to accommodate Block 2 Procurement samples; the four destined for each of the secondary sites and the remainder for the Pasadena site will be installed within the next few months, as weather permits.

## C. PROBLEM/FAILURE ANALYSIS

During this quarter 26 new problem/failure reports (PFRs) were generated and 25 PFR analyses were completed. As of December 31, 1977, 107 PFRs were in the system; 50 of these had been disposed of. Review of the types of problems that are being experienced as a result of environmental testing shows the following breakdown:

| | |
|---|---|
| Design problems | 46 |
| Workmanship problems | 41 |

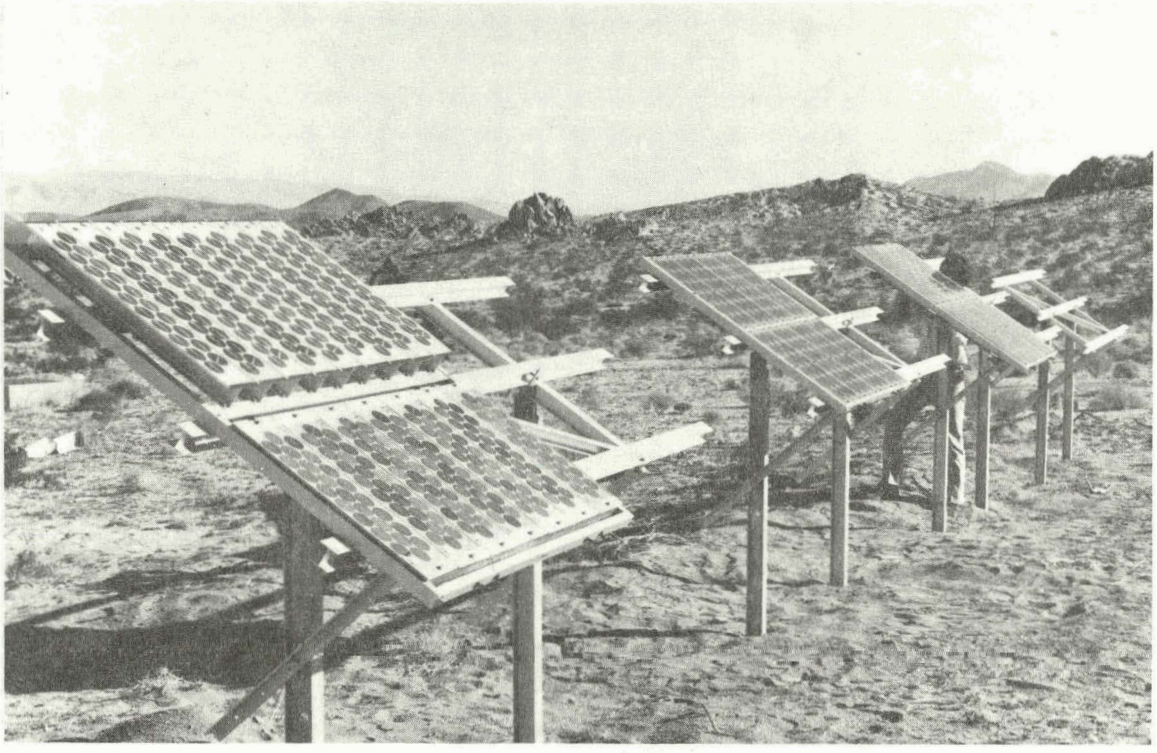

Figure 9-5. Modules Installed for Field Testing - Goldstone Site

| | |
|---|---|
| Manufacturing problems | 9 |
| Test equipment problems | 11 |

The problem analysis further shows that 55% of the problems are materials-related, e.g., delamination of encapsulants, cracking encapsulants, warpage of modules, stressing or breaking of interconnects, bubbles, fractured terminals, cell discoloration, encapsulation discoloration, and flux/corrosion. The remaining 45% relate to electrical performance, degradation of power output, opens, intermittents, and electrical isolation problems.

A PFR operations procedure is being prepared for release during the next quarter. This procedure will formalize the reporting, analysis and corrective action responses to provide more uniform reporting from JPL operations and test and applications projects.

A major analysis completed during this quarter involved samples of a design procured separately from the Block 1 Procurement. Test modules exhibited a variety of electrical isolation problems and opens after being subjected to environmental stress. The encapsulation system was found to be sensitive to humidity and humidity/freezing environments:

insulation resistance between cells and substrate dropped from greater than 100 megohms to as low as 6,000 ohms by the end of the test.

The JPL failure laboratory has developed a nondestructive method of locating open circuits within a module through use of capacitance and dissipation factor measurements of each solar cell. This is accomplished by connecting one terminal of the capacitance bridge to the positive side of the cell string and the other terminal to an aluminum foil electrode the size of one cell; the latter is placed, in sequence, over each cell as data are recorded. The values of capacitance and dissipation factor change abruptly at the cell with open circuit.

## D. PERFORMANCE MEASUREMENT STANDARDIZATION

In accordance with agreements reached at the last JPL/LeRC meeting on measurement standards, further interlaboratory measurement comparisons have been performed. The measurements were made using JPL and LeRC Large Area Pulsed Solar Simulators (LAPSS) and Small Area Pulsed Solar Simulators (SAPSS); identical standard cells and solar modules were used. The results show excellent agreement -- typically within 1%. A summary report of these data will be presented at the Semiannual Photovoltaic Program Review in San Diego in January.

Intermediate standard cells for the Block 2 Procurement were received from LeRC in November and December. Characterization tests and comparison with Block 1 Procurement standards is nearly complete. Delivery of intermediate standards to the manufacturers has begun; completion is anticipated by mid-January 1977.

Characterization testing of Spectrolab prototype modules in support of performance measurement standardization has been completed. These tests included empirical determination of power, voltage, and current temperature coefficients and red/blue short-circuit current ratios. The temperature coefficients permit extrapolation of performance data to the contractually required 60°C from ambient measurements. The red/blue ratio results will be compared to those for standard cells to verify that the standards are spectrally representative of production modules.

# SECTION X

# LARGE SCALE PRODUCTION TASK

During the last quarter of 1976, the Block 1 Procurement* of solar cell modules, including the 15 kilowatt "add-on" buy, was completed. The Block 2 Procurement* of solar cell modules was initiated; design and development are currently in progress.

## Block 1 Procurement

The Block 1 Procurement was initiated with five contractors for the procurement of 46 kilowatts of modules. One contractor was terminated and the procurement was continued with four contractors; 6,563 modules, equivalent to 55.26 kilowatts of power, had been delivered as of December 25, 1976. The module delivery status is given below.

| Contract (kW) | JPL Contract No. | Modules Delivered | Power Delivered (kW) | |
|---|---|---|---|---|
| Solar Power (15) | BQ633039 | 1,037 | 15.0 | (completed) |
| Solar Power-Add-On Buy (15) | | 828 | 12.0 | (in process) |
| M7 International (3) | (Terminated) | 52 | 0.26 | |
| Solarex (10) | BQ649006 | 1,046 | 10.0 | (completed) |
| Sensor Tech (8) | 954387 | 1,600 | 8.0 | (completed) |
| Spectrolab (10) | BQ649005 | 2,000 | 10.0 | (completed) |
| Total (46) | | 6,563 | 55.26 | |

The Block 1 Procurement was essentially based on state-of-the-art module technology. The primary objective of the buy was to provide modules to meet the needs of the ERDA Test and Demonstration Program. A secondary objective was to assess the capability of performance of the modules in a terrestrial environment.

Ten modules from each manufacturer were subjected to qualification tests. The tests included electrical performance, thermal cycles,

*New terminology: Block 1 Procurement - formerly called the 46 kilowatt procurement; Block 2 Procurement - formerly the 130 kilowatt procurement.

and temperature/humidity tests. The tests revealed several deficiencies, some related to module design and some to manufacturing quality. Modifications in design and process improvements were incorporated to virtually eliminate these problems. Key specifications for the Block 1 Procurement solar array modules are shown in Table 10-1.

As a result of the extensive testing and analysis performed on the modules, a great deal of knowledge concerning module design strength capability and module design weaknesses was obtained. As a result of the Block 1 Procurement experience, the following observations can be made:

(1) Because of its high cost and difficulty of application, the silicone encapsulant material cannot be readily incorporated into low-cost large scale production. It is suggested that an investigation be carried out to find a suitable alternative material.

(2) According to the module manufacturers, the cost of labor associated with manufacturing the modules could be reduced by designing the modules larger and thus reducing the quantity of modules required.

Block 2 Procurement

Block 2 Procurement incorporates additional environmental and performance requirements and modifies others to align the module qualification tests to the terrestrial environment. A requirement for a 4 x 4-foot envelope for module packaging was introduced. The purpose of the requirement is to make easier the installation and utilization of the module in the ERDA Demonstration and Test Program. Table 10-2 shows key specifications for the Block 2 Procurement solar array modules.

Table 10-1. Key Specifications for the LSSA Block 1 Procurement

| Test | Conditions and Requirements |
|---|---|
| Electrical Performance | 100 $mW/cm^2$ at 28°C |
| Temperature Cycling | 100 cycles, -40 to +90°C at less than 100°/hr |
| Temperature/Humidity | 168 hours, 95% relative humidity at 70°C |

Table 10-2. Key Specifications for the LSSA Block 2 Procurement Solar Array Modules

| Test | Conditions and Requirements |
|---|---|
| Electrical Performance | 100 $mW/cm^2$ at 60°C |
| Temperature Cycling | 50 cycles, -40 to +90°C |
| Humidity | 5 cycles, 95% RH, 23 to 41°C |
| Wind Loading | 100 cycles, ±50 lb/ft |
| Insulation Resistance | 100 MΩ, 1000 Vdc |
| High Voltage Breakdown | 1500 Vdc, 1 minute |
| Packaging Envelope | Envelope 4 x 4-foot frame |
| Redundancy | Terminal and in some cases cell-to-cell redundancy |

During the last quarter of 1976, the Block 2 Procurement effort was in the design and development phase. The power of the modules scheduled to be delivered by each contractor is shown in Table 10-3.

Table 10-3. Modules To Be Delivered - Block 2 Procurement

| Contractor | JPL Contract No. | Power of Modules (kW) |
|---|---|---|
| Solarex Corp. | 954577 | 30 |
| Sensor Technology | 954565 | 40 |
| Spectrolab | 954587 | 40 |
| Solar Power Corp. | BQ658202 | 15 |
| M7 International | (Terminated) | 5 |

The status and progress of each contractor is briefly described below.

Solarex

The preliminary module design review was held on October 29, 1976. Solarex is scheduled to start production of 30 prototype modules; 20 modules are to be shipped to JPL for qualification tests and 10 modules are to be tested by Solarex. Fabrication of the modules is scheduled for completion in December 1976.

Sensor Technology

The preliminary design review has been completed and fabrication of 30 prototype modules has started. Twenty modules were shipped to JPL on December 15, 1976 for JPL in-house qualification testing. The other 10 prototype modules are to undergo qualification tests at Sensor Technology. The final design review is scheduled for the first week in February 1977.

Spectrolab

Spectrolab has completed the preliminary design review. Prototype module testing has been completed by Spectrolab and JPL, with minimal electrical and mechanical degradation. Module production is expected to begin in January 1977.

Solar Power Corporation

The preliminary design review was completed by Solar Power. Authorization was given to Solar Power to start the fabrication of prototype modules. Completion of the prototype modules in January 1977 is expected.

The Block 2 Procurement is encountering delays. Some of the delays are attributable to:

(1) Implementation of the design changes resulting from design reviews.

(2) Contractor's inability to obtain materials in a timely manner.

(3) Delays due to changes to JPL Specification 5-342-1. The changes are generally directed toward improving the module design and/or performance capability.



NASA—JPL—Coml., L.A., Calif.